

REPORT NO. NADC-83116-60



DEVELOPMENT OF LATERAL-DIRECTIONAL EQUIVALENT SYSTEM MODELS FOR SELECTED U.S. NAVY TACTICAL AIRCRAFT

D. E. Bischoff and R. E. Palmer
Aircraft and Crew Systems Technology Directorate
NAVAL AIR DEVELOPMENT CENTER
Warminster, Pennsylvania 18974

NADC

SEPTEMBER 1983

Tech. Inf

19970605 008

FINAL REPORT
AIRTASK NO. A034-0000/001B/0F41-400-000

DTIC QUALITY INSPECTED 2

Approved for Public Release; Distribution Unlimited

Prepared For
NAVAL AIR SYSTEMS COMMAND
Department of the Navy
Washington, DC 20361

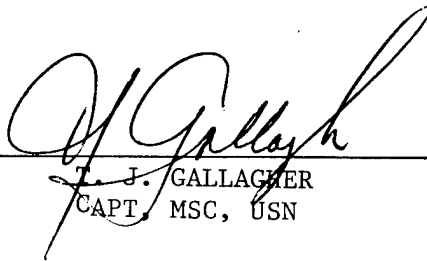
NOTICES

REPORT NUMBERING SYSTEM – The numbering of technical project reports issued by the Naval Air Development Center is arranged for specific identification purposes. Each number consists of the Center acronym, the calendar year in which the number was assigned, the sequence number of the report within the specific calendar year, and the official 2-digit correspondence code of the Command Office or the Functional Directorate responsible for the report. For example: Report No. NADC-78015-20 indicates the fifteenth Center report for the year 1978, and prepared by the Systems Directorate. The numerical codes are as follows:

CODE	OFFICE OR DIRECTORATE
00	Commander, Naval Air Development Center
01	Technical Director, Naval Air Development Center
02	Comptroller
10	Directorate Command Projects
20	Systems Directorate
30	Sensors & Avionics Technology Directorate
40	Communication & Navigation Technology Directorate
50	Software Computer Directorate
60	Aircraft & Crew Systems Technology Directorate
70	Planning Assessment Resources
80	Engineering Support Group

PRODUCT ENDORSEMENT – The discussion or instructions concerning commercial products herein do not constitute an endorsement by the Government nor do they convey or imply the license or right to use such products.

APPROVED BY: _____


J. J. GALLAGHER
CAPT, MSC, USN

DATE: _____

16 April 1984

REPORT DOCUMENTATION PAGE		READ INSTRUCTIONS BEFORE COMPLETING FORM
1. REPORT NUMBER NADC-83116-60	2. GOVT ACCESSION NO.	3. RECIPIENT'S CATALOG NUMBER
4. TITLE (and Subtitle) DEVELOPMENT OF LATERAL – DIRECTIONAL EQUIVALENT SYSTEM MODELS FOR SELECTED U.S. NAVY TACTICAL AIRCRAFT		5. TYPE OF REPORT & PERIOD COVERED Final 1 Oct. 1981 – 30 Nov. 1982
		6. PERFORMING ORG. REPORT NUMBER
7. AUTHOR(s) David E. Bischoff and Robert E. Palmer		8. CONTRACT OR GRANT NUMBER(s)
9. PERFORMING ORGANIZATION NAME AND ADDRESS Aircraft and Crew Systems Technology Directorate Naval Air Development Center Warminster, PA 18974		10. PROGRAM ELEMENT, PROJECT, TASK AREA & WORK UNIT NUMBERS AIRTASK No. A034-0000/001B/ OF41-400-000
11. CONTROLLING OFFICE NAME AND ADDRESS Naval Air Systems Command Department of the Navy Washington, D.C. 20361		12. REPORT DATE September 1983
		13. NUMBER OF PAGES
14. MONITORING AGENCY NAME & ADDRESS (if different from Controlling Office)		15. SECURITY CLASS. (of this report) Unclassified
		15a. DECLASSIFICATION/DOWNGRADING SCHEDULE
16. DISTRIBUTION STATEMENT (of this Report) Approved for public release; distribution unlimited		
17. DISTRIBUTION STATEMENT (of the abstract entered in Block 20, if different from Report)		
18. SUPPLEMENTARY NOTES		
19. KEY WORDS (Continue on reverse side if necessary and identify by block number) Aircraft Lateral Directional Flying Qualities Equivalent Systems Frequency Response Matching		
20. ABSTRACT (Continue on reverse side if necessary and identify by block number) The high order transfer functions representing the lateral directional responses to pilot control inputs were matched with low order equivalent forms in the frequency domain for five Navy tactical aircraft: the A-6, A-7, S-3, F-14, and F-18. The candidate low order equivalent forms investigated were: 1) the complete three degree of freedom representation of roll and sideslip angle responses, and 2) the single degree of freedom roll mode and Dutch roll approximations. Acceptable models were generally obtained for both forms. Simultaneous matching of sideslip and roll angle responses and/or apriori information for the roots was required to match the full		

20. ABSTRACT (Continued)

three degree of freedom forms. The equivalent system models are discussed in terms of their match statistics. The equivalent system modal parameters, when compared against the requirements of the military flying qualities specification, demonstrate Level 1 flying qualities for the conditions analyzed with the exception of roll angle time delay for the A-7 and F-18 airplanes. The A-7's lateral command augmentation structure results in Level 2-3 equivalent time delays, while the F-18's control force inputs produce Level 2 equivalent time delays.

TABLE OF CONTENTS

	Page
LIST OF FIGURES	iii
LIST OF TABLES	iv
LIST OF SYMBOLS	v
INTRODUCTION	1
BACKGROUND	1
PURPOSE	1
SCOPE	1
METHOD	2
RESULTS AND DISCUSSION	7
GENERAL	7
EQUIVALENT SYSTEM MODELS	7
S-3 Airplane	7
A-6 Airplane	14
A-7 Airplane	17
F-14 Airplane	34
F-18 Airplane	36
COMPARISON WITH SPECIFICATION REQUIREMENTS	42
CONCLUSIONS AND RECOMMENDATIONS	49
REFERENCES	50
APPENDIX	
A AIRCRAFT AND CONTROL SYSTEM DESCRIPTIONS	A-1
B SUMMARY OF EQUIVALENT SYSTEM MODELS	B-1

LIST OF FIGURES

Figure		Page
1	S-3 Roll Response – Approximate Form	10
2	S-3 Sideslip Response – Approximate Form	11
3	S-3 Roll Response – Approximate Form Plus Low Frequency Root	12
4	S-3 Sideslip Response – Approximate Form Plus Low Frequency Roots	13
5	S-3 Roll Response – Simultaneous Match	15
6	S-3 Sideslip Response – Simultaneous Match	16
7	A-6 Roll Response – Approximate Form	19
8	A-6 Sideslip Response – Approximate Form	20
9	A-6 Roll Response – Simultaneous Match	21
10	A-6 Sideslip Response – Simultaneous Match	22
11	A-7 Roll Response – Approximate Form, No Control Augmentation	25
12	A-7 Sideslip Response – Approximate Form, No Control Augmentation	26
13	A-7 Roll Response – Simultaneous Match, No Control Augmentation	28
14	A-7 Sideslip Response – Simultaneous Match, No Control Augmentation	29
15	Impact of Roll Command Augmentation on A-7 Roll Rate Response	30
16	A-7 Roll Response – Simultaneous Match, Command Augmentation Included	32
17	A-7 Sideslip Response – Simultaneous Match, Command Augmentation Included ..	33
18	F-14 Roll Response – Simultaneous Match	36
19	F-14 Sideslip Response – Simultaneous Match	37
20	F-18 Roll Response – Simultaneous Match	40
21	F-18 Sideslip Response – Simultaneous Match	41
22	Roll Mode Results – Cruise Configuration	43
23	Roll Mode Results – Power Approach Configurations	44
24	Dutch Roll Mode Results – Cruise Configuration	45
25	Dutch Roll Mode Results – Power Approach Configuration	46
26	A-7 Time Delay Results	47
27	Time Delay vs. Roll Mode Time Constant – Approximate Form Results	48
A-1	S-3 Lateral Directional Control System	A-3
A-2	A-6 Lateral Directional Control System	A-6
A-3	A-7 Lateral Directional Control System	A-9
A-4	F-14 Lateral Directional Control System	A-12
A-5	F-18 Lateral Directional Control System	A-16
B-1	S-3 Roll Response – Simultaneous Match .71 Mach	B-3
B-2	S-3 Sideslip Response – Simultaneous Match .71 Mach	B-4
B-3	A-6 Roll Response – Simultaneous Match .72 Mach	B-6
B-4	A-6 Sideslip Response – Simultaneous Match .72 Mach	B-7
B-5	A-6 Roll Response – Simultaneous Match .87 Mach	B-8
B-6	A-6 Sideslip Response – Simultaneous Match .87 Mach	B-9
B-7	A-7 Roll Response – Simultaneous Match .30 Mach	B-11
B-8	A-7 Sideslip Response – Simultaneous Match .30 Mach	B-12
B-9	A-7 Roll Response – Simultaneous Match .90 Mach	B-13
B-10	A-7 Sideslip Response – Simultaneous Match .90 Mach	B-14
B-11	F-14 Roll Response – Simultaneous Match .715 Mach	B-16
B-12	F-14 Sideslip Response – Simultaneous Match .715 Mach	B-17
B-13	F-14 Roll Response – Simultaneous Match .795 Mach	B-18

LIST OF FIGURES (Continued)

Figure		Page
B-14	F-14 Sideslip Response – Simultaneous Match .795 Mach	B-19
B-15	F-14 Roll Response – Simultaneous Match .91 Mach	B-20
B-16	F-14 Sideslip Response – Simultaneous Match .91 Mach	B-21
B-17	F-14 Roll Response – Simultaneous Match Power Approach Configuration	B-22
B-18	F-14 Sideslip Response – Simultaneous Match Power Approach Configuration ...	B-23

LIST OF TABLES

Table		Page
I	Flight Conditions	2
II	S-3 Airplane Equivalent Transfer Functions	9
III	A-6 Airplane Equivalent Transfer Functions	18
IV	A-7 Airplane Equivalent Transfer Functions, No Prefilters	24
V	Effect of Initial Parameter Values on Roll Angle Matching	27
VI	A-7 Airplane Equivalent Transfer Functions, Prefilters Included	31
VII	F-14 Airplane Equivalent Transfer Functions	35
VIII	F-18 Airplane Equivalent Transfer Functions	39
A-I	S-3 Airplane Transfer Functions	A-4
A-II	A-6 Airplane Transfer Functions	A-7
A-III	A-7 Airplane Transfer Functions	A-10
A-IV	F-14 Airplane Transfer Functions	A-13
A-V	F-18 Airplane Transfer Functions	A-17
B-I	S-3 Aircraft Equivalent Parameter Results	B-2
B-II	A-6 Aircraft Equivalent Parameter Results	B-5
B-III	A-7 Aircraft Equivalent Parameter Results	B-10
B-IV	F-14 Aircraft Equivalent Parameter Results	B-15

LIST OF SYMBOLS

A_y	–	Lateral acceleration – ft/sec ²
K	–	Numerator gain
L	–	Rolling moment – ft lbs
M	–	Mismatch parameter
N	–	Yawing moment – ft lbs
p	–	Roll rate – rad/sec
r	–	Yaw rate – rad/sec
t	–	Time delay – sec
δa	–	Aileron deflection – rad
δa_p	–	Lateral control force – lb
δr	–	Rudder deflection – rad
δr_p	–	Rudder pedal force – lb
δ_{LAT}	–	Roll control input – rad or lb
δ_{PED}	–	Sideslip control input – rad or lb
ϕ	–	Bank angle – rad
β	–	Sideslip angle – rad
ζ	–	Damping ratio
ω	–	Frequency – rad/sec
$(\dot{\cdot})$	–	Time derivative

Subscripts

DR	–	Dutch Roll
e	–	Equivalent system
HOS	–	High Order System
LOS	–	Low Order System
r	–	Roll mode
s	–	Spiral mode

Transfer Function Root Representation

(σ)	–	Real root of value σ
$[\zeta, \omega]$	–	Imaginary root with damping ζ , frequency ω

INTRODUCTION

BACKGROUND

The Military Specification for Flying Qualities of Piloted Airplanes, MIL-F-8785B, (reference (a)), was developed largely from flight tests of classically responding unaugmented aircraft. Its quantitative requirements are generally expressed in terms of modal approximations which can be described mathematically by first or second order linear expressions. Advancements in aerodynamics and complicated control system augmentation schemes, prevalent in modern aircraft designs, have resulted in responses which are described by high order functions.

In an attempt to utilize the existing requirements in analyzing advanced aircraft/control system configurations, the concept of equivalent systems, has been introduced (reference (b)). A digital frequency domain equivalent system matching technique has been developed by Hodgkinson, et. al., and applied to the high order representations of experimental aircraft (reference (c)). The approach used was to approximate the high order response to pilot control input transfer functions of the subject aircraft with classical low order transfer functions describing the specification requirements, augmented with a time delay. This equivalent time delay approximates the phase lag introduced by the high frequency control system components. Within the scope of the initial investigations, it was determined that the linear modal requirements of MIL-F-8785B, when augmented by a requirement on time delay, are appropriate for specifying the handling qualities of the advanced high order configurations of tomorrow's airplanes (reference (d)). This approach has been incorporated in the latest revision to the MIL-SPEC, MIL-F-8785C, and the proposed MIL standard and Handbook, reference (e) and (f) respectively, which states:

"The contractor shall define equivalent classical systems which have responses most closely matching those of the actual aircraft."

The parameters defining the resulting equivalent system (frequency, damping ratio, time constants etc.) rather than any modes of the high order system, are to be compared with the specification requirements. Guidance as to how the contractor shall proceed with his equivalent system definition is addressed in the proposed MIL Handbook, Volume II of reference (f).

The Naval Air Development Center, as part of its effort in identifying flying qualities criteria for manned aircraft, undertook the determination of equivalent system descriptions of current Navy tactical aircraft. The determination of classical pitch-rate short-period models for current fleet aircraft was reported in reference (g). This report presents similar results for the lateral-directional responses of the same U.S. Navy aircraft.

PURPOSE

The purpose of this effort was to investigate the utility of the equivalent systems approach to defining the dynamic lateral-directional flying qualities parameters of augmented aircraft. This report presents equivalent low order system models for current U.S. Navy tactical aircraft and compares them with the modal requirements of MIL-F-8785C, reference (e).

SCOPE

Lateral-directional modal responses for the A-6, A-7, F-14, F-18 and S-3 aircraft were analyzed in this effort. Where applicable, each aircraft was assumed to have its Stability/Control Augmentation System (SAS/CAS) ON. The flight conditions investigated included both Power Approach (PA) and Cruise (CR) configurations as presented in table I.

TABLE I. FLIGHT CONDITIONS

Aircraft	Configuration	Gross Weight (lb)	CG Position (% MAC)	Altitude (ft)	Airspeed (M/KEAS)
A-6	CR	39505	23.6	20000	0.4 0.72 0.87
S-3	CR	36320	21.7	15000	0.36 0.71
F-14	CR	51015	8.2	15000	0.40 0.715 0.795 0.91 0.183/121
	PA		44030		
A-7	CR	21890	30.0	15000	0.3 0.6 0.9
F-18	CR	29930	25.0	10000	0.5

METHOD

Frequency response matching techniques were utilized to determine low order equivalent systems describing the complex aircraft high order representations. Digital computer programs, prepared by the McDonnell Aircraft Company, utilized a direct Rosenbrock search algorithm (reference c) to match a Bode plot describing the high order pilot input to aircraft output transfer function with an equivalent low order system. Since this analysis is concerned with determining equivalent lateral-directional models, the roll and sideslip angle responses to pilot control inputs were analyzed.

In order to use the matching routines, a description of the frequency response of the system to be matched is required. This may be in the form of either (1) transfer functions or (2) numerical phase-gain data obtained at various input frequencies. Since only limited numerical response data is available for the subject airplanes (and it is generally corrupted with instrumentation noise and air turbulence) the transfer function input approach was chosen. Each aircraft's transfer functions describing the desired responses were obtained either directly from available information (A-7) or computed via NADC transfer function programs from stability and control derivative information (A-6, S-3, F-14, F-18). Reference (h) through (m) were used to obtain this information as well as a description of the respective control systems. With the aircraft's unaugmented dynamics thus obtained, the control components present in each aircraft's control system (i.e., actuators, stick feel system, feedback loops, compensation networks, etc.) were added to obtain the high order transfer function describing each aircraft/control system combination and flight condition. Brief descriptions of the aircraft and their respective control systems are presented in appendix A.

The equivalent low order systems were obtained via a frequency response matching technique which minimizes a mismatch function. This mismatch function is defined as the weighted sum of the squares of the differences in magnitude and phase angle between the high and low order systems at a number of discrete frequencies. Quantitatively, this can be expressed as:

$$M = \frac{20}{n} \sum_{\omega_1}^{\omega_n} [(G_{HOS} - G_{LOS})^2 + .01745 (\Phi_{HOS} - \Phi_{LOS})^2] \quad (1)$$

where G equals the gain in decibels and Φ is the phase in degrees. Summing the mismatch function over a number of frequencies, evenly spaced on a logarithmic scale, is similar to minimizing the integral of the square of the error on a Bode plot. As a result, it is possible to qualitatively compare the matches with the quantitative mismatch results. The frequency range over which the minimization was conducted was chosen to span the pilot's primary frequency range of interest (0.1 – 10 rad/sec).

The frequency response matching procedure enables the analyst to match any high order system with any desired low order system format. Restricting the scope of this analysis to the determination of dynamic lateral directional characteristics establishes the possible forms of the low order system to be matched. Beginning with the three degree of freedom equations of motion describing the lateral directional responses, the MIL-SPEC dynamic lateral directional characteristics (ζ_{DR} , ω_{DR} , τ_r and τ_s) can be obtained from the transfer functions relating roll angle and sideslip angle response to control deflection:

$$\frac{\phi(s)}{\delta_a(s)} = \frac{L\delta_a (s^2 + 2\zeta_\phi\omega_\phi s + \omega_\phi^2)}{(s+1/\tau_r) (s+1/\tau_s) (s^2 + 2\zeta_{DR}\omega_{DR}s + \omega_{DR}^2)} \quad (2)$$

$$\frac{\beta(s)}{\delta_r(s)} = \frac{N\delta_r (s+1/\tau_{\beta_1}) (s+1/\tau_{\beta_2}) (s+1/\tau_{\beta_3})}{(s+1/\tau_r) (s+1/\tau_s) (s^2 + 2\zeta_{DR}\omega_{DR}s + \omega_{DR}^2)} \quad (3)$$

Equations (2) and (3) can be further simplified by decoupling the lateral and directional modes of motion. Assuming only a single degree of freedom roll response, the roll equation of motion yields the following approximate transfer function:

$$\frac{\phi(s)}{\delta_a(s)} = \frac{L\delta_a}{s (s+1/\tau_r)} \quad (4)$$

Similarly by eliminating the rolling degree of freedom, the Dutch roll approximation may be expressed as:

$$\frac{\beta(s)}{\delta_r(s)} = \frac{N\delta_r}{(s^2 + 2\zeta_{DR}\omega_{DR}s + \omega_{DR}^2)} \quad (5)$$

In matching the response of high order and/or closed loop control systems to pilot command inputs, the control input required in equations (2) through (5) is the cockpit control force or deflection.

The inclusion of control system components in the high order system may result in high frequency phase responses which exceed the phase asymptotes of the classical systems. Therefore, the equivalent system procedure augments equations (2) through (5) via the addition of a time delay. This delay introduces phase lag without altering the gain characteristics. The resulting equivalent systems may then be expressed as follows:

Complete three degree of freedom

$$\frac{\phi(s)}{\delta_{ap}(s)} = \frac{K_{\phi} (s^2 + 2\zeta_{\phi}\omega_{\phi}s + \omega_{\phi}^2) e^{-t_{\phi}s}}{(s+1/\tau_r) (s+1/\tau_s) (s^2 + 2\zeta_{DR}\omega_{DR}s + \omega_{DR}^2)} \quad (6)$$

$$\frac{\beta(s)}{\delta_{rp}(s)} = \frac{K_{\beta} (s+1/\tau_{\beta_1}) (s+1/\tau_{\beta_2}) (s+1/\tau_{\beta_3}) e^{-t_{\beta}s}}{(s+1/\tau_r) (s+1/\tau_s) (s^2 + 2\zeta_{DR}\omega_{DR}s + \omega_{DR}^2)} \quad (7)$$

Approximate forms:

$$\frac{\phi(s)}{\delta_{ap}(s)} = \frac{K_{\phi} e^{-t_{\phi}s}}{s (s+1/\tau_r)} \quad (8)$$

$$\frac{\beta(s)}{\delta_{rp}(s)} = \frac{K_{\beta} e^{-t_{\beta}s}}{(s^2 + 2\zeta_{DR}\omega_{DR}s + \omega_{DR}^2)} \quad (9)$$

In order to further simplify the approximate forms, roll rate, rather than roll angle, was used to evaluate the roll response. The approximate roll rate response appears as:

$$\frac{p(s)}{\delta_{ap}(s)} = \frac{K_{\phi} e^{-t_{\phi}s}}{(s+1/\tau_r)} \quad (10)$$

Equations (6) and (7) have been implemented by Hodgkinson in a digital computer program called LATFIT, reference (n). This program allows for either individual or simultaneous matching of the roll angle and sideslip responses. When using the LATFIT program, initial estimates for the unknown parameters must be supplied by the analyst.

It should be noted that the guidance for determining equivalent system models given in reference (f) is to individually match the approximate sideslip response via equation (9) to obtain Dutch roll information and the complete roll rate response via

$$\frac{p(s)}{\delta_{ap}(s)} = s \frac{\phi(s)}{\delta_{ap}(s)} = s \cdot \text{equation (6)} \quad (11)$$

to obtain roll mode information. It will be shown in the Results and Discussion section that it is often necessary to match the sideslip and bank angle responses simultaneously, in which case consistent models should be utilized.

In performing the equivalent system match, the analyst worked interactively with the program to determine which of the decision variables to vary in the search for the equivalent low order system. In general, the procedure outlined below was utilized:

- a) Initially, the ϕ and β response transfer functions were matched independently with the approximate forms of the low order equivalent system. (This step was, in general, easily accomplished and provided qualitatively acceptable matches when compared in both the frequency and time domains.)
- b) Secondly, improvement in the mismatch function was evaluated by obtaining the complete low order forms, equations (6) and (7). This was accomplished by starting ζ_{DR} , ω_{DR} , τ_r , and the time delays from the approximate form results. In addition ζ_ϕ , ω_ϕ , and τ_{β_2} were either started at their high order system values or at values close to ζ_{DR} , ω_{DR} , and τ_r , respectively. The remaining factors, τ_{β_1} , τ_{β_2} , and τ_s , which were generally outside the frequency range of interest, were held fixed at their high order system values.

The proximity of the roll angle numerator and denominator oscillatory roots, as well as one of the sideslip numerator time constants (τ_{β_2}) and the roll mode time constant, restricted the low order equivalent system determination when matching ϕ and β independently with the complete form (step b). This problem could be alleviated by fixing the numerator roots at their high order system value or by simultaneously matching ϕ and β while constraining the equivalent denominators to be identical. While the former case generally produced satisfactory results, knowledge of the numerator roots may not always be available prior to the matching process. In the latter case the roll mode time constant, identifiable from the roll response, helped to locate the sideslip numerator root while the Dutch roll roots, identifiable from the sideslip response, helped to locate the roll angle numerator roots.

When individual control system roots were present in the frequency range of interest, as with prefilters for example, the problems associated with determining an acceptable equivalent system match were compounded.

The following technique (further explained in the Results and Discussion section) was found to overcome these problems with a minimum amount of computational effort:

- a) Determine an approximate denominator root location using equations (9) and (10).
- b) Simultaneously match equations (6) and (7) in the following sequence (Fix τ_{β_1} , τ_{β_3} , and τ_s at their corresponding high order system values in these runs):
 1. Fix ζ_{DR} , ω_{DR} , and τ_r at the values obtained in step a. Match all remaining parameters (beginning with $\zeta_\phi \approx \zeta_{DR}$, $\omega_\phi \approx \omega_{DR}$, and $\tau_{\beta_2} \approx \tau_r$).
 2. Fix ζ_ϕ , ω_ϕ , and τ_{β_2} at the values obtained in step b.1. Start all other parameters from their step b.1 values and obtain a new match.

NADC-83116-60

At this point, all the parameters could be started at the results of step b.2 and freed in the matching algorithm to obtain a final match. However, the matching technique did not always provide a unique solution. In addition, the computational effort expended was not justified by the small mismatch improvement generally obtained. Therefore, the technique utilized was to terminate the matching procedure after step b.2 and compare those resulting equivalent parameters with the MIL-F-8785C requirements.

In performing these matches, the "goodness of fit" was determined quantitatively by the value of the mismatch parameter and qualitatively from Bode plots and time history responses to unit impulse and step control inputs. Although no minimum value of mismatch has been conclusively established, several guidelines have been proposed. Hodgkinson (reference c), initially recommended that a good match is obtained when the mismatch function is less than or equal to 10. In a limited experimental effort by Smith (reference o), pilot ratings were correlated with various levels of mismatch. These results indicated that pilots were insensitive to analytical mismatches up to 200 in the frequency range of 0.1 to 10.0 radians/second.

RESULTS AND DISCUSSION

GENERAL

Approximate and complete lateral directional equivalent system models were determined for the A-6, A-7, S-3, F-14, and F-18 airplanes. Each of these airplanes incorporates rate and/or acceleration feedback for stability augmentation. The A-7, F-14 and F-18 airplanes include forward loop control augmentation. Similar techniques were utilized to obtain the equivalent system matches for each of these airplanes.

In general, acceptable equivalent system models were developed for each of these aircraft. The greatest difficulties were experienced for those configurations with forward loop prefilter like components whose frequencies lie in the range of 0.1 – 10 rad/sec. The purpose of these prefilters is to provide attenuation of high frequency inputs. The overall effect is to impose both an attenuation and a lag on the system response. The equivalent system model reflects this effect via a modified modal response parameter and a significant increase in time delay.

Comparisons of the equivalent system parameters with the specification requirements of reference (c) resulted in Level 1 flying qualities for all but a few cases. At .3M, the A-7 equivalent roll mode time constant exceeds the Level 1 boundary. Also, the F-18 configuration investigated exceeds the roll numerator time delay requirement of 0.10 seconds.

EQUIVALENT SYSTEM MODELS

The emphasis in lateral directional equivalent systems matching has been centered on the roll and sideslip responses, the parameters of which are necessary for comparison with the requirements of MIL-F-8785C. Initial matches were obtained for the roll and sideslip angle responses to pilot control input transfer functions for the S-3 and A-6. In general, these configurations were characterized by the bare airframe augmented by control surface actuators and rate feedbacks. From these configurations, a basic understanding of the frequency response matching process was obtained. Subsequently, the effect of compounding dynamic components such as lateral acceleration feedback and forward loop lags were investigated for the A-7, F-14, and F-18 aircraft.

S-3 Airplane

The S-3 airplane's lateral directional control system utilizes feedback from the yaw rate gyro to augment the aircraft's basic Dutch roll characteristics. The resulting roll and sideslip angle responses to pilot control inputs can be represented by fifth and sixth order numerators, respectively, over an eighth order denominator. The feedback components add a numerator and denominator root in the vicinity of 0.35 rad/sec while the actuator adds a single denominator root at approximately 22 rad/sec in the lateral axis and 29 rad/sec in the directional axis. Because of the proximity of the added feedback roots, they effectively cancel each other while the actuator roots are outside the pilot's frequency range of interest. Approximate pole-zero cancellation of roots within the frequency range of interest results in a transfer function similar in form to that of the desired equivalent system. It is therefore expected that a close match of the higher order system will be obtained.

The McAir recommended matching procedure was utilized with the NAVFIT and LATFIT computer programs to determine an equivalent system for each of the flight conditions analyzed. Both the approximate and complete forms of the roll and sideslip angle transfer functions were used. The following discussion will focus on a representative case analyzed for the S-3 aircraft to demonstrate the matching procedures.

The equivalent system parameters, along with the high order system values, for the S-3 aircraft at 15,000 ft and 0.36M are shown in table II. The approximate forms (trials 1 and 2) yield good matches of roll mode time constant and Dutch roll frequency and damping ratio when compared to the high order system values. Equivalent time delays are acceptable and mismatch values are relatively low. The frequency and time responses for the high-order and low-order equivalent systems are compared in figures 1 and 2. As indicated in these figures, the frequency responses are relatively well matched in the region from .1 to 10 rad/sec. This impression is confirmed by the excellent match of rise time on roll rate (roll mode time constant and control power combination) and the oscillatory response in sideslip angle (frequency and damping). There are however, minor differences between the high-and low-order responses; the equivalent steady state response does not decay with time (a result of the large mismatch exhibited at frequencies less than 0.1 rad/sec) and the oscillatory roll response is absent in the low-order system. These differences result from their not being modelled in the approximate forms. Matching the complete forms should improve both of these areas.

Improvements in the steady state response can be demonstrated by adding the low frequency roots to the equivalent system models and identifying the roots over an expanded frequency range. The equivalent models can then be represented as:

$$\frac{\phi}{\delta_{LAT}} = \frac{K_{\phi} e^{-t_{\phi}s}}{(s + 1/\tau_r)(s + 1/\tau_s)} \quad (11)$$

$$\frac{\beta}{\delta_{PED}} = \frac{K_{\beta} (s + 1/\tau_{\beta_1}) e^{-t_{\beta}s}}{(s + 1/\tau_s)(s^2 + 2\zeta_{DR}\omega_{DR}s + \omega_{DR}^2)} \quad (12)$$

Expanding the frequency match range to encompass the added low frequency breakpoints, the results presented in trials 3 and 4 of table II were obtained. In the case of the roll response, the NAVFIT program was used, with arbitrary initial parameter values, to obtain the results shown. However, in the case of the sideslip response, it was necessary to utilize the identified roll mode spiral root as a starting point, in the NAVFIT program, in order to obtain satisfactory results.

The mismatch between the high-and low-order system roll response was greatly improved, as shown in figure 3. The only remaining discrepancy between the two systems is now the absence of the oscillatory component in the low order response. The differences in the high- and low-order sideslip response are now almost imperceptible, as shown in figure 4.

Having demonstrated the ability to identify the low frequency roots, and the associated mismatch improvement, τ_s and τ_{β_1} were fixed at their known high-order values in all subsequent runs in order to simplify the matching process.

The complete form equations were used in an attempt to further improve the response matches in the mid frequency range. In this case, independently matching the roll or sideslip angle responses was difficult due to the proximity of several numerator and denominator roots. The oscillatory roll angle response roots $[\zeta_{\phi}, \omega_{\phi}]$ and $[\zeta_{DR}, \omega_{DR}]$ were close enough to prevent the search algorithm from identifying realistic values. Similar difficulties were also encountered for the sideslip angle response due to the proximity of a sideslip numerator constant (τ_{β_2}) and the roll mode time constant (τ_r). This difficulty was overcome (trials 5 and 6 of table II) by fixing the parameters ζ_{ϕ} , ω_{ϕ} , and τ_{β_2} at their high order system values or starting them very close to these values. The resulting match statistics indicate a decrease in both the roll and sideslip mismatch.

TABLE II
 S-3 AIRPLANE EQUIVALENT TRANSFER FUNCTIONS
 Roll and Sideslip Angle Response to Cockpit Control Inputs
 Configuration CR 15,000 ft 0.36M

PARA-METER	HOS VALUES	APPROXIMATE FORMS										COMPLETE FORMS										SIMUL-TANEOUS ϕ & β
		INDEPENDENT					INDEPENDENT					INDEPENDENT					INDEPENDENT					
		P	β	ϕ	β	ϕ	β	ϕ	β	ϕ	β	ϕ	β	ϕ	β	ϕ	β	ϕ	β			
TRIAL #		1	2	3	4	5	6	7	8	9	10											
ORDER	-	0/1	0/2	0/2	1/3	2/4	3/4	2/4	3/4	2/4	3/4	3/4	2/4	3/4	2/4	3/4	2/4	3/4	2/4 & 3/4	11		
FREQUENCY RANGE	-	.1 - 10.	.1 - 10.	.001 - 10.	.001 - 10.	.1 - 10.	.001 - 10.	.001 - 10.	.001 - 10.	.1 - 10.	.1 - 10.	.001 - 10.	.001 - 10.	.1 - 10.	.1 - 10.	.1 - 10.	.1 - 10.	.1 - 10.	.1 - 10.	0.1 - 10.		
K_ϕ	290.2	58.3		58.4		51.5							55.4			52.0				53.9		
ζ_ϕ	0.38	-				0.38*							0.37			0.47				0.37		
ω_ϕ	1.99	-				1.99*							2.14			2.05				2.00		
t_ϕ	-	0.069		0.072		0.056							0.063			0.056				0.060		
K_β	11.35		24.4		24.1		0.384						0.371							0.384		
τ_{β_1}	-60.64				-62.54		-60.64*						-60.64*							-60.64*		
τ_{β_2}	0.390						0.390*						0.320							0.400		
τ_{β_3}	0.015						0.015*						0.015*							0.015*		
t_β	-		0.013		0.015		0.034						0.031							0.034		
τ_r	0.38	0.312		0.305			0.384						0.312*							0.355		
τ_s	166.69			160.6	161.4		166.69*						166.69*							166.69*		
ζ_{DR}	0.31		0.28		0.28		0.29						0.28*							0.29		
ω_{DR}	2.11		2.14		2.15		2.10						2.14*							2.08		
M_ϕ	-	18.2		9.1		1.2							2.9			0.9				1.8		
M_β	-		14.8		2.5		2.2						3.2							2.2		

* Fixed parameter
 (Note: See Appendix B for summary of all flight conditions.)

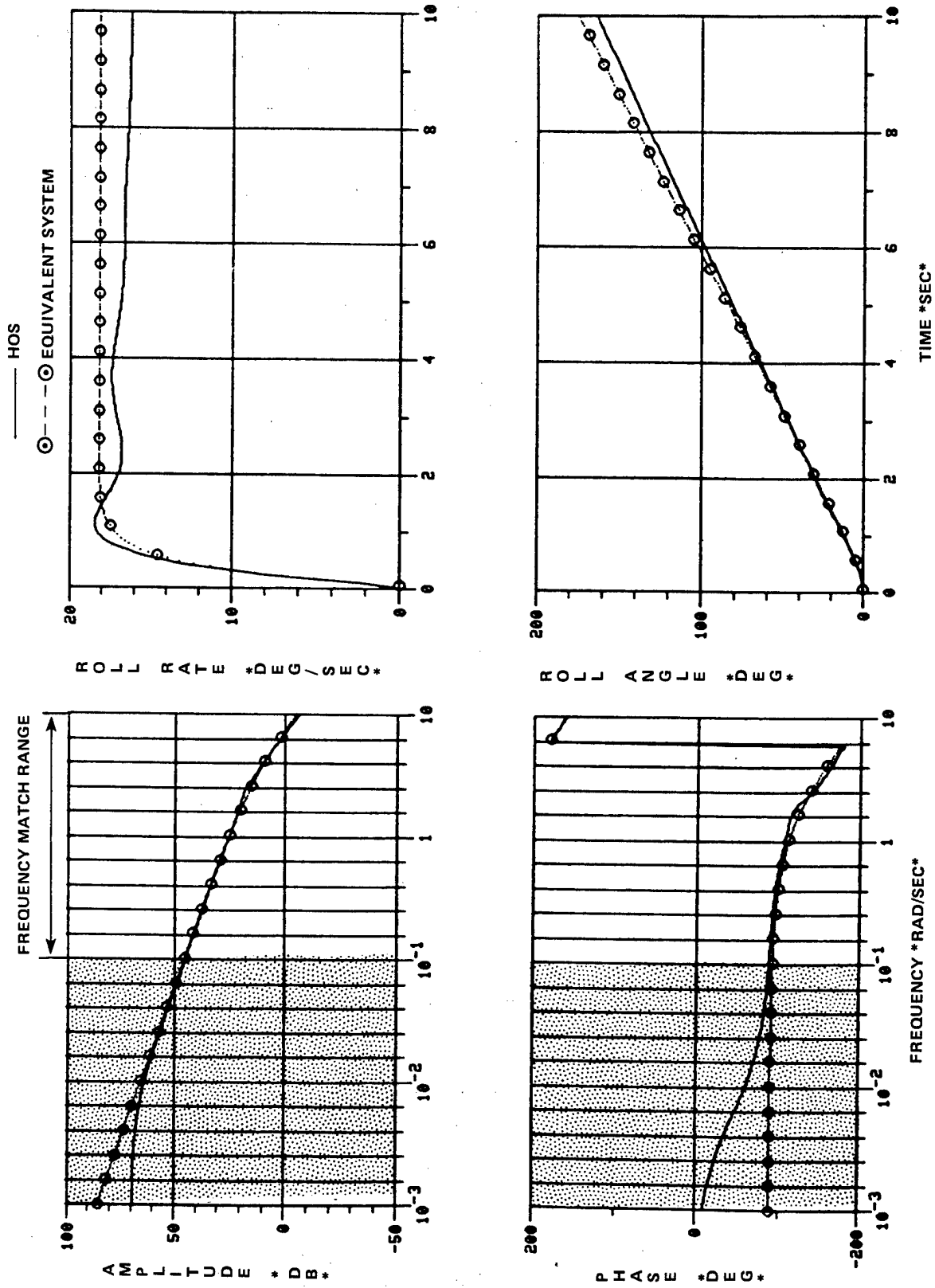


Figure 1. S-3 Roll Response - Approximate Form (Trial 1)

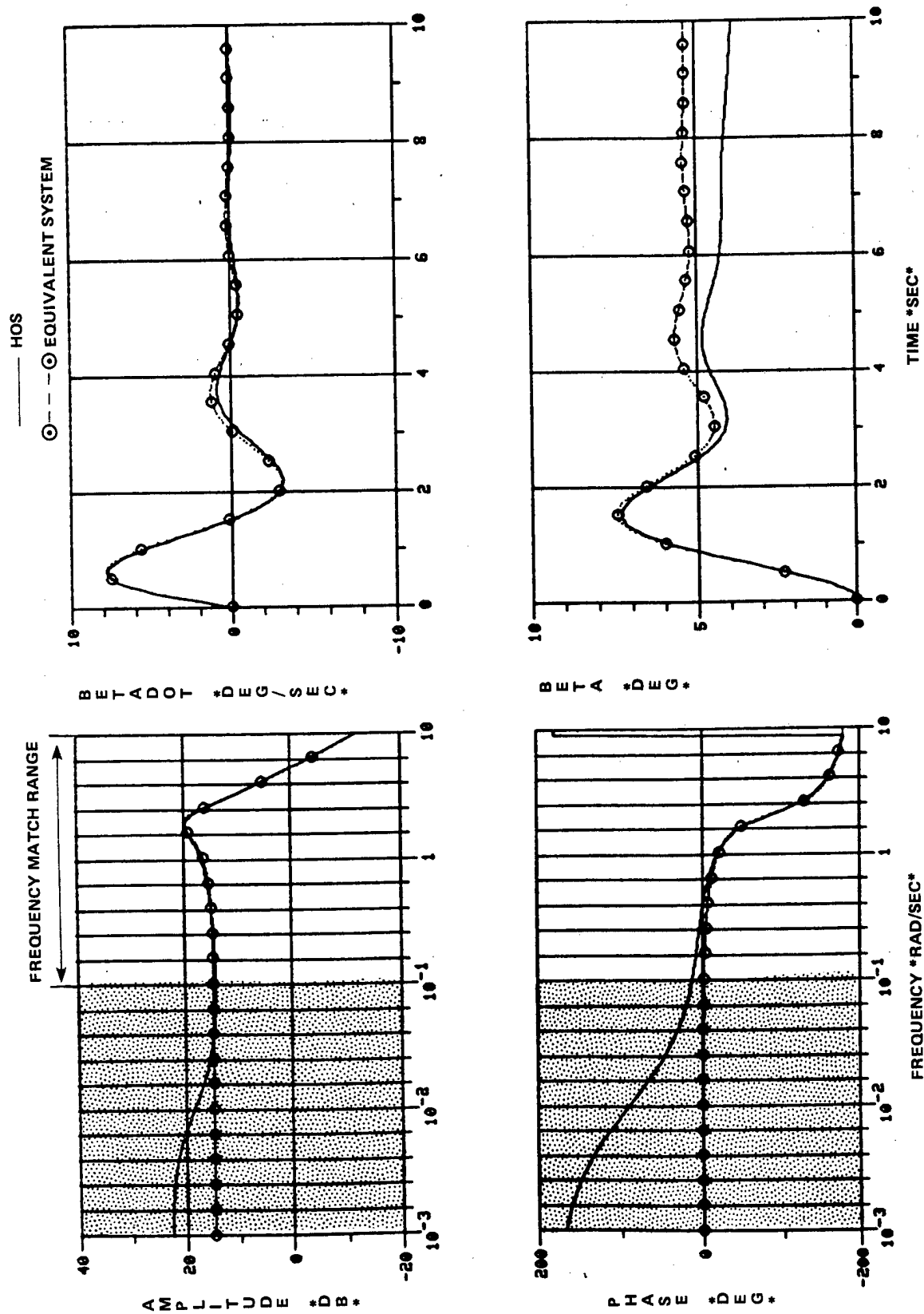


Figure 2. S-3 Sideslip Response - Approximate Form (Trial 2)

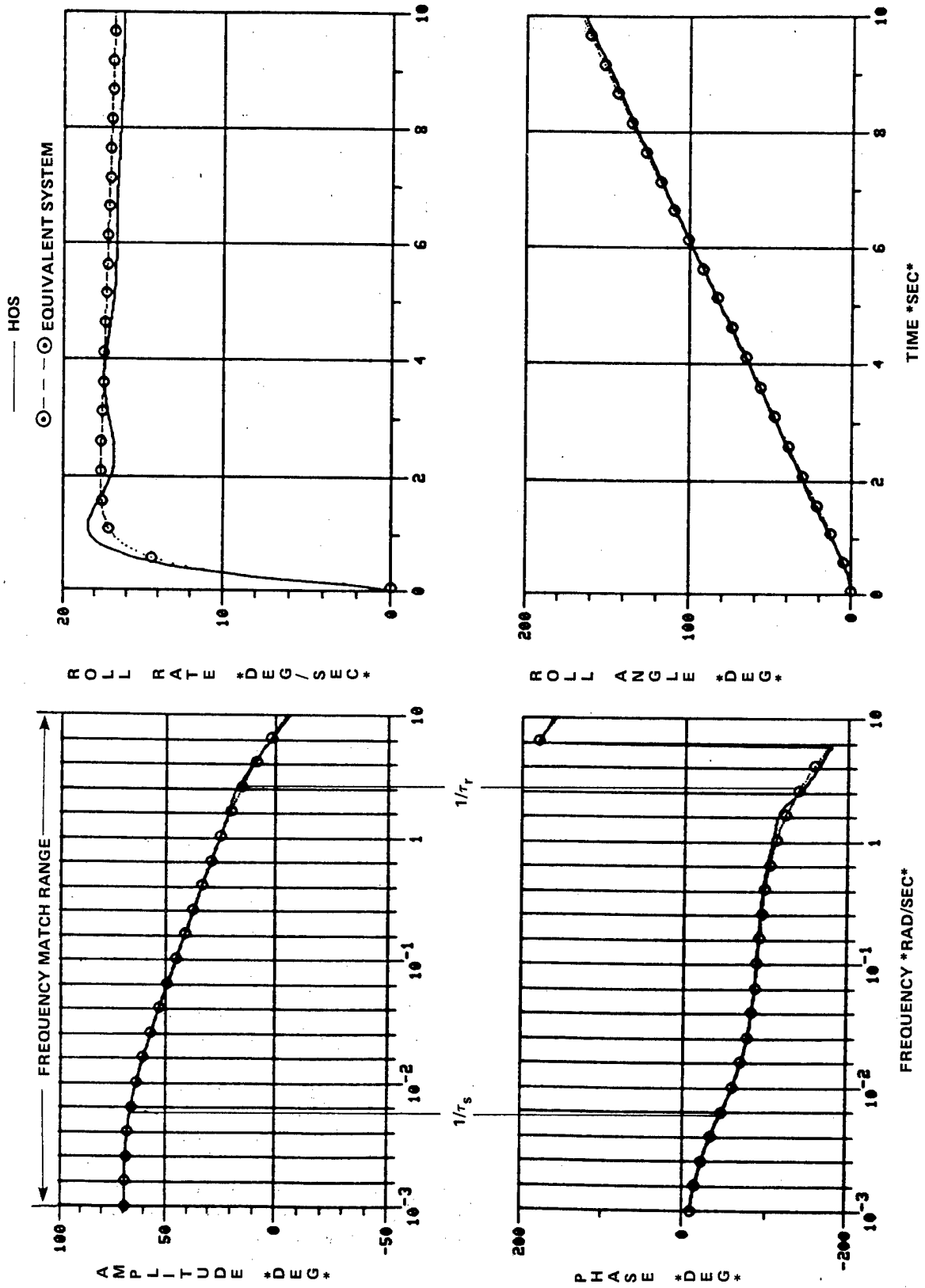


Figure 3. S-3 Roll Response — Approximate Form Plus Low Frequency Root (Trial 3)

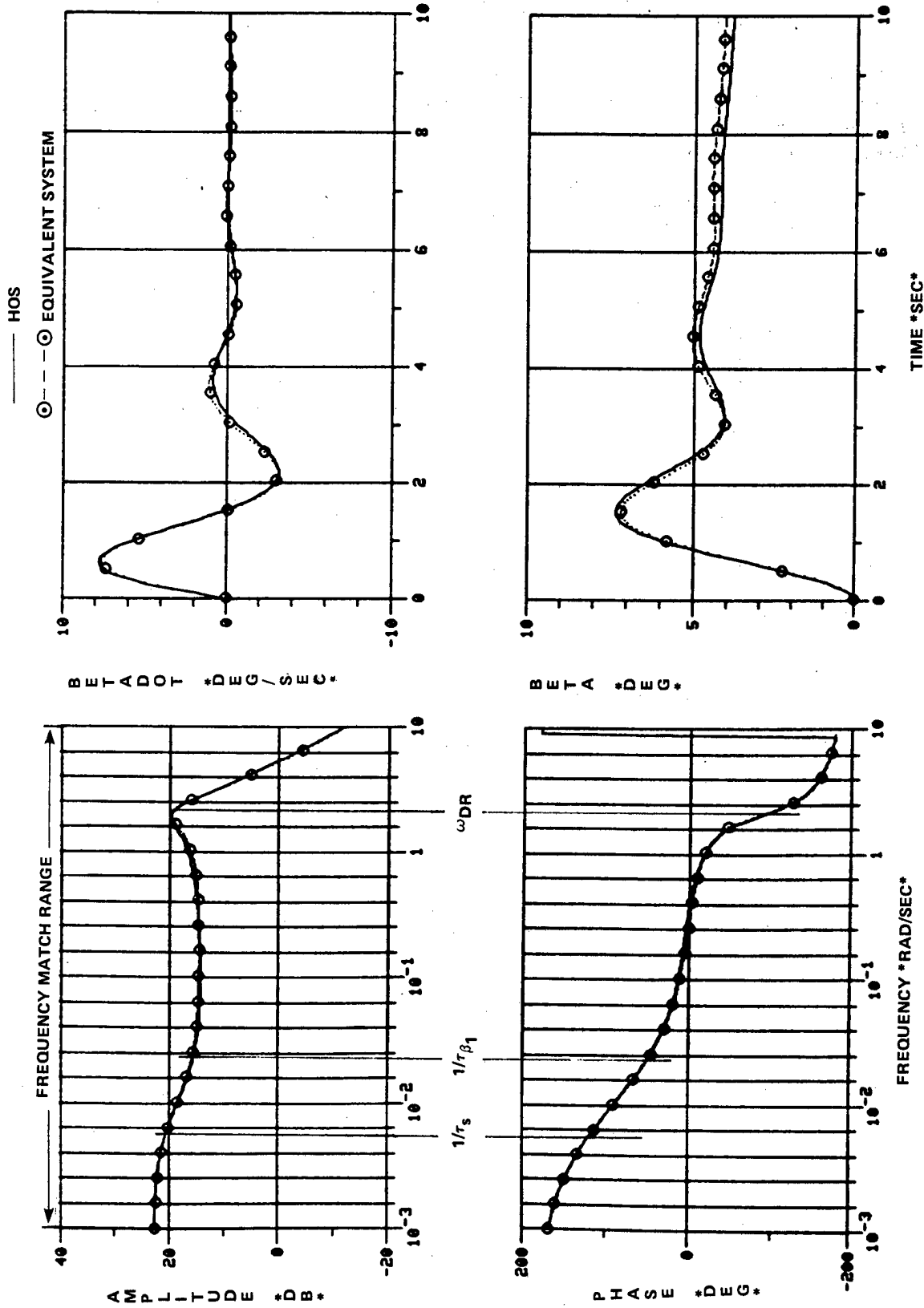


Figure 4. S-3 Sideslip Response - Approximate Form Plus Low Frequency Roots (Trial 4)

Also evident is that the roll mode time constant identified for each case closely agrees with the high order system value. This technique, however, requires apriori knowledge of the high order system modal parameters, which may not always be available.

The lack of apriori knowledge of the high order system numerator roots can be avoided by either 1) fixing the denominator values at the identified approximate form results and performing the required match, or 2) simultaneously matching roll and sideslip angle responses while constraining the equivalent denominators to be identical. The first procedure is demonstrated in trials 7 and 8 of table II. The results obtained show only slight variations from those obtained by identifying denominator roots with the numerator roots held fixed. Then beginning with the roots at these latest locations, it was possible to free all parameters, as demonstrated in trials 9 and 10 of table II.

In the second procedure, the Dutch roll roots, easily identified from the sideslip response, helped to locate the roll angle numerator roots while the roll mode time constant, easily identified from the roll angle response, helped to locate the sideslip numerator root. The results for this procedure are presented in the final column of table II. Excellent agreement was obtained between all high- and low-order modal parameters investigated along with extremely low values of mismatch. Frequency and time responses for the simultaneous matching procedure are presented in figures 5 and 6. Excellent agreement is shown between the high- and low-order systems with the oscillatory component of the roll response now being identified.

The approximate and complete form sideslip angle results provide additional insight into the time delay parameter. In the approximate form, the time delay accounts for the total phase lag imparted by high frequency roots, whereas in the complete system, a high frequency aircraft numerator root ($1/\tau\beta_3$) is included in the equivalent model. Since this numerator root adds high frequency phase lead, the complete form time delay has been increased in order to match the overall high frequency phase characteristics. The approximate time delay can therefore be interpreted as representing the overall aircraft/control system lag experienced by the pilot, while the complete system time delay represents the time delay contribution arising from the control system.

The equivalent system models obtained for the S-3 airplane flight conditions investigated are summarized in Appendix B.

A-6 Airplane

The A-6 airplane utilizes both roll rate and yaw rate feedbacks to augment the aircraft's basic lateral-directional stability characteristics. The resulting control system descriptions add numerator and denominator roots in the vicinity of 0.2 to 0.5 rad/sec while the flaperon and rudder actuators add denominator roots at approximately 19.6 and 27.0 rad/sec, respectively.

The following discussion is for a representative flight condition (0.40M, 20,000 ft altitude) for the A-6 airplane. Results for all flight conditions analyzed are summarized in Appendix B.

Transfer functions describing the airplane's roll and sideslip angle responses to pilot control inputs can be represented by fifth and sixth order numerators, respectively, over an eighth order

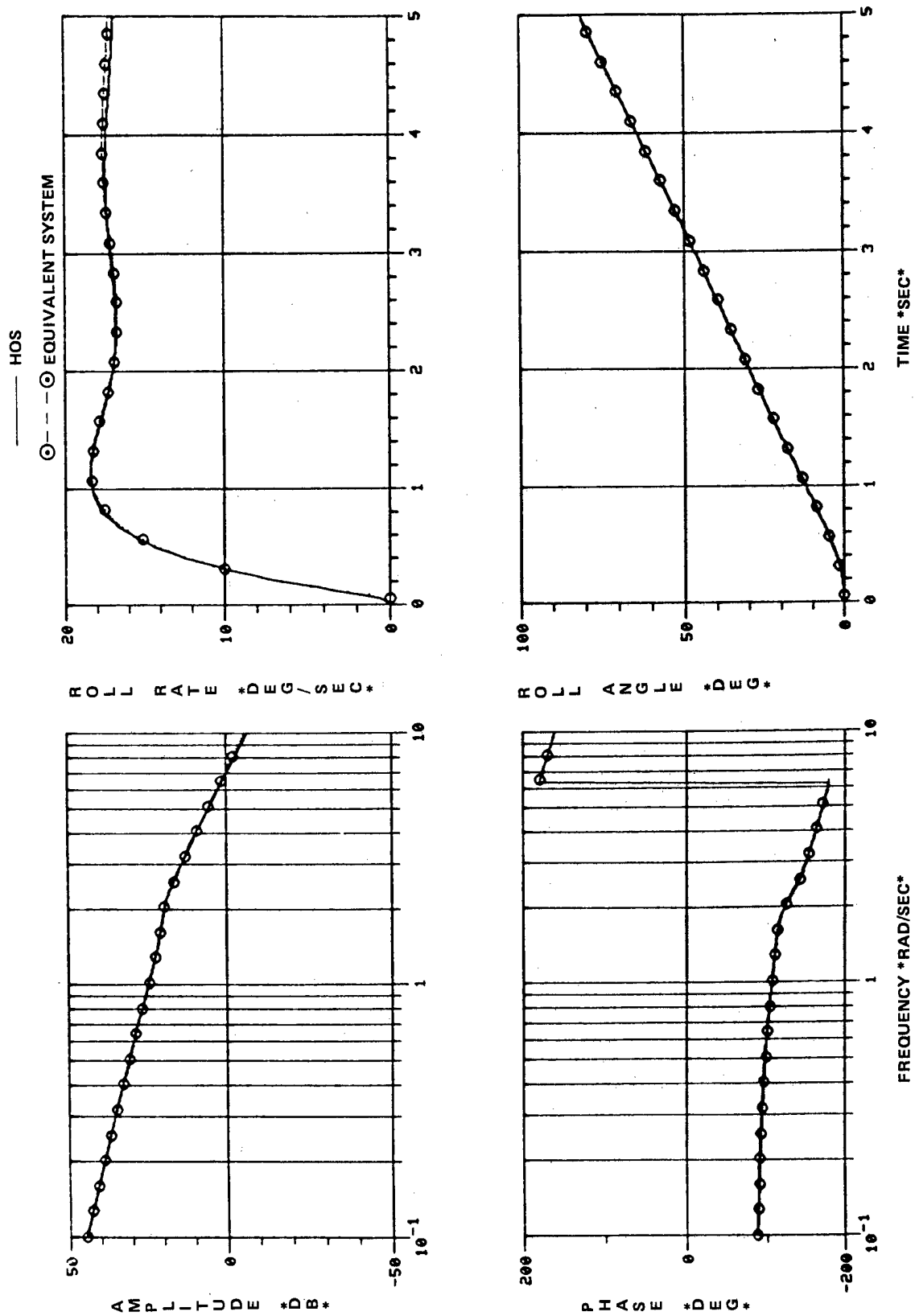


Figure 5. S-3 Roll Response - Simultaneous Match

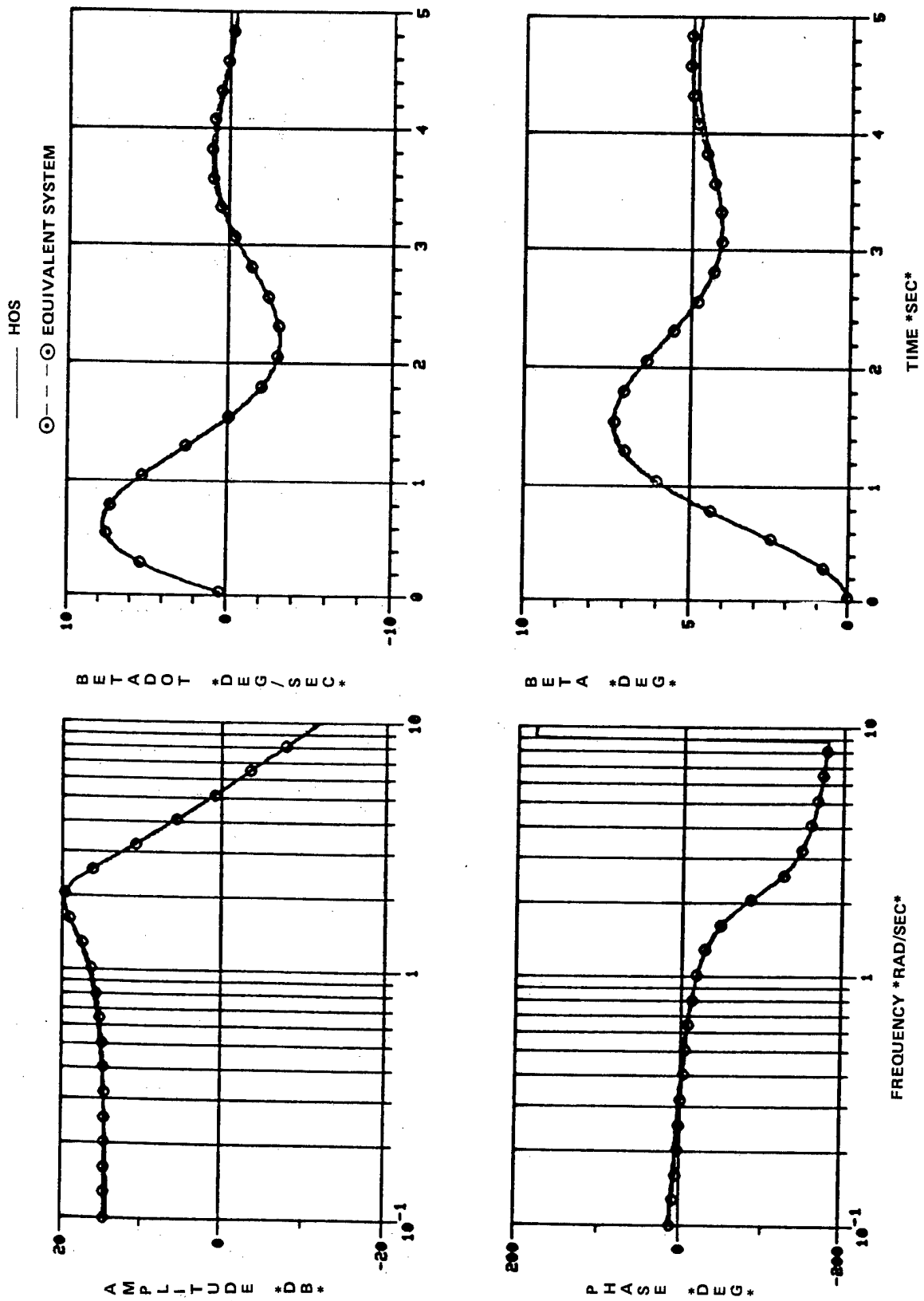


Figure 6. S-3 Sideslip Response — Simultaneous Match

denominator. Inspection of the high-order system roots in the frequency range of interest yields the following observations:

- a) Utilizing approximate pole-zero cancellation, only one significant numerator, and two significant denominator roots remain in the roll rate transfer function. The effect of these roots is to provide magnitude attenuation of 20 db per decade of frequency and a high frequency phase lag approximately 90 deg less than that at low frequencies. Since these are the same response characteristics exhibited by the low order system model it can be expected that an equivalent system match can be readily determined.
- b) Applying approximate pole-zero cancellation to the sideslip response, only a single pair of oscillatory denominator roots remains in the frequency range of interest. Since the form of the low order system is identical to this representation of the high order system, an excellent sideslip angle match is anticipated.

These observations are borne out in the equivalent system results presented in table III.

Good matches of both the roll rate and sideslip angle responses via the approximate forms were obtained, as shown in figures 7 and 8.

The complete form matching technique results are similar to those obtained for the S-3 airplane. In the case of the independent response parameter matching technique it was again necessary to fix ζ_ϕ and ω_ϕ at their high order system values. Significant differences are noted between the bank and sideslip angle results for τ_r and ζ_{DR} , while ω_{DR} shows only minor differences.

In order to obtain a consistent set of modal parameters, it was necessary to simultaneously match both bank and sideslip angle responses, while constraining the identified denominators to be identical. The numerator parameters, ζ_ϕ , ω_ϕ and τ_{β_2} were again allowed to go free in the matching process. The results, presented in table III, are seen to be a compromise on the individually determined low-order systems — the mismatch values are increased and the denominator parameters, τ_r , ζ_{DR} , and ω_{DR} lie near the values obtained for the independent matching technique. Figures 9 and 10 show the frequency and time responses for these simultaneous matches.

The mismatch values for both the approximate and complete forms are higher than those obtained for the S-3 airplane. The question of acceptable mismatch was addressed by Smith, Hodgkinson, and Snyder (reference p). Based on limited experimental data, they concluded that pilot ratings were insensitive to analytical mismatch values up to 190. Since the maximum value obtained for the A-6 airplane was 145.4, these matches were considered to be acceptable. Figures 7 and 8 show the frequency and time responses for the approximate forms and graphically illustrate these levels of mismatch.

A-7 Airplane

The A-7 airplane utilizes forward path compensation as well as yaw and roll rate feedback, as described in Appendix A, to augment the aircraft's basic stability characteristics. The roll and sideslip angle responses to pilot control inputs can be represented by seventh and tenth order numerators, respectively, over twelfth order denominator transfer functions. The forward mechanical path includes feel system components which introduce first order roots at approximately 12 rad/sec. The electrical, or command augmentation, feed forward path includes prefilter type components at 3 and 10 rad/sec. The 3 rad/sec root lies well within the frequency range of interest and could be expected to cause problems in obtaining an equivalent system match. The feedback components

TABLE III

A-6 AIRPLANE EQUIVALENT TRANSFER FUNCTIONS
 Roll and Sideslip Angle Response to Cockpit Control Inputs
 CR 20,000 FT 40 M

	HOS VALUES	APPROXIMATE FORM		COMPLETE FORM		
		INDEPENDENT		INDEPENDENT		SIMULTANEOUS
		P	β	ϕ	β	ϕ & β
K_ϕ	17.84	.670	—	.702	—	.646
ζ_ϕ	.283	—	—	.283*	—	.194
ω_ϕ	1.77	—	—	1.77*	—	1.56
t_ϕ	—	.0076	—	.018	—	.0077
K_β	.0078	—	.0293	—	.0003	.0003
$\tau_{\beta 1}$	-131.58	—	—	—	-131.58*	-131.58*
$\tau_{\beta 2}$.148	—	—	—	.172	.692
$\tau_{\beta 3}$.010	—	—	—	.010*	.010*
t_β	—	—	.025	—	.034	.042
τ_r	.156	.461	—	.767	.181	.642
τ_s	105.26	—	—	105.26*	105.26*	105.26*
ζ_{DR}	.269	—	.251	.465	.258	.299
ω_{DR}	1.73	—	1.736	2.17	1.74	1.71
M_ϕ	—	145.4	—	101.0	—	121.8
M_β	—	—	4.4	—	.46	4.2

*Fixed parameter

(Note: See Appendix B for summary of all flight conditions)

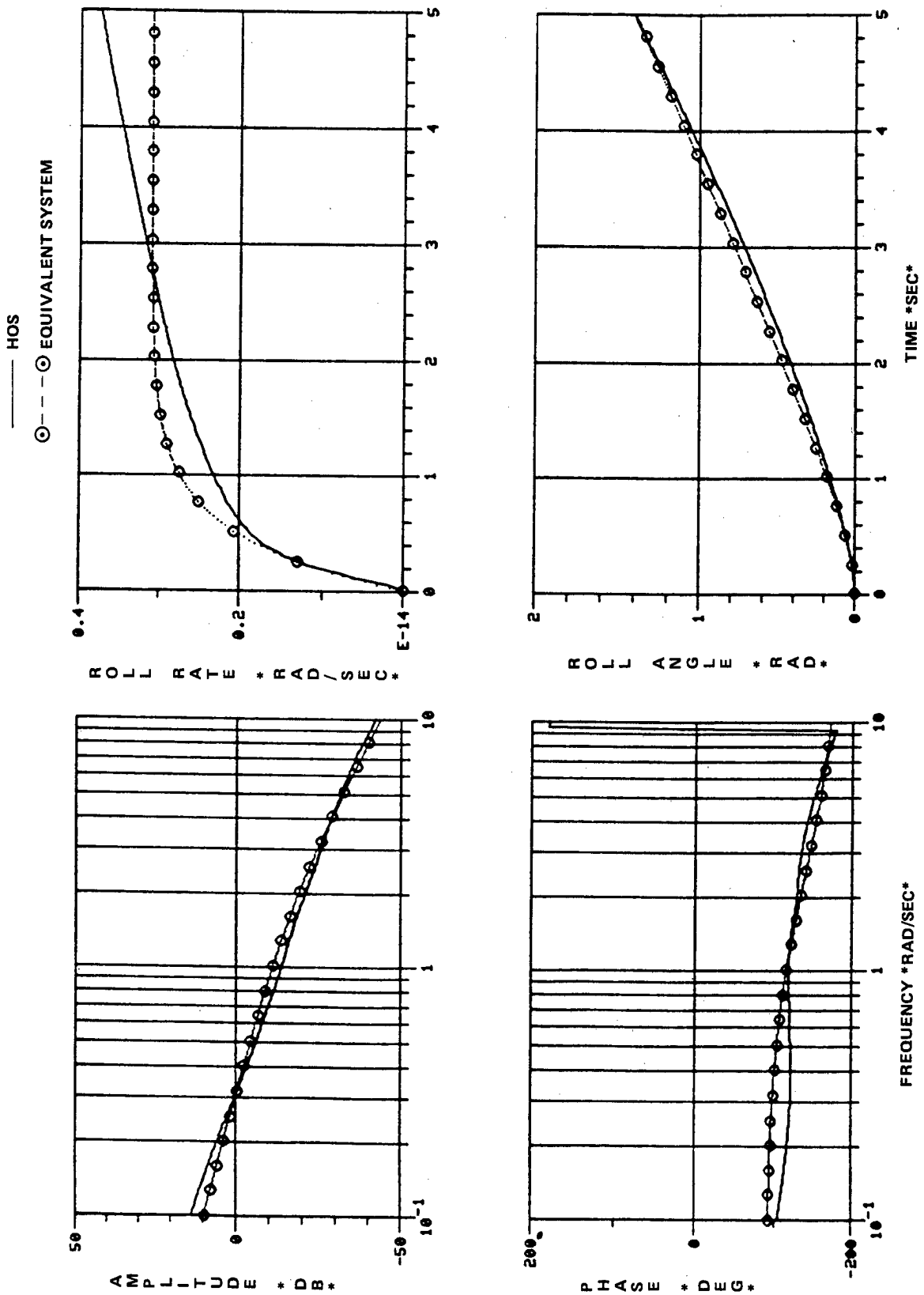


Figure 7. A-6 Roll Response — Approximate Form

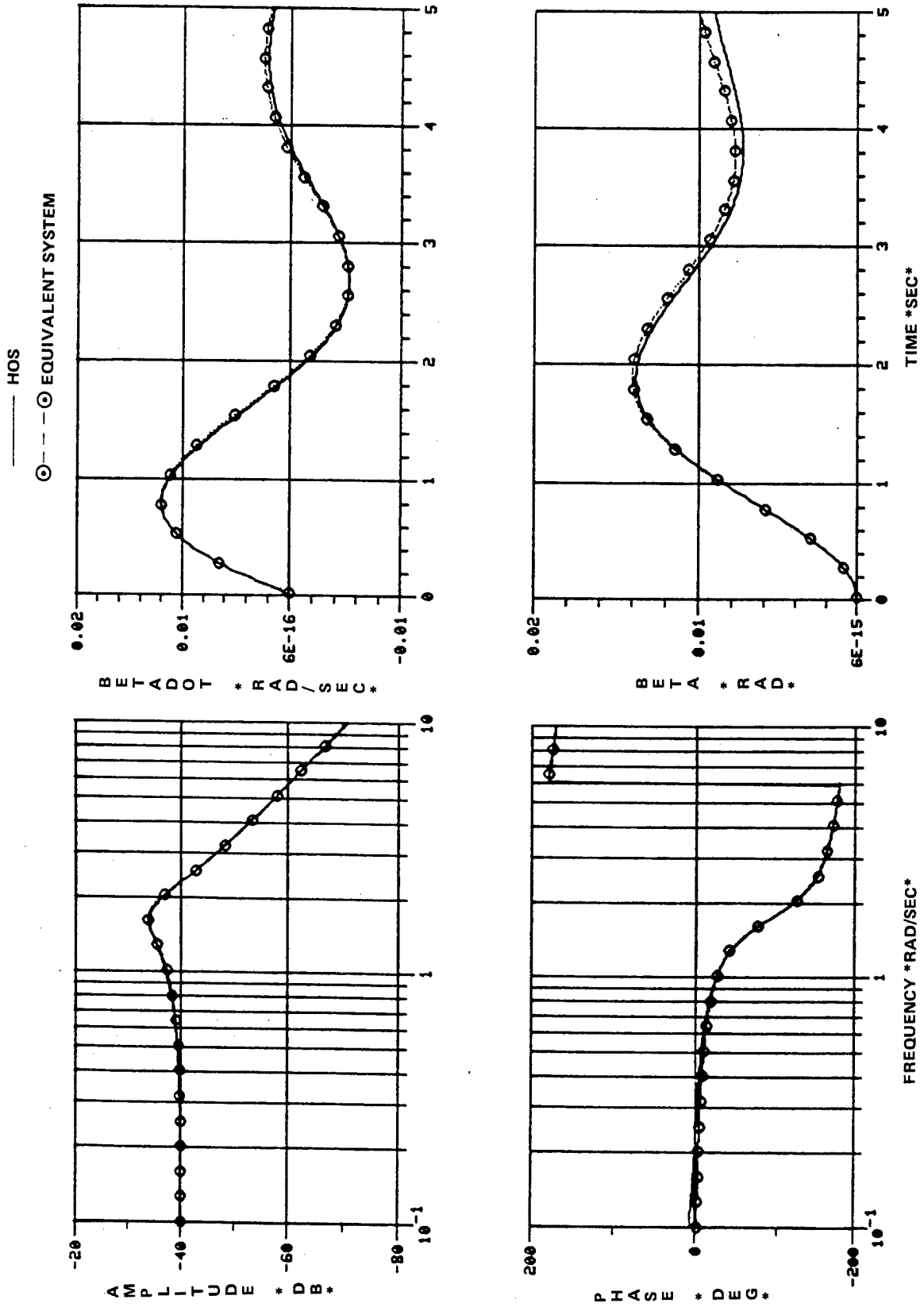


Figure 8. A-6 Sideslip Response — Approximate Form

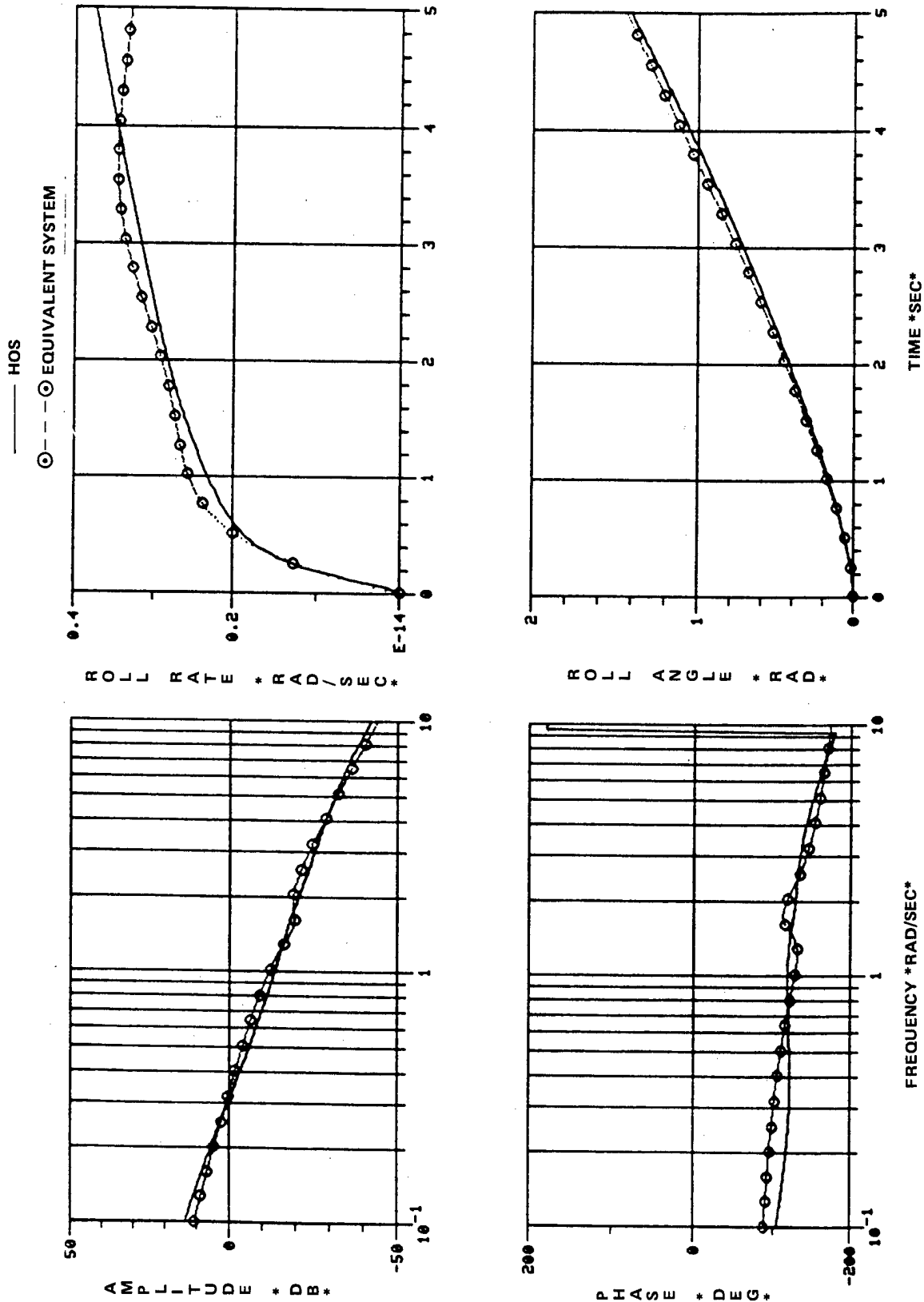


Figure 9. A-6 Roll Response — Simultaneous Match

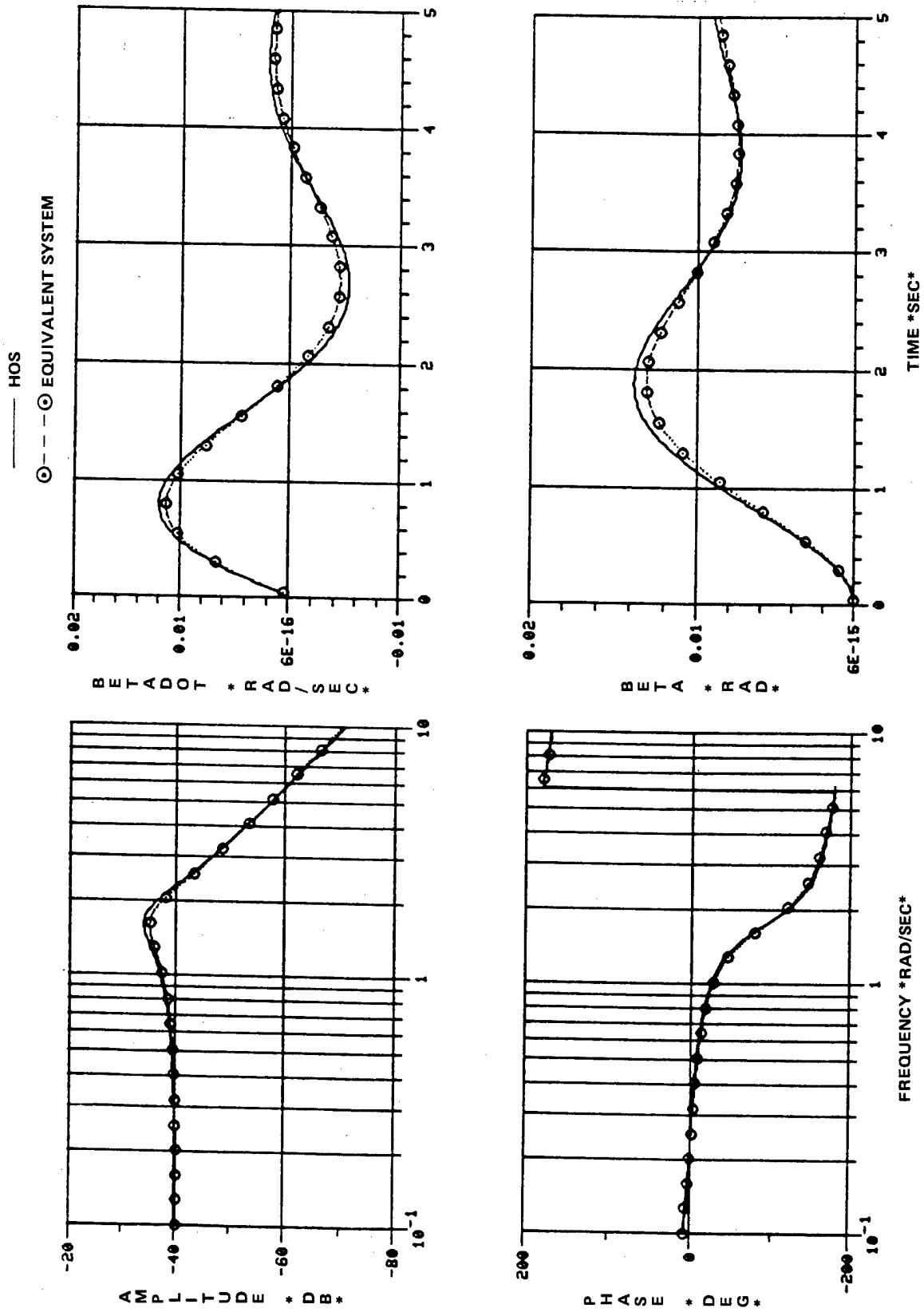


Figure 10. A-6 Sideslip Response — Simultaneous Match

add numerator and denominator roots in the vicinity of both 1 and 31 rad/sec, which approximately cancel each other. In addition, the surface actuators add denominator roots at approximately 20 rad/sec, which are outside the frequency range of interest.

The following discussion is for a representative flight condition at 0.6 Mach and 15,000 ft altitude. The results for all A-7 conditions analyzed are summarized in Appendix B. This discussion is divided into the results with and without the control augmentation path prefilters, as significant differences were obtained.

Table IV summarizes the results obtained for the A-7 aircraft at 15,000 ft and 0.60 M without the control augmentation path prefilters. Using the approximate forms for the low order system, good match statistics were obtained when compared to the high order system values. Roll mode time constant shows excellent agreement, while Dutch roll frequency and damping ratio show only minor differences. The mismatch function was relatively low for both the roll and sideslip angle responses.

Frequency and time response comparisons for the approximate forms are presented in figures 11 and 12. The only significant differences occur in the steady state portions of the responses which may be attributed to the lack of a spiral mode root in the equivalent systems.

The complete form results are also shown in table IV. Again, ζ_ϕ , ω_ϕ , and τ_{β_2} had to be either fixed at or started very close to their high order system values. If these parameters were not fixed, their resulting values were not unique but rather varied as their initial value varied. This was especially true of the roll angle response as show in table V. Unique values for τ_{β_1} and τ_r could be determined when matching sideslip angle along, but only after a very large number of iterations had been completed.

This difficulty was overcome by simultaneously matching the roll and sideslip angle responses as was previously done for the S-3 and A-6 aircraft. Table IV presents the results of this simultaneous match for the A-7 and indicates good match statistics. The mismatch functions are very low while the modal parameters are very close to the high order system values. Frequency and time history responses for these results are shown in figures 13 and 14. There is essentially no difference between the high order and the low order equivalent systems. The steady state responses identified with the simultaneous matching technique show a significant improvement when compared to the approximate form (figures 11 and 12).

The inclusion of the roll command augmentation in the forward loop had a significant impact on both the commanded response and the equivalent system model. The purpose of the prefilters is to provide attenuation of inputs at frequencies greater than approximately 3 rad/sec. The effect of this attenuation is to impose a lag in the roll response to step control inputs as shown in figure 15.

Approximate pole-zero cancellation of the high order bank angle response, in the frequency range of interest, results in a second over fifth order transfer function. Since this representation is different from that of the equivalent models, difficulties in obtaining an equivalent system match can be anticipated. The additional phase lag introduced by the command augmentation prefilters is accounted for in the equivalent system model via the time delay. However, since there are also gain modifications resulting from the prefilters in the frequency range of interest, which are not accounted for in the equivalent system model, the resulting equivalent system parameters are, at best, an average characteristic reflecting the contribution of aircraft and control system components. This condition is reflected in the equivalent system parameters for the A-7 aircraft as shown in table VI.

TABLE IV

A-7 AIRPLANT EQUIVALENT TRANSFER FUNCTIONS, NO PREFILTERS
 Roll and Sideslip Angle Response to Cockpit Control Inputs
 CR 15,000 FT. 0.6 M
 CONTROL AUGMENTATION OFF

	HOS VALUES	APPROXIMATE FORM		COMPLETE FORM		
		INDEPENDENT		INDEPENDENT		SIMULTANEOUS
		ϕ	β	ϕ	β	ϕ & β
K_ϕ	422.2	23.2	—	21.25	—	20.16
ζ_ϕ	.56	—	—	.56*	—	.449
ω_ϕ	2.02	—	—	2.02*	—	1.92
t_ϕ	—	.053	—	.045	—	.040
K_β	.0011	—	.0061	—	.000066	.000065
$\tau_{\beta 1}$	-1250.0	—	—	—	-1250.0*	-1250.0*
$\tau_{\beta 2}$.198	—	—	—	.195	.408
$\tau_{\beta 3}$.009	—	—	—	.009*	.009*
t_β	—	—	.032	—	.060	.058
τ_r	.20	.20	—	.23	.14	.25
τ_s	37.45	—	—	37.45*	37.45*	37.45*
ζ_{DR}	.49	—	.40	.49	.38	.39
ω_{DR}	2.03	—	2.29	2.06	2.15	2.01
M_ϕ	—	20.1	—	0.35	—	0.86
M_β	—	—	10.4	—	7.0	4.1

* Fixed parameter

(Note: See Appendix B for summary of all flight conditions)

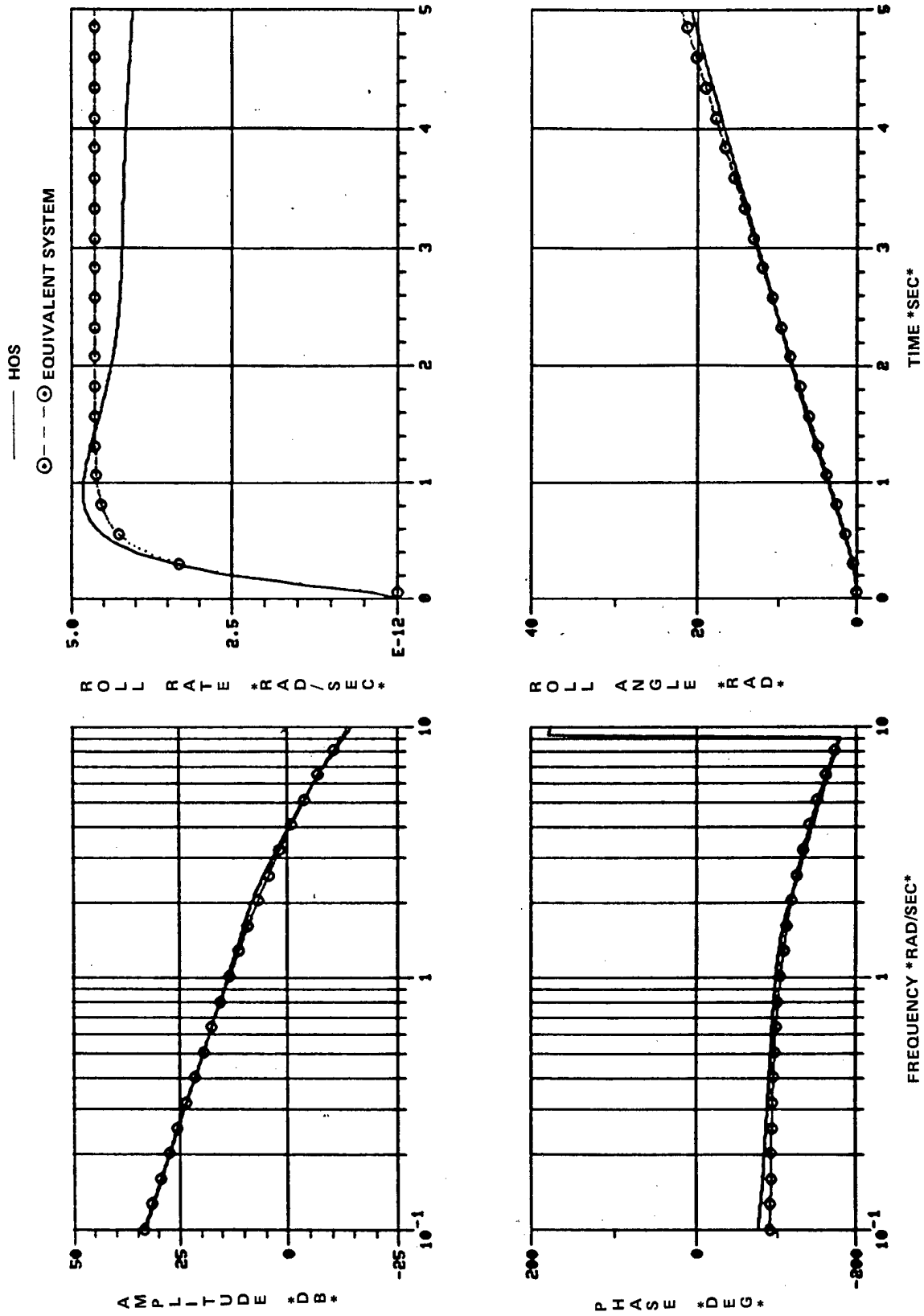


Figure 11. A-7 Roll Response - Approximate Form, No Control Augmentation

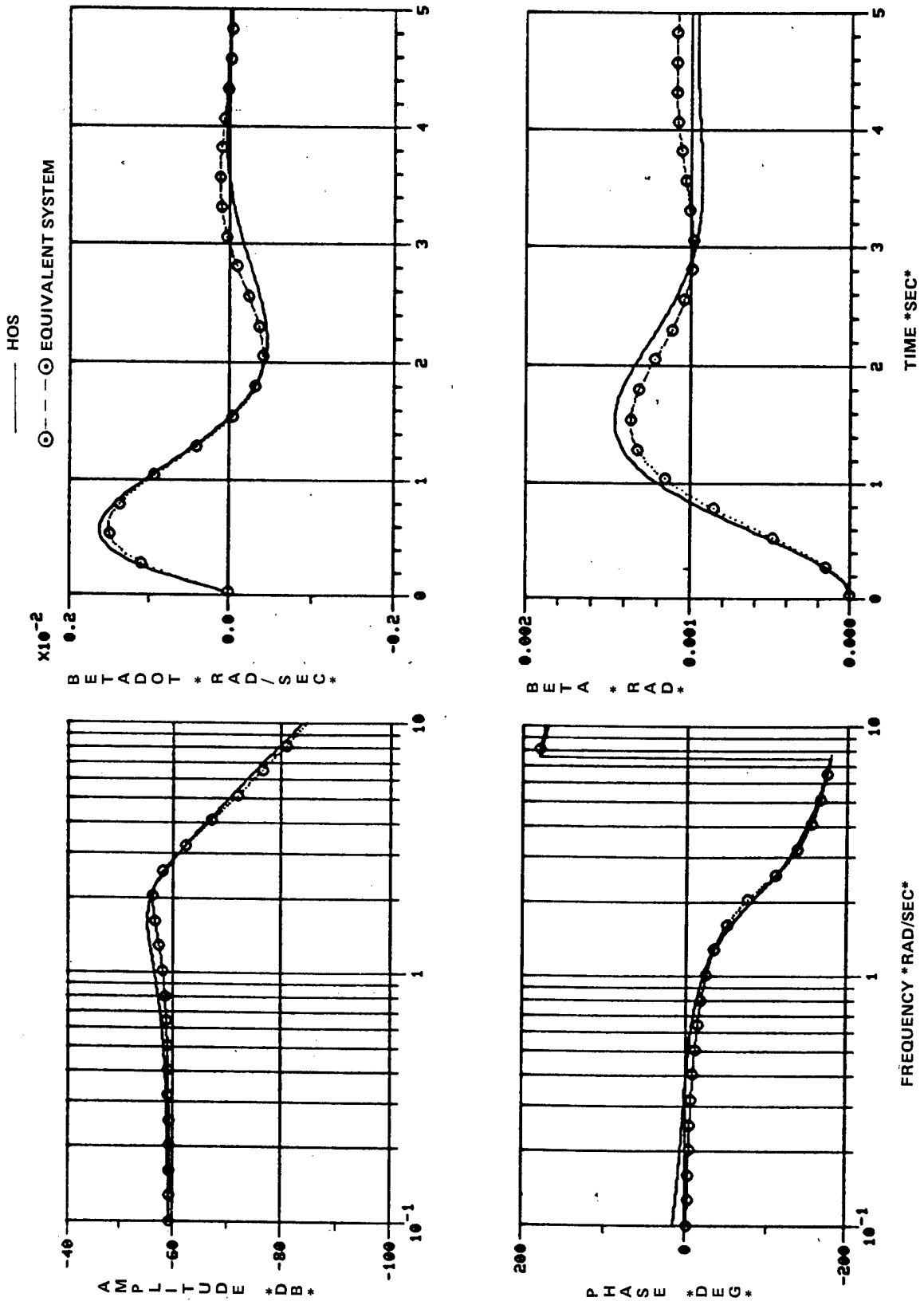


Figure 12. A-7 Sideslip Response — Approximate Form, No Control Augmentation

TABLE V

EFFECT OF INITIAL PARAMETER VALUES ON ROLL ANGLE MATCHING
 A-7 Airplane 0.6 Mach, 15,000 FT Altitude
 Control Augmentation Off

	HOS	APPROXIMATE	COMPLETE			
			INITIAL	FINAL	INITIAL	FINAL
K_ϕ	422.2	23.2	5.0	19.0	5.0	17.4
ξ_ϕ	.56	—	.20	1.26	.10	1.60
ω_ϕ	2.02	—	3.0	2.67	1.0	4.50
τ_r	.20	.20	.25	.59	.25	.38
ξ_{DR}	.49	—	.35	.96	.35	1.22
ω_{DR}	2.03	—	2.5	4.20	2.5	5.39
t_ϕ	—	.053	.05	.036	.05	.032
M_ϕ	—	20.1	—	0.39	—	0.35

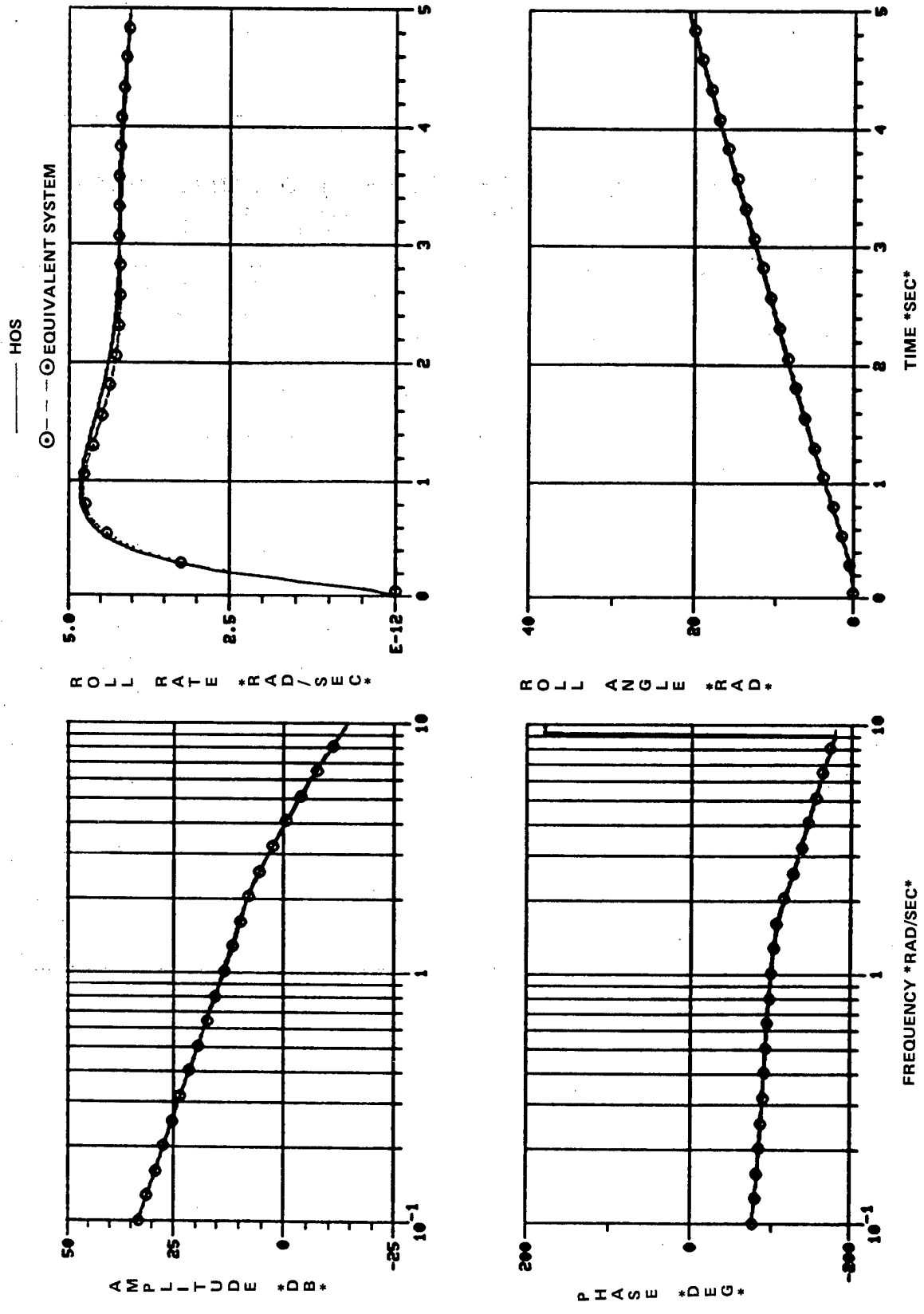


Figure 13. A-7 Roll Response — Simultaneous Match, No Control Augmentation

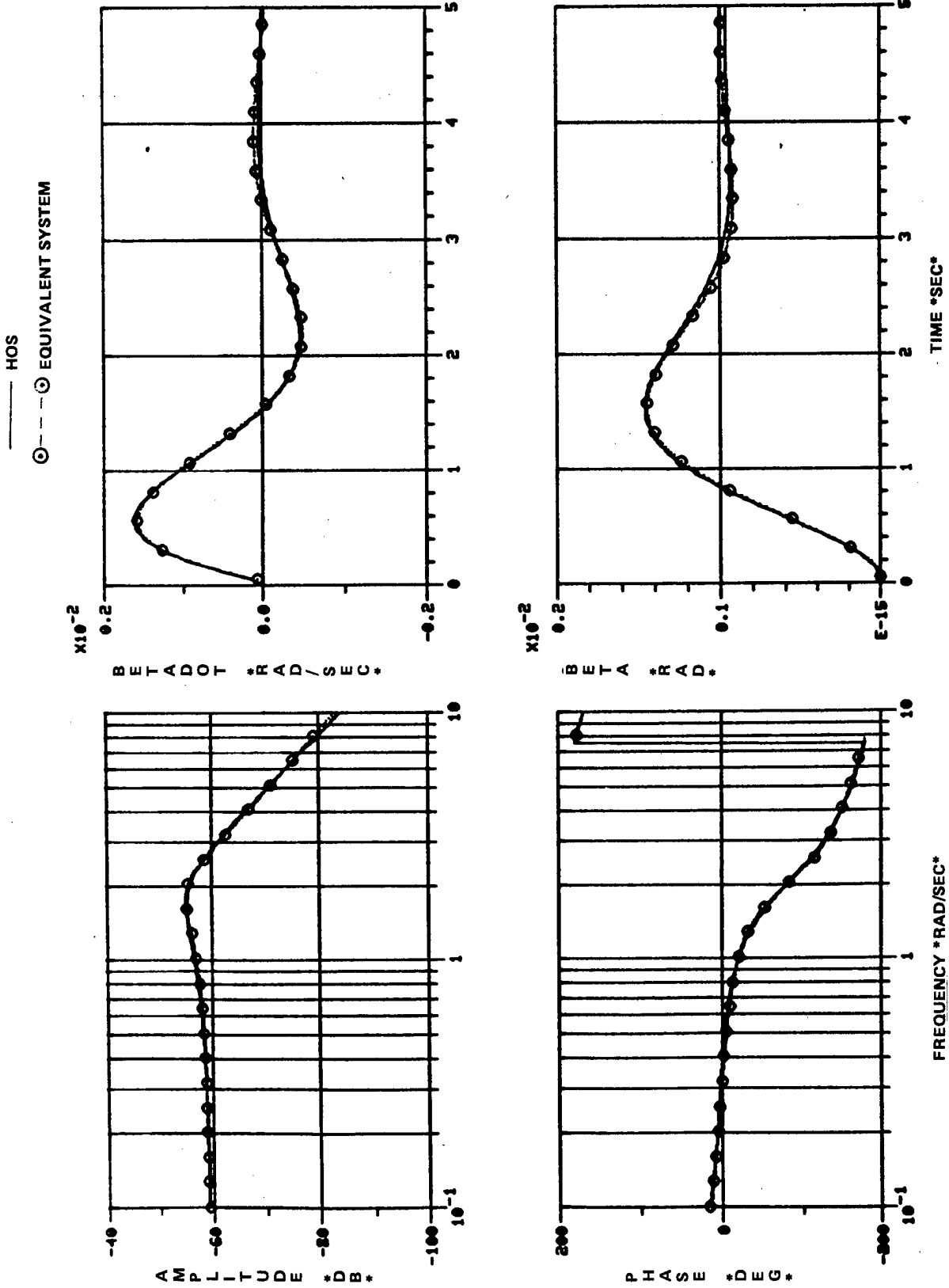


Figure 14. A-7 Sideslip Response — Simultaneous Match, No Control Augmentation

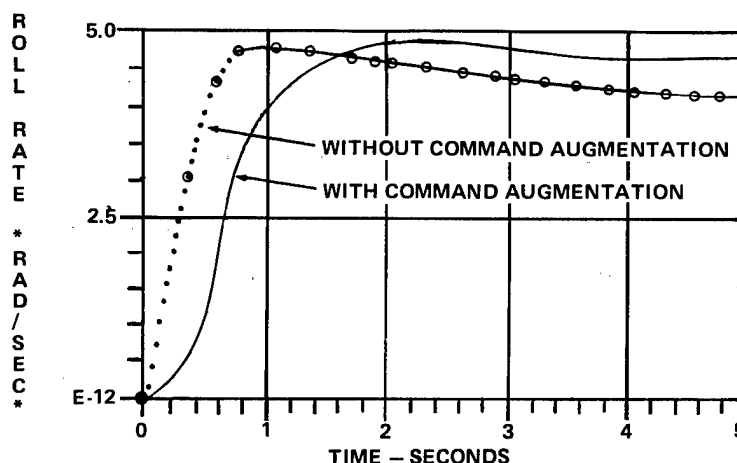


Figure 15. Impact of Roll Command Augmentation on A-7 Roll Rate Response

Referring first to the approximate form results, it can be seen that the time delay and roll mode time constant are considerably larger than those for the Command Augmentation OFF results of table IV. Likewise, the bank angle mismatch has increased significantly, reflecting the difficulty in obtaining a good match with the additional prefilter roots present in the high order system. The sideslip response, which is unaffected by the lateral command augmentation, yields the same equivalent system as shown in table IV.

The complete form bank angle results (trial 3 of table VI) again illustrate the difficulties experienced in obtaining equivalent system results with a closeness of numerator and denominator roots. Although very excellent match statistics are obtained ($M_\phi = 2.7$), the modal parameters identified are completely unrealistic. It was again necessary to either fix the numerator roots at their known higher order system value (Trial 4), or iteratively fix first the denominator roots at the approximate form results (Trial 5) and then fix the resulting numerator roots (Trial 6). This latter method was found to be 1), the most straightforward approach, assuming that no information concerning the root location was available a priori and 2), give the most consistent results. Independent matching of the sideslip response was again easily accomplished, although the identified roll mode time constant was inconsistent with any of the other results. It should be possible to improve the roll mode time constant identified in the sideslip response by again iteratively fixing and freeing the denominator and numerator terms respectively. However, since it has already been shown, for the S-3 and A-6 airplanes, that simultaneous matching of bank and sideslip angles simplifies the matching procedure, no additional independent matches were performed.

Freeing all of the modal parameters in the simultaneous technique again provided the lowest mismatch statistics but resulted in unrealistic modal parameters (Trial 8 of table VI). It was again necessary to iteratively fix and free the denominator (beginning with the approximate form results) and numerator terms, respectively, in order to obtain the equivalent system model (Trials 9 and 10).

Frequency and time history comparisons for the high order and equivalent system models, with Command Augmentation ON, are presented in figures 16 and 17. The differences evident in these two figures reflect the impact of not explicitly including the control system roots in the equivalent system modelling process. It would be possible to add the additional roots in the equivalent system model (see for example, reference (g)). However, the resulting modal parameters would not be consistent with the comparison data base used to generate the specification requirements of references (a) and (e).

TABLE VI
 A-7 AIRPLANE EQUIVALENT TRANSFER FUNCTIONS, PREFILTERS INCLUDED
 Roll and Sideslip Angle Response to Cockpit Control Inputs
 Configuration CR 15,000 feet/0.6 Mach
 Command Augmentation ON

PARAMETER	HOS VALUES	APPROX. FORM	COMPLETE FORM									
			INDEPENDENT MATCHING					SIMULTANEOUS MATCHING				
			P	β	ϕ	ϕ	ϕ	ϕ	ϕ	ϕ	β	ϕ & β
TRIAL			1	2	3	4	5	6	7	8	9	10
K_ϕ	13540.		7.9		1.97	6.27	5.93	5.75		5.25	5.9	5.97
ζ_ϕ	0.56				2.32	0.56*	0.686	0.686*		1.09	0.693	0.693*
ω_ϕ	2.02				4.63	2.02*	2.528	2.528*		1.79	2.558	2.558*
t_ϕ	-		0.237		0.135	0.210	0.204	0.202		0.193	0.203	0.205
K_β	0.0011			0.0061					0.000061	0.000061	0.000057	0.000058
$\tau_{\beta 1}$	-1250.								-1250.			
$\tau_{\beta 2}$	0.197								0.545	1.75	0.642	0.642*
$\tau_{\beta 3}$	0.009								0.009			
t_β	-			0.032					0.052	0.052	0.045	0.045
τ_r	0.20				1.01				0.37	1.33	0.60*	0.589
τ_s	370.4				370.4			0.77				
ζ_{DR}	0.50			0.40	0.74	0.33	0.40*	0.38	0.41	0.49	0.40*	0.42
ω_{DR}	2.0			2.29	3.06	2.14	2.29*	2.48	2.03	2.20	2.29*	2.271
M_ϕ	-		84.8		2.7	36.9	31.3	26.2	2.6	23.7	31.2	31.2
M_β	-			10.4						2.3	8.6	7.6

* Fixed parameter

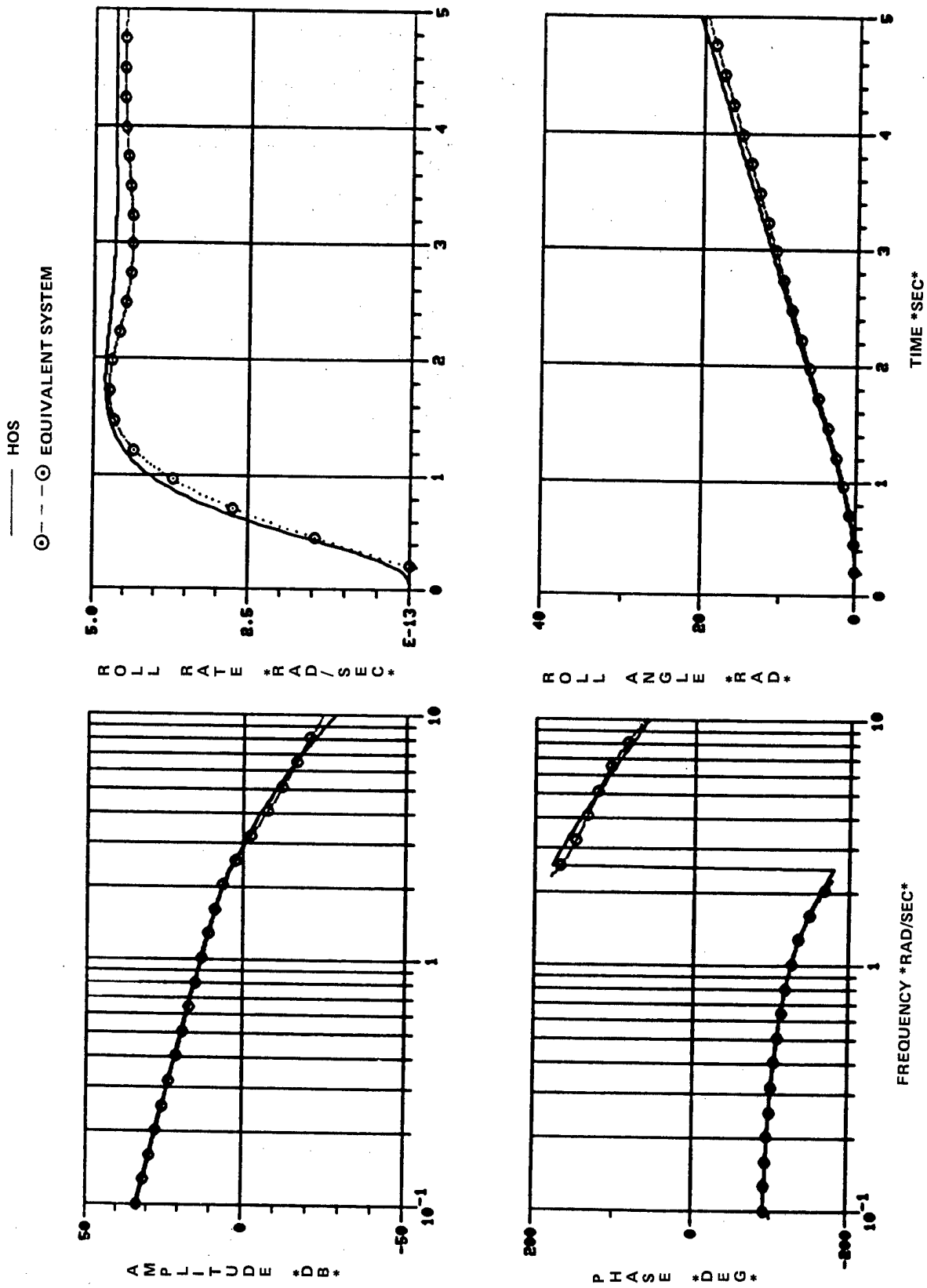


Figure 16. A-7 Roll Response - Simultaneous Match, Command Augmentation Included

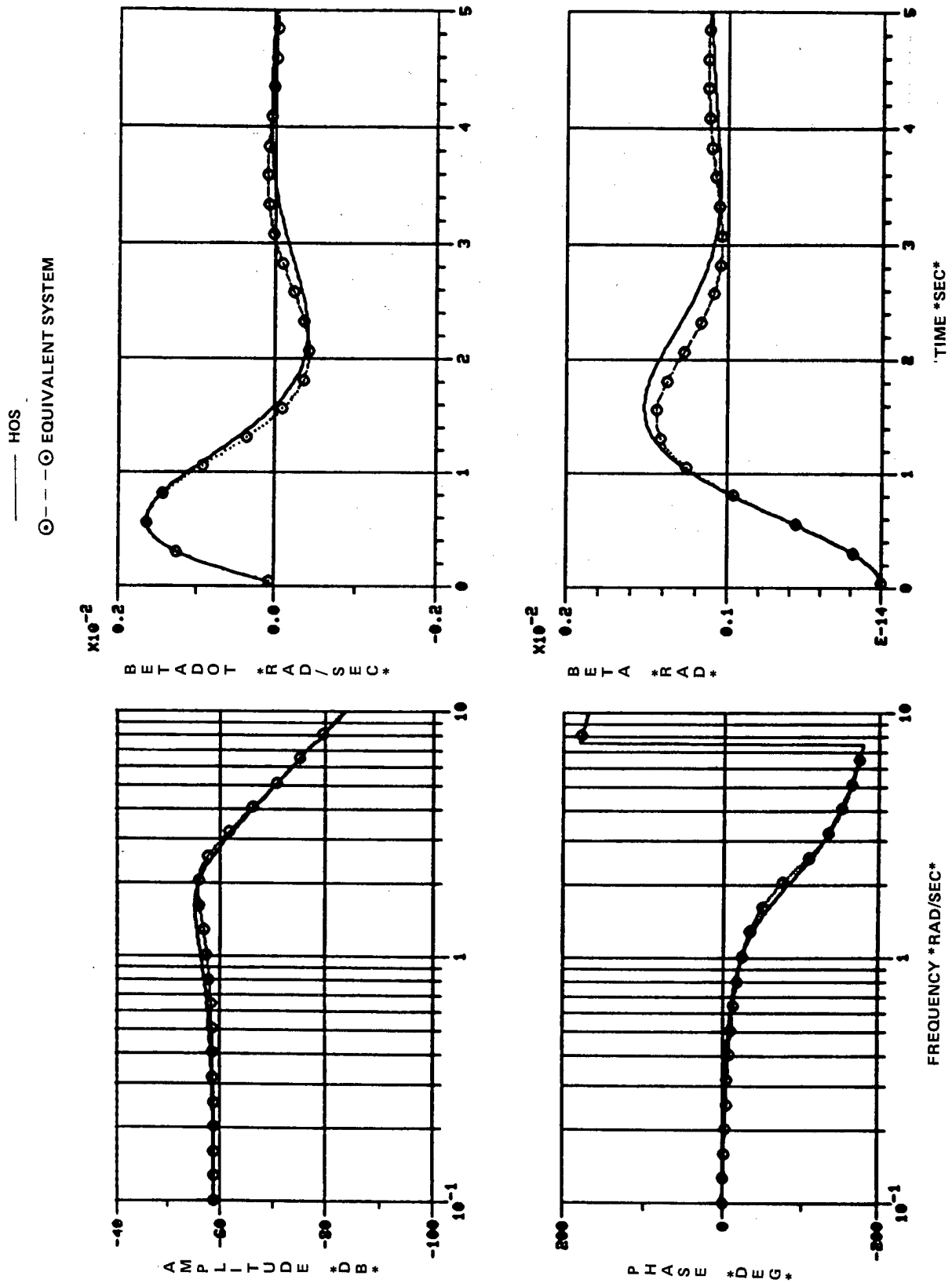


Figure 17. A-7 Sideslip Response - Simultaneous Match, Command Augmentation Included

F-14 Airplane

The lateral directional control system for the F-14 aircraft incorporates roll rate, yaw rate and lateral acceleration feedbacks as well as a lateral stick to differential stabilizer feed forward command to augment the airplane's basic response characteristics. As shown in Appendix A, the lateral augmentation patch incorporates a prefilter at a frequency of 2.0 rad/sec. Initially, this prefilter may be expected to impact the determination of an equivalent model in much the same way that the A-7's command prefilter did. However, the architecture of the two systems is somewhat different: in the A-7 airplane, the augmented command signal is fed to both the differential tail and spoilers while for the F-14, the augmented command is directed only to the differential tail, thereby minimizing the prefilter impact on the total response model. The transfer functions representing the roll and sideslip angle response to pilot commanded inputs for the F-14 are seventh and eighth order numerators, respectively, over a tenth order denominator.

Cancelling numerator and denominator roots of similar magnitudes and eliminating those outside the 0.1 to 10.0 rad/sec frequency range, the roll transfer function reduces to a second over fourth order response. Since the low order equivalent form is also a second over fourth order response, good matches were anticipated. In fact, low order equivalents of these transfer functions were readily obtained. The equivalent system parameters for a representative case of 15,000 ft and 0.40 Mach are presented in table VII. The best matches were again obtained when the simultaneous matching technique was utilized. In this instance, it was not necessary to fix any of the equivalent system parameters in the range of .1 to 10 rad/sec. The corresponding frequency and time history responses, shown in figures 18 and 19 indicate virtually no difference between the high and low order systems. The results for all F-14 airplane flight conditions analyzed are presented in Appendix B.

TABLE VII

F-14 AIRPLANE EQUIVALENT TRANSFER FUNCTIONS
 Roll and Sideslip Angle Response to Cockpit Control Inputs
 CR 15,000 FT .40 M

	HOS VALUES	APPROXIMATE FORM		COMPLETE FORM				
		INDEPENDENT		INDEPENDENT				SIMULTANEOUS
		P	β	ϕ		β		ϕ & β
K_ϕ	13.19	.683	—	.66	.67	—	—	.64
ζ_ϕ	.70	—	—	.70*	.59	—	—	.73
ω_ϕ	1.28	—	—	1.28*	1.68	—	—	1.04
t_ϕ	—	.054	—	.048	.049	—	—	.045
K_β	.111	—	.267	—	—	.0065	.0062	.0062
$\tau_{\beta 1}$	-34.48	—	—	—	—	-34.48*		-34.48*
$\tau_{\beta 2}$.388	—	—	—	—	.388*	1.53	1.935
$\tau_{\beta 3}$.02	—	—	—	—	.02*		.02*
t_β	—	—	.020	—	—	.06	.056	.054
τ_r	.36	.671	—	.55	.53	.23	.55*	.701
τ_s	-62.50	—	—	-62.50*		-62.50*		-62.50*
ζ_{DR}	.61	—	.491	.55	.49*	.43	.53	.591
ω_{DR}	1.07	—	1.515	1.18	1.515*	1.31	1.06	1.06
M_ϕ	—	12.6	—	1.8	4.1	—	—	1.4
M_β	—	—	38.0	—	—	18.3	2.6	1.5

*Fixed parameter

(Note: See Appendix B for summary of all flight conditions)

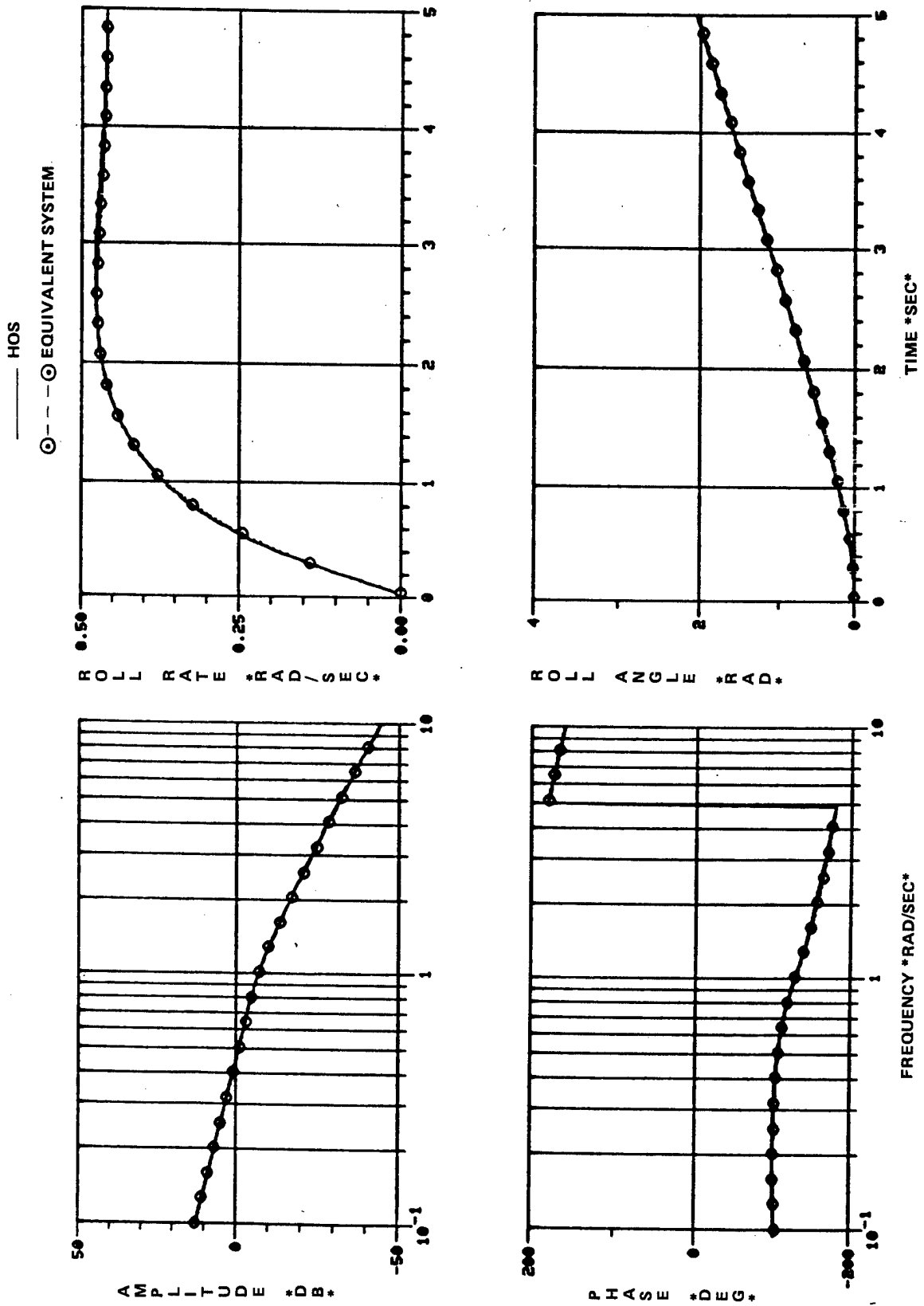


Figure 18. F-14 Roll Response - Simultaneous Match

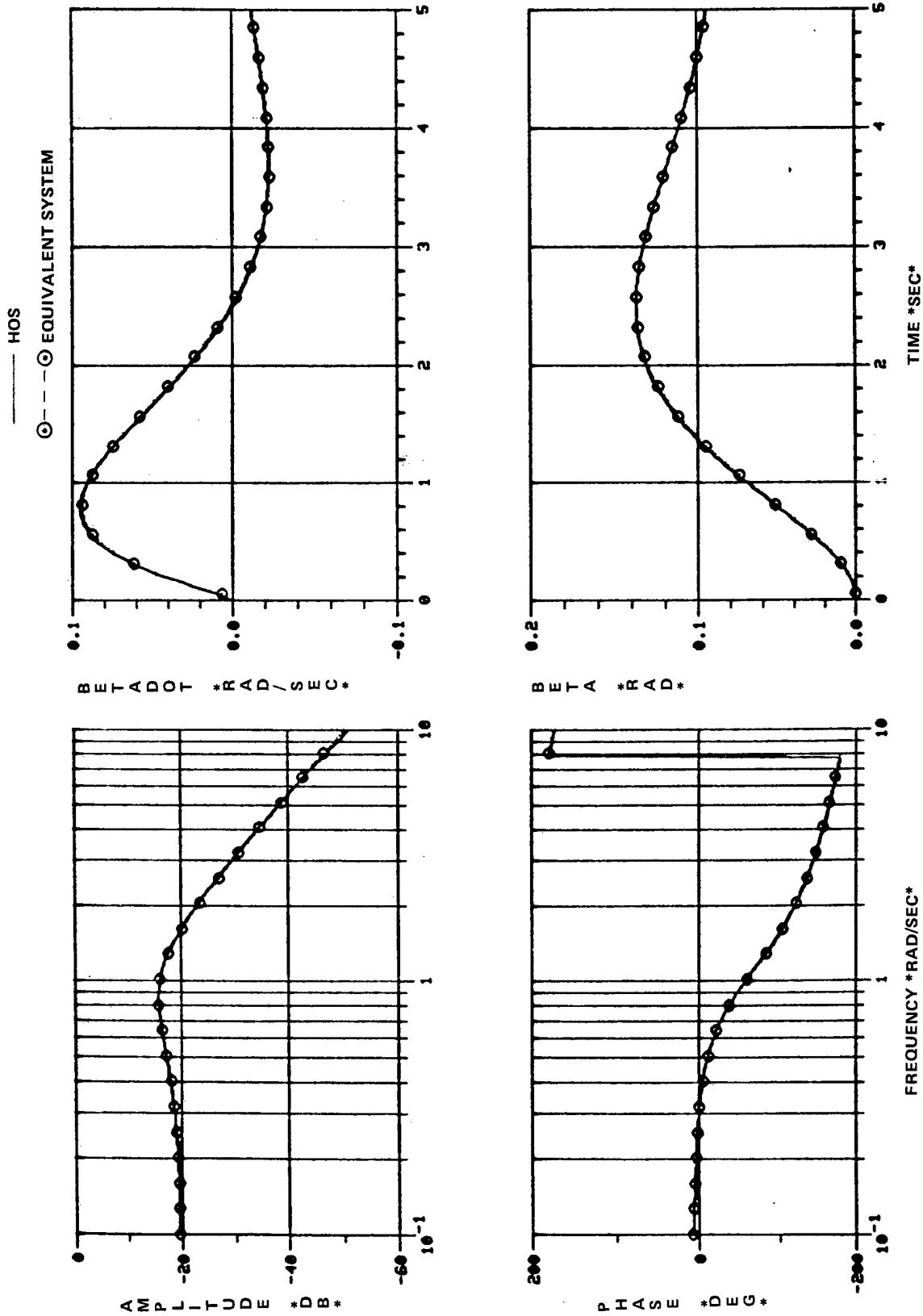


Figure 19. F-14 Sideslip Response -- Simultaneous Match

F-18 Airplane

The F-18 lateral directional control system is part of a highly complex digital flight control system. Lateral acceleration, roll rate and yaw rate signals are shaped and gain scheduled before being summed with the command input signals. The transfer functions representing the F-18 airplane's roll and sideslip angle responses are composed of 20th and 22nd order numerators, respectively, over a 25th order denominator, as presented in Appendix A. Many of these roots occur at frequencies higher than 10 rad/sec and will primarily contribute to an equivalent time delay. Eight of the denominator roots lie in the frequency range of .1 to 10 rad/sec, making it difficult to identify the dominant modes of these responses. Approximate pole-zero cancellation of roots in this range results in 0/2nd order representations for both transfer functions. Previous experience leads to the expectation that equivalent system models will be easily obtained from these representations. A good sideslip match can be expected while the bank angle response should include a large time delay due to the additional (uncancelled) root in the high order model.

The expected equivalent system results were, in fact, obtained, as shown in table VIII. The approximate forms were readily matched and exhibit relatively low mismatch values. The roll rate approximation exhibits a large time delay and a roll mode time constant different from that obtained from simply tracking the aircraft root in the high order system representation. The equivalent Dutch roll damping is similar to that of the high order oscillatory root while the equivalent frequency is somewhat higher. Simultaneous roll and sideslip angle matching (with all roots in the frequency range of .1 to 10 rad/sec allowed to go free) resulted in excellent matches as shown in table VIII. Similar trends to the approximate mode were obtained, except that the Dutch roll frequency mode closely matched that of the high order system oscillatory root.

Frequency and time history matches for the simultaneous match results are presented in figures 20 and 21. Only minor differences between the high order and low order equivalent system models are evident, as is to be expected from the low (≈ 4.5) mismatch values obtained.

TABLE VIII

F-18 AIRPLANE EQUIVALENT TRANSFER FUNCTIONS
 Roll and Sideslip Angle Response to Cockpit Control Inputs
 CR 10,000 FT .50 M

	HOS VALUES	APPROXIMATE FORM		COMPLETE FORM		
		INDEPENDENT		INDEPENDENT		SIMULTANEOUS ϕ & β
		P	β	ϕ	β	
K_ϕ	$.105 \times 10^7$	31.4	—	—	—	28.56
ζ_ϕ	.61	—	—	—	—	.595
ω_ϕ	1.46	—	—	—	—	1.37
t_ϕ	—	.151	—	—	—	.141
K_β	44.8	—	.416	—	—	.0092
$\tau_{\beta 1}$	-125.0	—	—	—	—	-125.0*
$\tau_{\beta 2}$	1.066	—	—	—	—	1.257
$\tau_{\beta 3}$.021	—	—	—	—	.021*
t_β	—	—	0	—	—	0
τ_r	.150	.331	—	—	—	.614
τ_s	-312.5	—	—	—	—	-312.5*
ζ_{DR}	.59	—	.56	—	—	.635
ω_{DR}	1.60	—	2.23	—	—	1.76
M_ϕ	—	10.9	—	—	—	4.4
M_β	—	—	26.4	—	—	4.7

* Fixed parameter

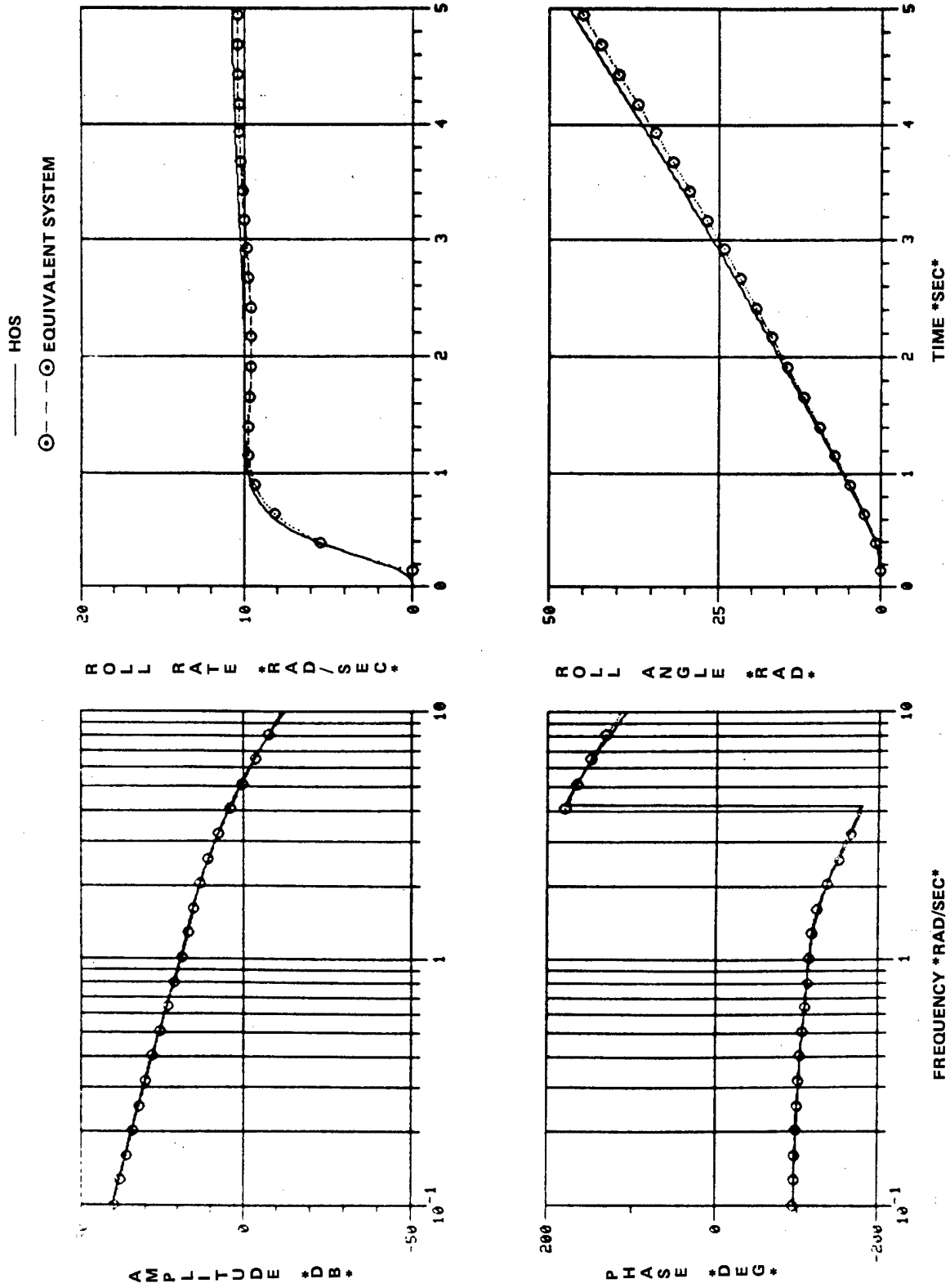


Figure 20. F-18 Roll Response — Simultaneous Match

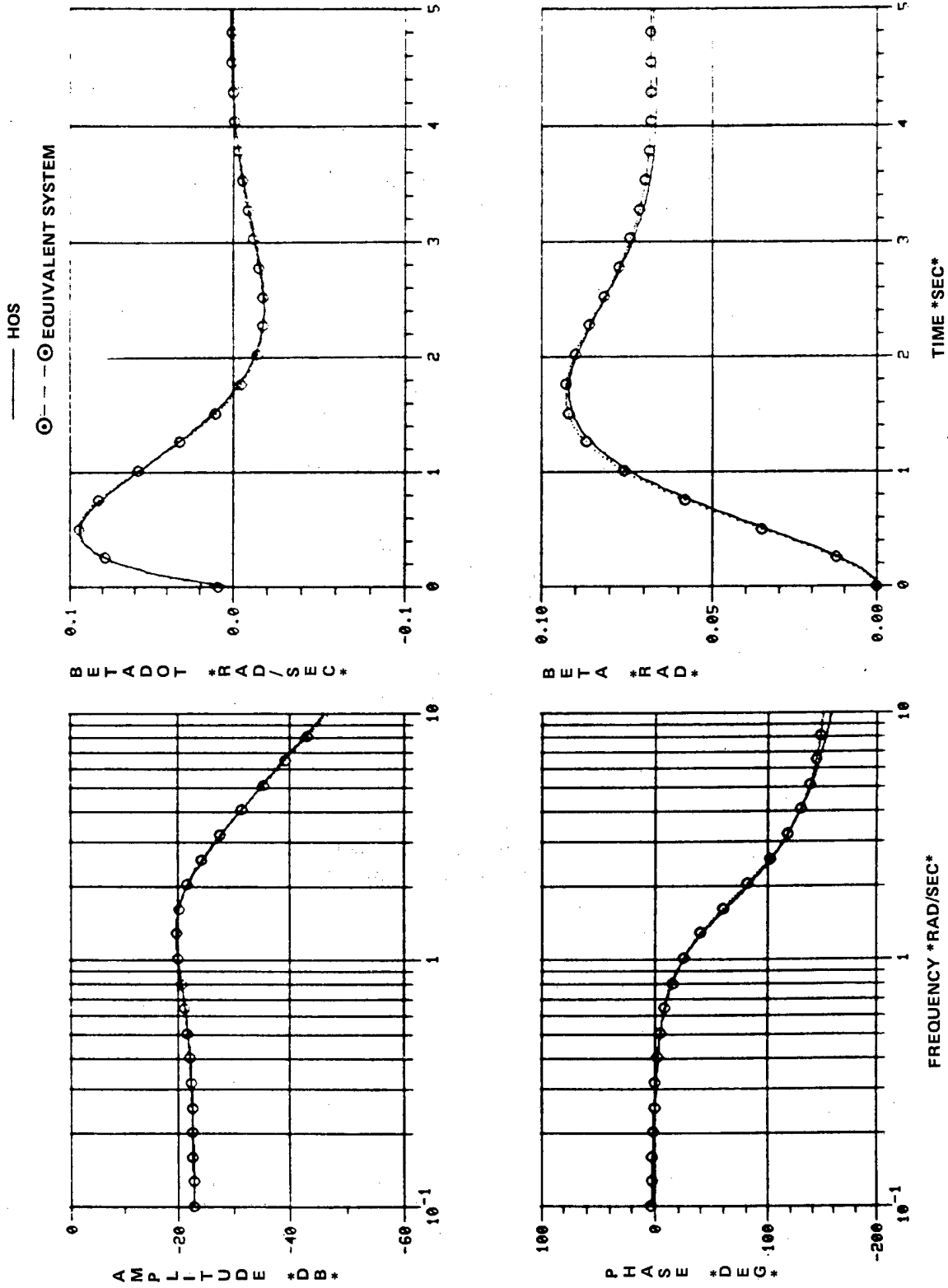


Figure 21. F-18 Sideslip Response — Simultaneous Match

COMPARISON WITH SPECIFICATION REQUIREMENTS

The lateral directional modal parameters resulting from the equivalent system analysis were compared against the requirements of reference (f) to determine specification compliance. Consistent trends were obtained for the equivalent system parameters resulting from the approximate and complete formats for all five aircraft analyzed as shown in figures 22, 23, 24, and 25.

There are differences evident in the modal parameters resulting from the approximate and complete equivalent system formats. In both the cruise and power approach configurations, the equivalent Dutch roll damping exhibited the largest differences, with the complete format results being from 5 to 25% higher than those for the approximate form. The complete form equivalent Dutch roll frequency was slightly reduced from that of the approximate form, while roll mode time constant showed a slight increase for the approximate form. The differences in roll mode time constant were only significant in two cases: 1) the A-6 airplane, for which the complete form roll mode time constant was consistently 0.2 seconds or more greater than that of the approximate form, and 2) the A-7 airplane at 0.3 Mach number.

All conditions analyzed met the Category A, Level 1, Dutch roll frequency and damping requirements of MIL-F-8785C. The F-14 and F-18 aircraft met the configuration CO (Combat) and GA (Ground Attack) requirement that damping ratio be greater than 0.4, at all flight conditions analyzed, while the other three aircraft only meet this requirement at the highest Mach numbers investigated.

The requirement that roll mode time constant be less than 1.0 second was met by all five airplanes, at all conditions analyzed, except one; the A-7 airplane at 0.3 Mach number. This configuration exhibited the largest discrepancy between the approximate and complete formats and was also the most difficult configuration to match due to the proximity of its higher order system roots.

Equivalent time delays also exhibited consistent trends. The complete format generally resulted in lower roll and sideslip angle time delays than determined for the approximate forms. The differences were, however, small and of little consequence in the resulting time history responses to control inputs.

The identified time delays met the Level 1 requirements of MIL-F-8785C at all conditions analyzed except for roll angle commands in the A-7 and F-18 aircraft. In the case of the A-7, presented in figure 26, these large time delays arise from the lateral command augmentation roots which are not explicitly modelled in the equivalent system format, as discussed previously. Flight experience with the A-7 airplane does not indicate any handling quality discrepancies which might be expected from time delays of this magnitude.

The F-18 aircraft, as modelled in this analysis, utilizes control force inputs in a highly complex digital flight control system. The stick force filters and sensors necessary to transmit the commanded force to the flight control system result in the large equivalent time delay shown in figure 22. The latest revision to the F-18 flight control system does not use control force inputs. Instead, control position inputs are utilized, eliminating the need for force prefilters. The removal of these prefilters has reduced the time delays to less than 0.10 seconds, which fall within the Level 1 boundaries as defined by reference (f).

A lateral high order system test program flown on the NT-33 airplane (reference (q)) suggests that roll mode time constant be plotted against time delay to determine lateral flying qualities characteristics. The time delay parameter in reference p was determined graphically and is slightly different from that arising from the equivalent system method used herein. Therefore the configurations of reference (q) were analyzed by the present methodology and the boundaries of reference (q) replotted as shown in figure 27 along with the approximate form results obtained in this analysis. The A-6, F-14 and S-3 aircraft results all lie within the Level 1 region, while the A-7 and F-18 results lie in the Level 2-3 regions.

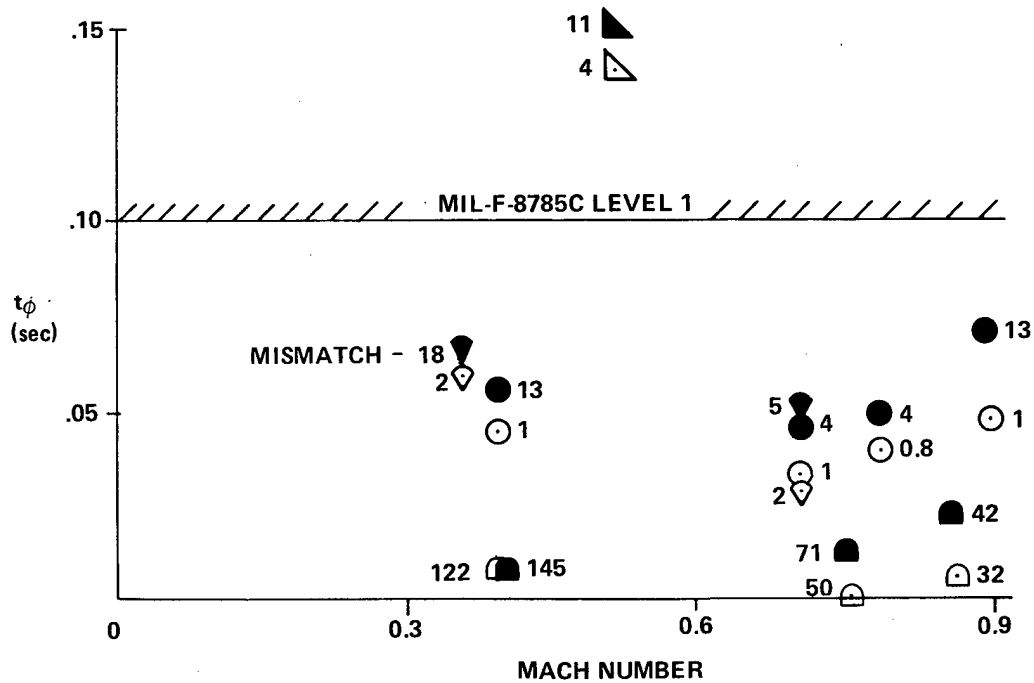
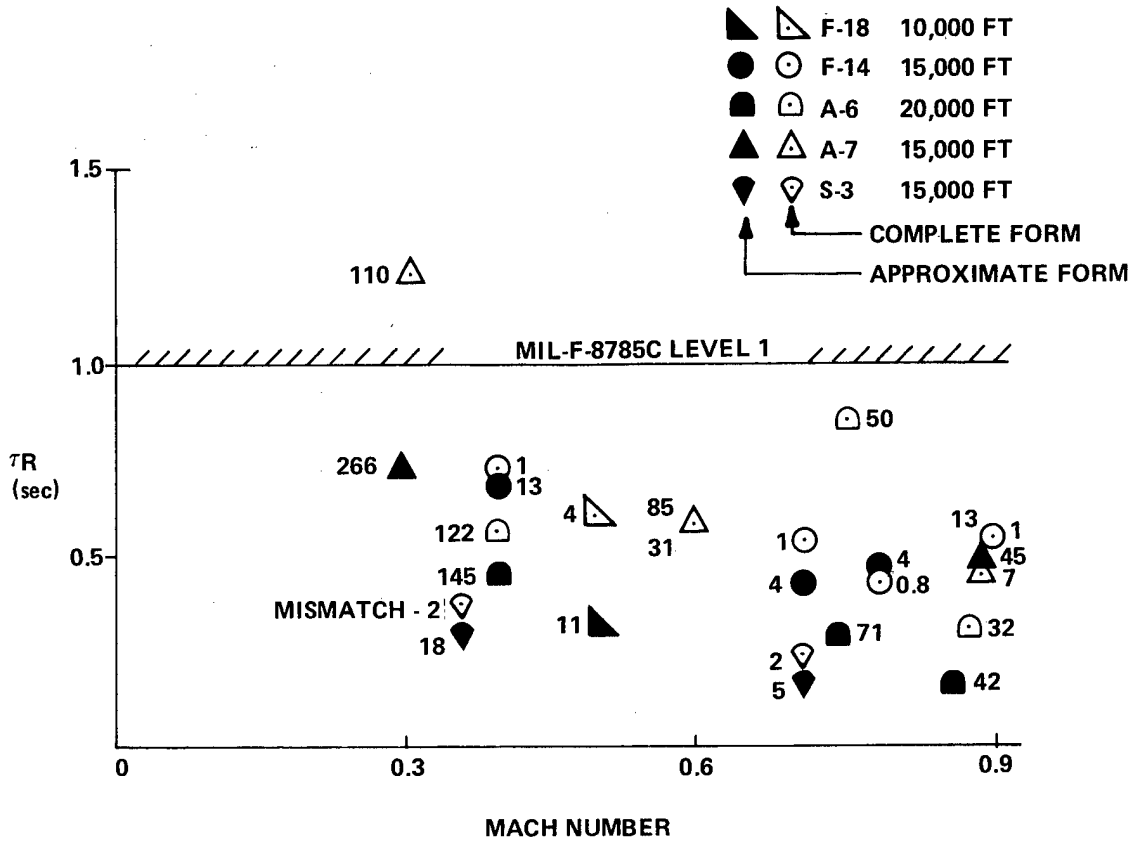


Figure 22. Roll Mode Results – Cruise Configurations

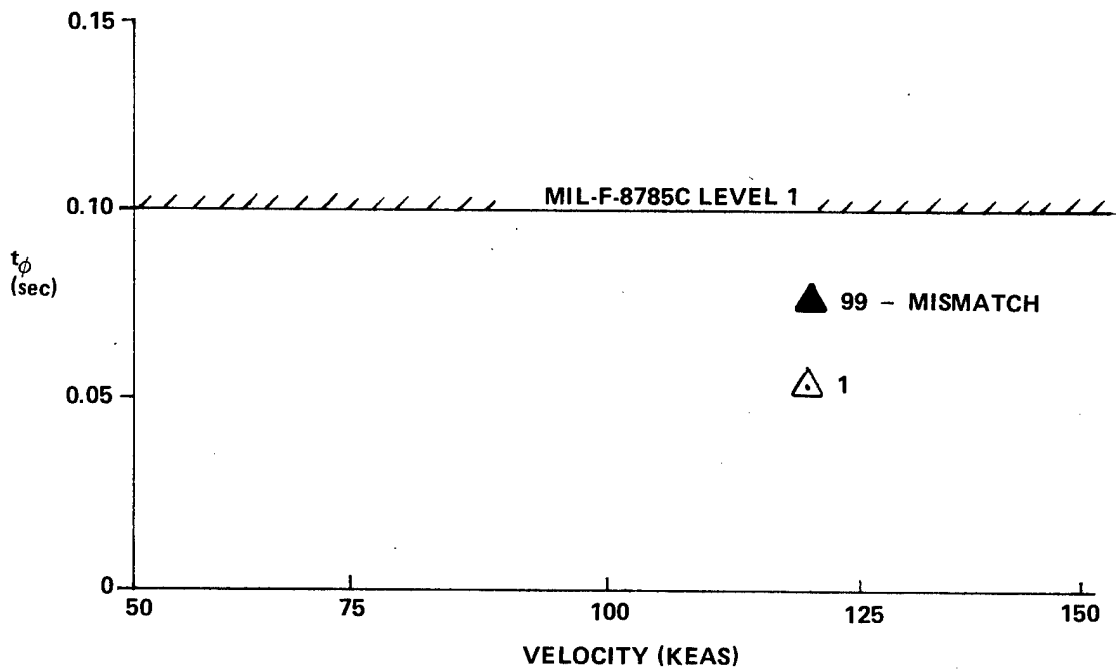
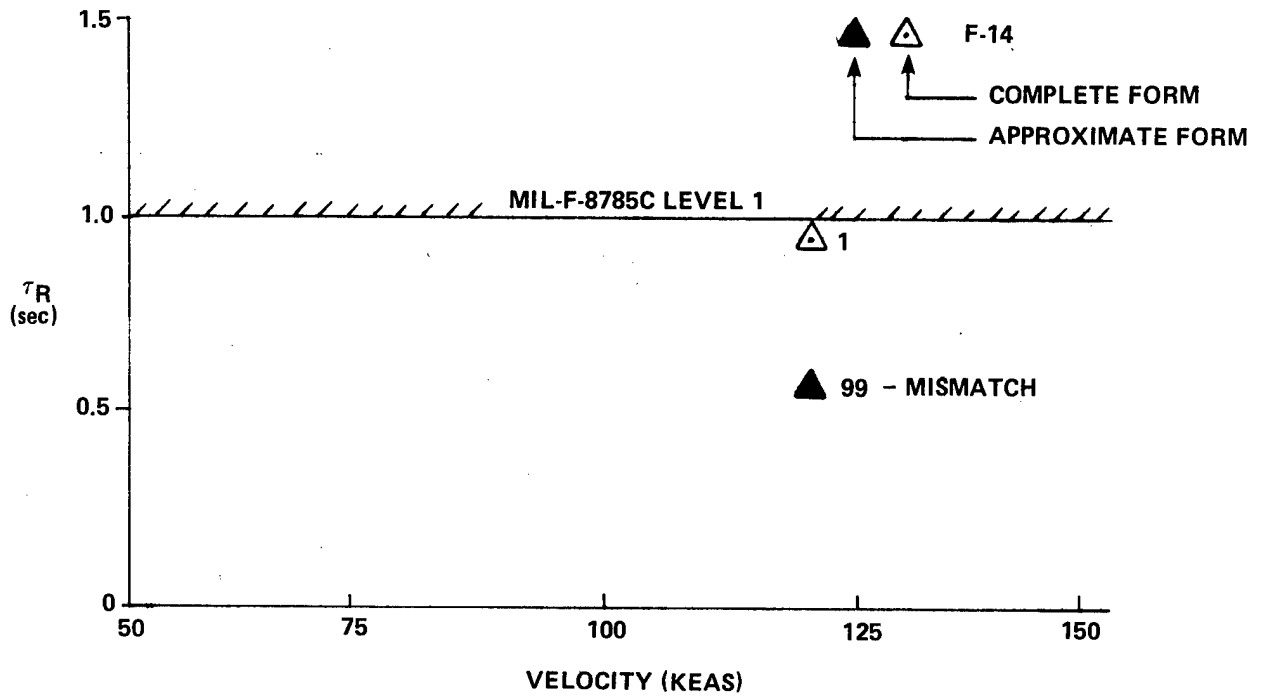


Figure 23. Roll Mode Results – Power Approach Configurations

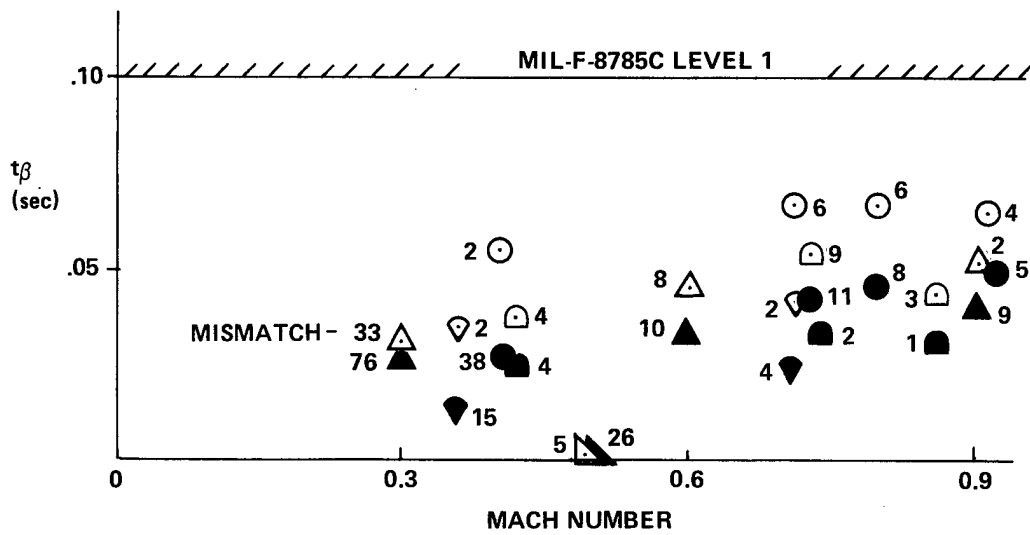
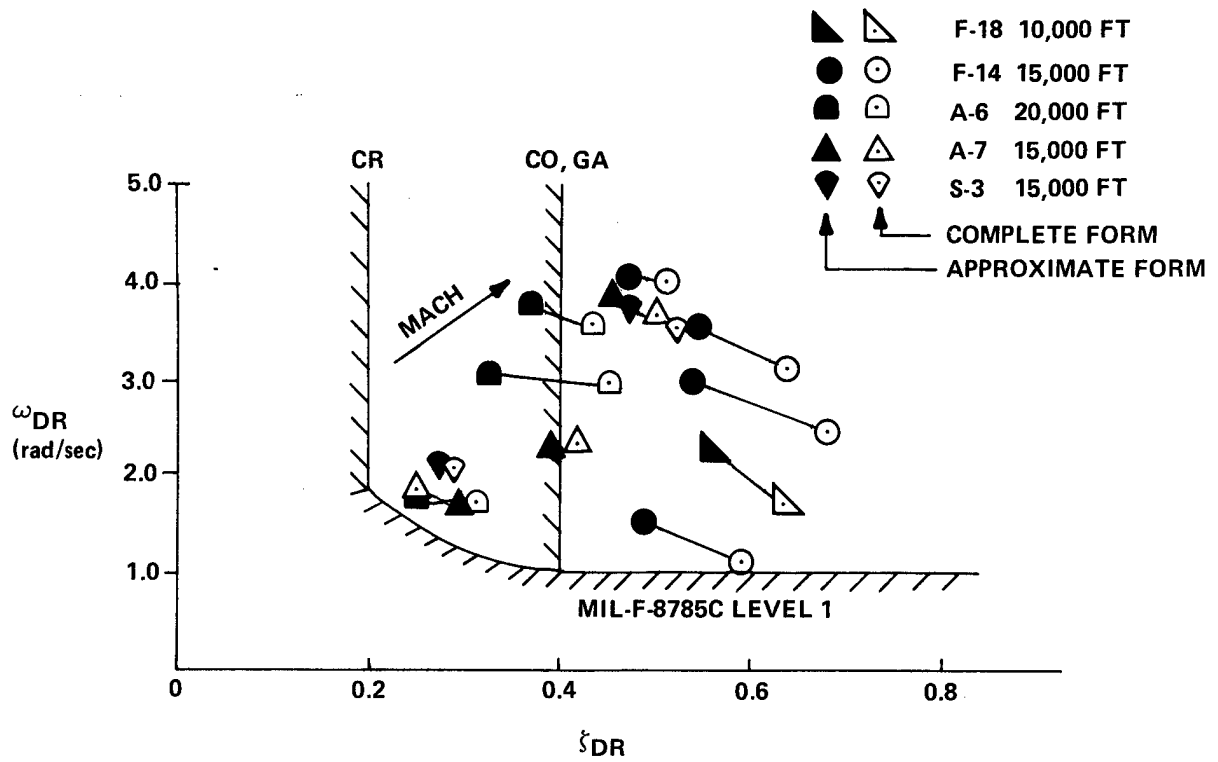


Figure 24. Dutch Roll Mode Results – Cruise Configuration

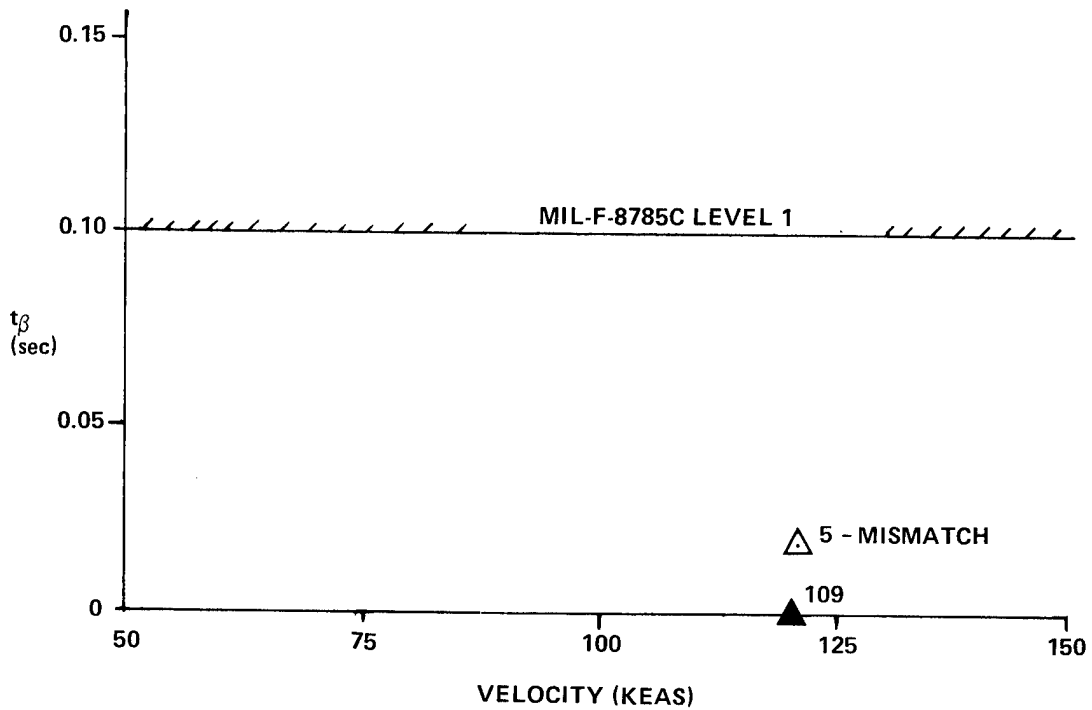
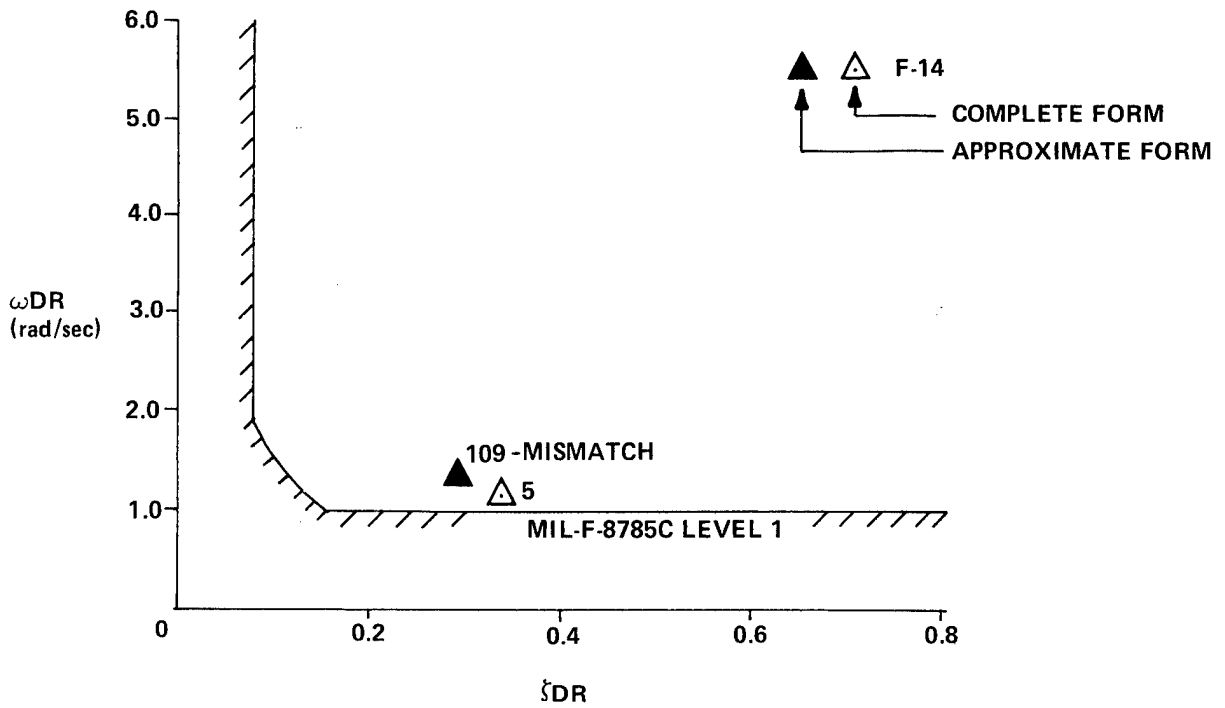


Figure 25. Dutch Roll Mode Results – Power Approach Configuration

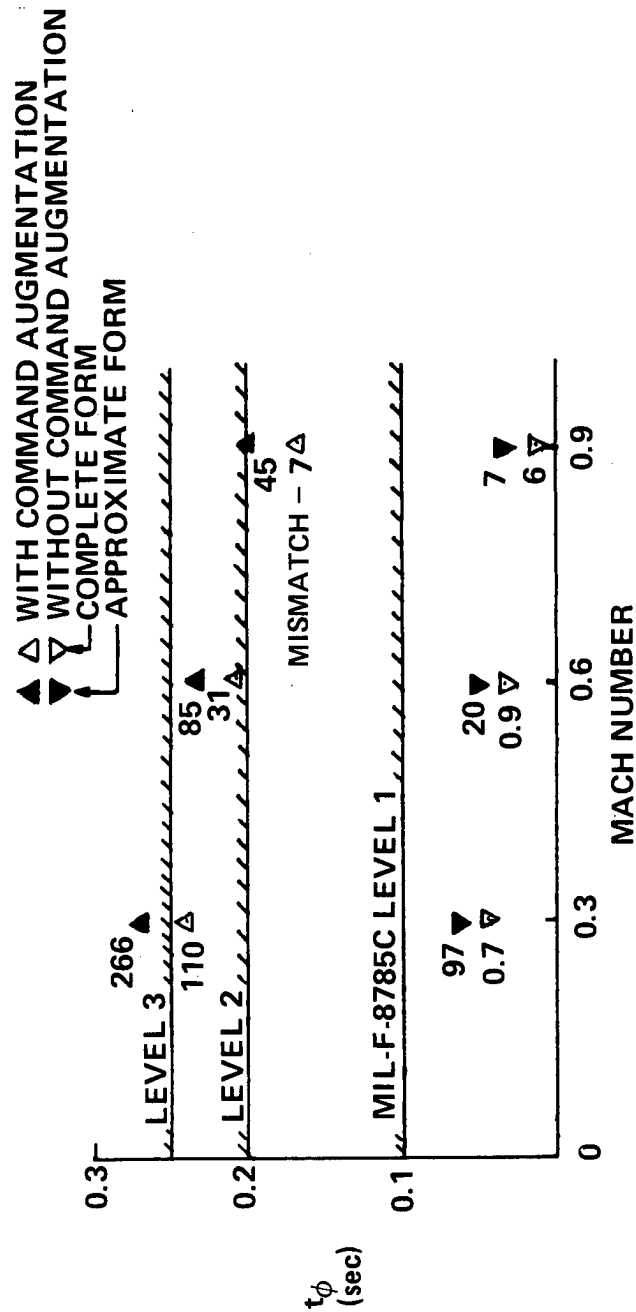


Figure 26. A-7 Time Delay Results

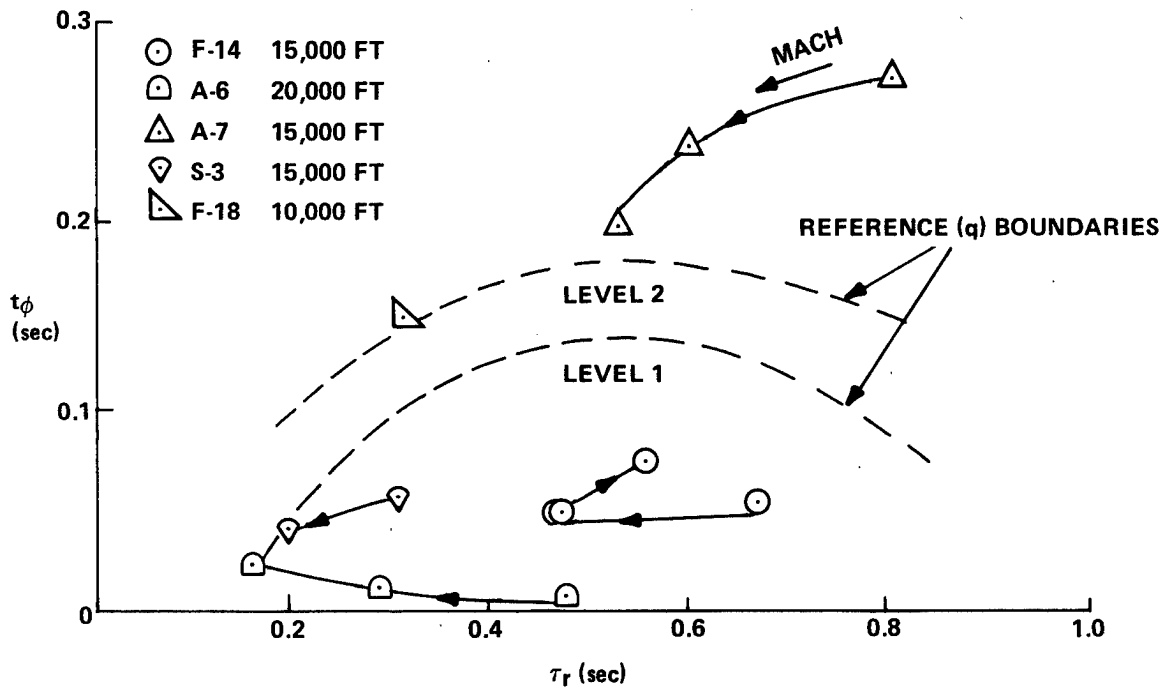


Figure 27. Time Delay vs. Roll Mode Time Constant – Approximate Form Results

CONCLUSIONS AND RECOMMENDATIONS

Lateral directional equivalent system models have been determined for five tactical Navy aircraft using both single degree of freedom roll and Dutch roll approximations and complete three degree of freedom formats for the low order systems. Mismatch between the high and low order systems was improved by using the complete format. However, the resulting approximate and complete modal parameters were not, with the possible exception of Dutch roll damping ratio, significantly different. When only denominator characteristics are desired, the single degree of freedom roll mode and Dutch roll approximate formats should be used to match roll rate and sideslip angle, respectively. These approximate models will provide acceptable equivalent system parameters for comparison against the MIL-SPEC requirements.

For those instances in which numerator characteristics are desired, the complete three degree of freedom equivalent system formats must be used. For these cases, an iterative matching procedure, in which numerator and denominator roots are alternately fixed and freed has been developed to optimize the matching procedure.

The identified equivalent system parameters reflect Level 1 flying qualities for the conditions analyzed when compared against the requirements of MIL-F-8785C with the exception of roll angle time delays for the A-7 and F-18 airplanes. These results indicate Level 2-3 equivalent time delays.

It is recommended that these frequency response matching techniques be applied to other types of aircraft to determine their low-order equivalent systems. Specific aircraft types for which these techniques would be applicable include VSTOL, rotary wing, and large aircraft. These analyses should include both the longitudinal and lateral-directional axes and would provide data for examining aircraft flying qualities requirements.

REFERENCES

- a. Anonymous, "Military Specification, Flying Qualities of Piloted Airplanes," MIL-F-8785B, 7 Aug 1969
- b. Stapleford, R.L., McRuer, D.T., Hoh, R.H., Johnston, D.E. and Heffley, R.K., "Outsmarting MIL-F-8785B(ASG), The Military Flying Qualities Specification," STI-TR-190-1, Aug 1971.
- c. Hodgkinson, J., LaManna, W.J. and Heyde, J.L., "Handling Qualities of Aircraft with Stability and Control Augmentation Systems – A Fundamental Approach," Aeronautical Journal, Feb 1976.
- d. A'Harrah, R.C., Hodgkinson, J. and LaManna, W.J., "Are Today's Specifications Appropriate for Tomorrow's Airplanes?," AGARD Flight Mechanics Symposium on Stability and Control, Ottawa, Canada, Sep 1978.
- e. Anonymous, "Military Specification, Flying Qualities of Piloted Airplanes," MIL-F-8785C, 5 Nov 1980.
- f. Hoh, Roger H., et al, "Proposed MIL Standard and Handbook – Flying Qualities of Air Vehicles," AFWAL-TR-82-3081, Volumes I and II, Nov 1982.
- g. Bischoff, D.E., "Development of Longitudinal Equivalent System Models for Selected U.S. Navy Tactical Aircraft," NAVAIRDEVCEN Report No. NADC 81069-60, 1 Aug 1981.
- h. Teper, Gary L., "Aircraft Stability and Control Data," STI Technical Report 176-1, Apr 1969.
- i. "An Aerodynamic Stability and Control Data Summary for Several Selected Military Aircraft, Vol I: Conventional Aircraft," NAVAIRDEVCEN Report No. NADC-AM-7106, 28 Sept 1971
- j. "Grumman Aerospace Corporation Report XA1128-116-1," 31 Oct 1968.
- k. Grumman Aerospace Corp. Report No. A51-335-R-77-01, "F-14A Stability and Control and Flying Qualities Report, Status IV," 16 Dec 1977.
- l. Lockheed California Company Report No. LR 24405, "S-3A Preliminary Automatic Flight Control System Report," 1 Mar 1971
- m. McDonnell Douglas Corp. Report No. MDC A3957, "F-18 Aerodynamic Stability and Control and Flying Qualities Report (U)," Rev A of 10 Mar 1980.
- n. Hodgkinson, J., Givan, M.E., "Lateral-Directional Equipment System Frequency Curve Fit," McDonnell Douglas Corp. Computer Program LATFIT, 25 October 1978.
- o. Hodgkinson, J. and Buckley, J., "General Purpose Frequency Response Curve Fit (Arbitrary Order)," McDonnell Douglas Corp. Computer Program NAVFIT, 25 Oct 1978.
- p. Smith, Rogers, E., Hodgkinson, J. and Synder, R.C., "Equivalent System Verification and Evaluation of Augmentation Effects on Fighter Approach and Landing Flying Qualities," AFWAL-TR-81-3116, Sep 1981.

NADC-83116-60

- q. Monagan, S.J., Smith, R.E., and Bailey, R.E., "Lateral Flying Qualities of Highly Augmented Fighter Aircraft", Calspan Report No. 6645-F-8, March 1982.
- r. "MAINSTREAM-EKS Programmer's Manual, EASY5 Dynamic Analysis System User's Guide," BCS Document 10208-001-R1

APPENDIX A

AIRCRAFT AND CONTROL SYSTEM DESCRIPTIONS

Data describing each of the airplanes and their respective control systems were obtained from available stability and control reports, references (g) thru (l). This appendix briefly describes the subject airplanes and presents a block diagram of their respective lateral directional control system as modelled in this analysis.

NADC-83116-60

S-3 – The S-3 airplane is a twin turbofan powered, land and carrier based, subsonic, antisubmarine warfare aircraft. Lateral directional control is accomplished via a mechanical control system which operates the ailerons, rudder, and spoilers. Control stick dynamics were not included in this model of the S-3 aircraft. The aircraft's basic stability is augmented through the feedback of both roll rate and yaw rate. A block diagram of the S-3's lateral directional control system, as modelled in this analysis, is presented in figure A-1. The transfer functions representing the S-3 airplane are presented in table A-1.

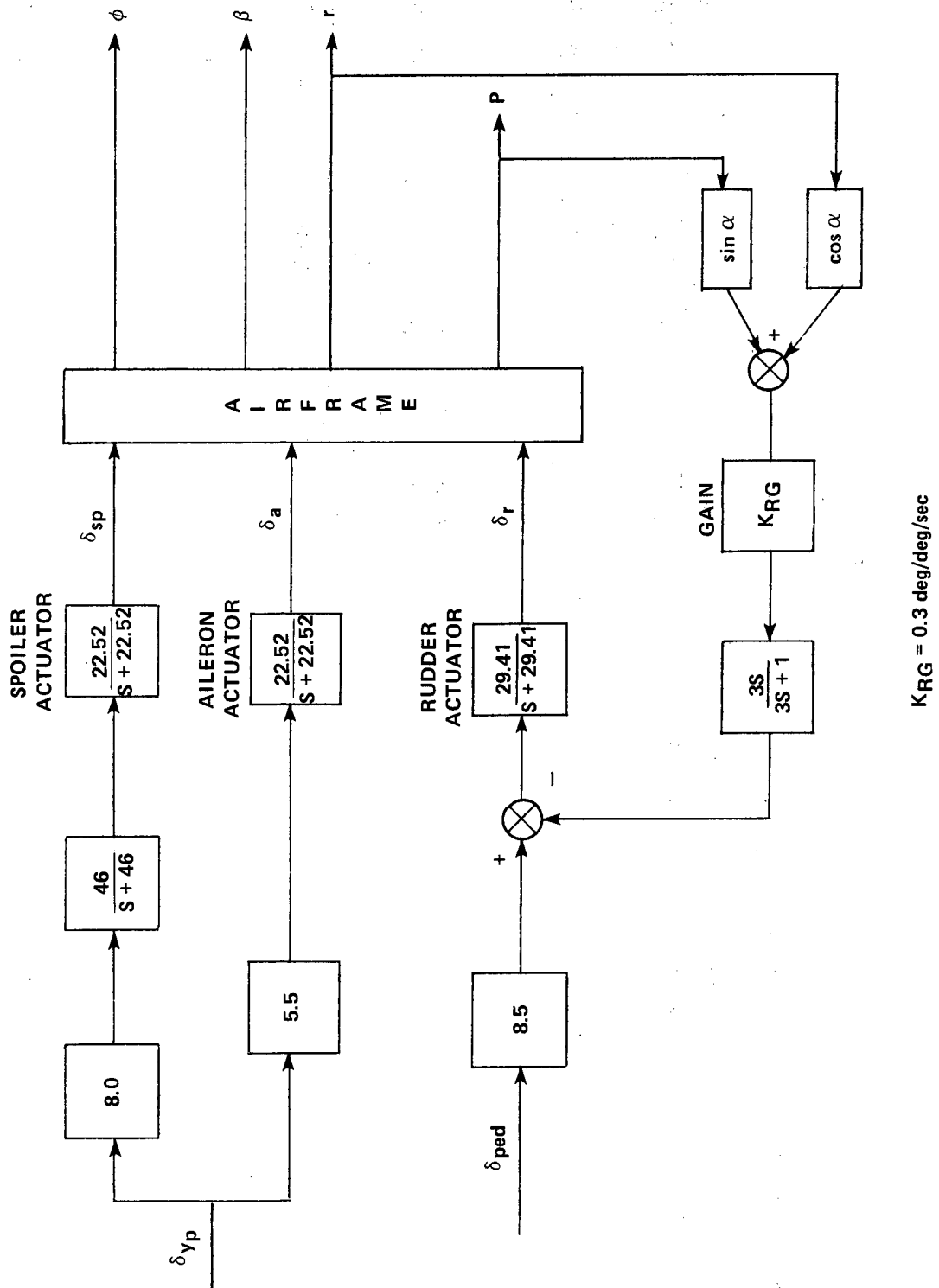


Figure A-1. S-3 Lateral-Directional Control System

TABLE A-1
S-3 AIRPLANE TRANSFER FUNCTIONS

<u>CONFIGURATION</u>	<u>ALTITUDE (ft)</u>	<u>AIRSPEED (M/KEAS)</u>	<u>TRANSFER FUNCTION</u>
CR	15,000	0.36/179	$\frac{\phi}{\delta y_p} = \frac{290.2 (.354) (193.4) (28.49) [38, 1.99]}{(2.607) (.381) (.006) (22.52) (46.0) (28.54) [.31, 2.11]}$
			$\frac{\beta}{\delta_{ped}} = \frac{11.35 (.333) (-.0165) (64.61) (2.563) (22.52) (46.0)}{(2.607) (.381) (.006) (22.52) (46.0) (28.54) [.31, 2.11]}$
CR	15,000	0.71/353	$\frac{\phi}{\delta y_p} = \frac{815.4 (.343) (90.52) (26.55) [.53, 3.89]}{(.369) (.008) (6.219) (22.52) (46.0) (26.69) [.51, 3.74]}$
			$\frac{\beta}{\delta_{ped}} = \frac{13.32 (.333) (-.0006) (151.8) (6.241) (46.0) (22.52)}{(.369) (.008) (6.219) (26.69) (46.0) (22.52) [.51, 3.74]}$

A-6 — The A-6 airplane is a twin turbojet, land and carrier based, subsonic, all-weather attack aircraft. A block diagram of the A-6's lateral directional control system, as modelled in this analysis, is presented in figure A-2. The control stick and rudder pedals are linked directly to their corresponding surface actuators by a system of pushrods, bellcranks, and cables. Lateral control is obtained through the use of flaperons while directional control is provided by a single rudder. The basic stability of the airplane is augmented through the feedback of roll rate and yaw rate to obtain the desired response.

The transfer functions representing the A-6 airplane's response to cockpit control deflections, obtained via the Boeing Computer Services program, EASYS (reference r), are presented in table A-11.

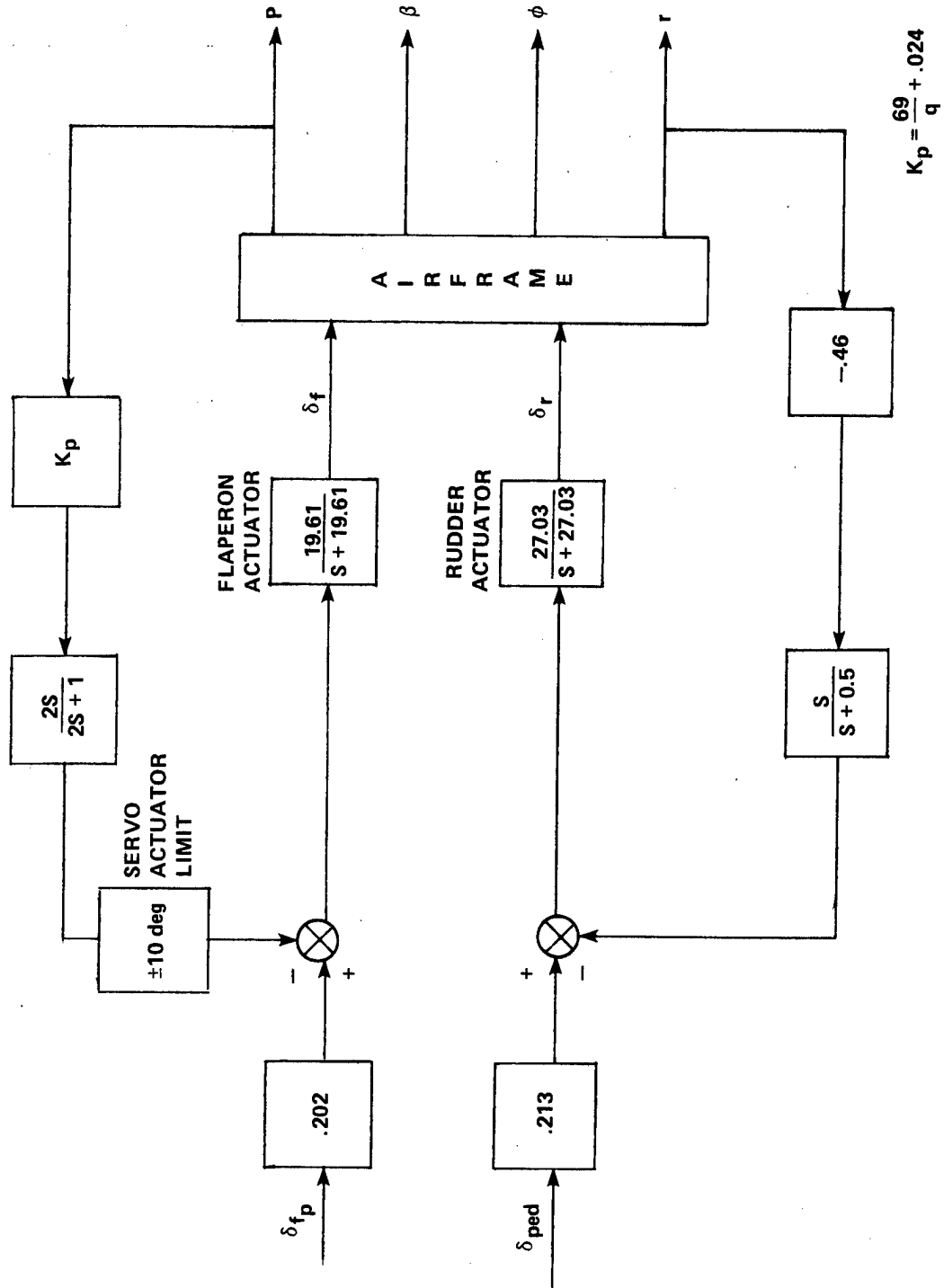


Figure A-2. A-6 Lateral-Directional Control System

TABLE A-II
A-6 AIRPLANE TRANSFER FUNCTIONS

<u>CONFIGURATION</u>	<u>ALTITUDE (ft)</u>	<u>AIRSPEED (M/KEAS)</u>	<u>TRANSFER FUNCTION</u>
CR	20,000	0.40/179	$\frac{\phi}{\delta f_p} = \frac{17.84 (.50) (.555) (26.32) [.283, 1.77]}{(.0095) (.172) (.555) (6.43) (15.48) (26.39) [.269, 1.73]}$
			$\frac{\beta}{\delta ped} = \frac{.0078 (-.0076) (.184) (.502) (6.76) (15.06) (101.3)}{(.0095) (.172) (.555) (6.43) (15.48) (26.39) [.269, 1.73]}$
CR	20,000	0.72/323	$\frac{\phi}{\delta f_p} = \frac{66.74 (.5) (.547) (24.80) [.41, 3.28]}{(.00861) (.240) (.549) (25.10) [.995, 12.00] [.361, 3.14]}$
			$\frac{\beta}{\delta ped} = \frac{.148 (.006) (.236) (.507) (141.8) [.928, 12.88]}{(.00861) (.240) (.549) (25.10) [.995, 12.00] [.361, 3.14]}$
CR	20,000	0.87/390	$\frac{\phi}{\delta f_p} = \frac{101.3 (.5) (.538) (24.68) [.415, 3.60]}{(.0069) (.303) (.539) (24.61) [.39, 3.65] [.952, 13.25]}$
			$\frac{\beta}{\delta ped} = \frac{.156 (.0057) (.30) (.50) (157.8) [.924, 13.89]}{(.0069) (.303) (.539) (24.61) [.39, 3.65] [.952, 13.25]}$

A-7 — The A-7 airplane is a single place turbo fan powered, land and carrier based, light attack aircraft. An irreversible mechanical system is utilized to produce lateral directional control with both stability and control augmentation. The stability augmentation system provides roll rate and yaw rate feedback signals to augment the aircraft's basic stability characteristics. The command augmentation system feeds control force signals forward through a prefilter as a means of increasing the pilot's commanded input. A block diagram of the A-7's lateral directional control system, as modelled in this analysis, is presented in figure A-3. The transfer functions representing the A-7 airplane's response to pilot force commands are presented in table A-III.

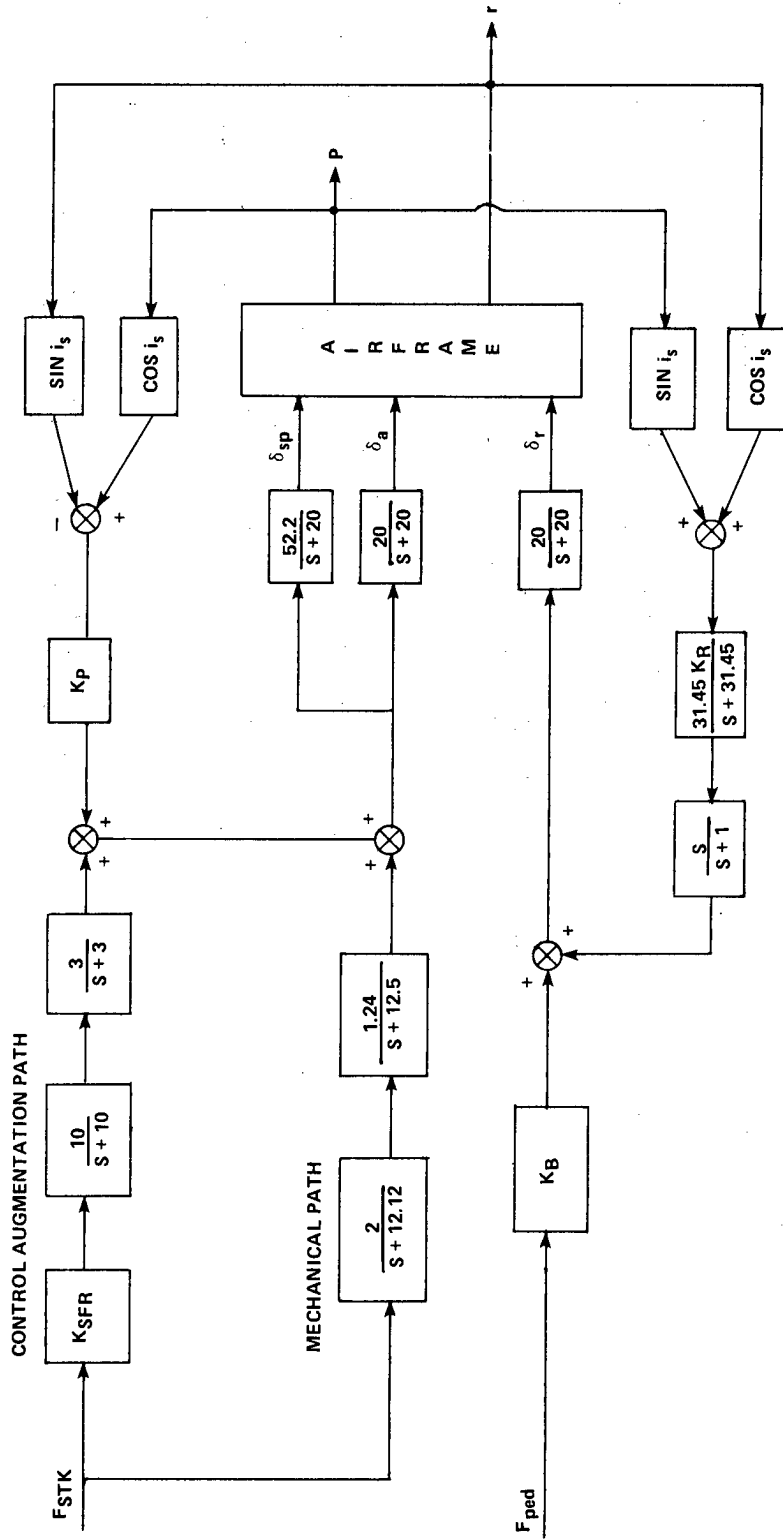


Figure A-3. A-7 Lateral-Directional Control System

TABLE A-III
A-7 AIRPLANE TRANSFER FUNCTIONS

<u>CONFIGURATION</u>	<u>ALTITUDE (ft)</u>	<u>AIR SPEED (M/KEAS)</u>	<u>TRANSFER FUNCTIONS</u>
CR	15,000	0.30/149	$\frac{\phi}{F_{STK}} = \frac{2886. (32.16) (18.8) (1.26) [.996, 11.99] [.30, 1.17]}{(32.14) (18.86) (19.57) (12.5) (10.0) (12.12) (3.0) (1.018) (1.525) (.045) [.34, 1.58]}$
			$\frac{\beta}{F_{ped}} = \frac{.00061 (31.45) (65.08) (19.68) (12.12) (12.5) (10.0) (3.0) (1.485) (1.0) (-.029)}{(32.14) (18.86) (19.57) (12.5) (10.0) (12.12) (3.0) (1.018) (1.525) (.045) [.34, 1.58]}$
CR	15,000	0.60/298	$\frac{\phi}{F_{STK}} = \frac{13540. (15.77) (33.64) [.996, 11.99] [1.595] [.56, 2.02]}{(33.57) (16.36) (17.28) (12.5) (12.12) (10.0) (5.015) (1.648) (3.0) (.0027) [.50, 2.0]}$
			$\frac{\beta}{F_{ped}} = \frac{.0011 (-.0008) (1.0) (3.0) (5.073) (10.0) (12.12) (12.5) (17.63) (31.45) (113.2)}{(33.57) (16.36) (17.28) (12.5) (12.12) (10.0) (5.015) (1.648) (3.0) (.0027) [.50, 2.0]}$
CR	15,000	0.90/447	$\frac{\phi}{F_{STK}} = \frac{18550. [.58, 4.13] (34.58) (13.27) [.996, 11.99] (1.209)}{[.57, 3.85] [.992, 14.2] (34.52) (12.12) (12.5) (11.49) (10.0) (3.0) (1.306) (.0158)}$
			$\frac{\beta}{F_{ped}} = \frac{.0011 (.0019) (1.0) (3.0) (10.0) (12.12) (12.5) (31.45) (169.9) [.995, 13.15]}{[.57, 3.85] [.992, 14.2] (34.52) (12.12) (12.5) (11.49) (10.0) (3.0) (1.306) (.0158)}$

F-14 — The F-14 airplane is a twin turbo-fan powered, land and carrier based, supersonic fighter aircraft. Lateral directional control is accomplished via an irreversible mechanical flight control system which transmits cockpit control commands to a differential stabilizer, spoilers, and rudders. The airplane's basic stability is augmented through the feedback of roll rate, yaw rate, and lateral acceleration to obtain the desired response. A block diagram of the F-14's lateral directional control system, as modelled in this analysis, is presented in figure A-4. The transfer functions representing the F-14's response to cockpit control inputs are presented in table A-IV.

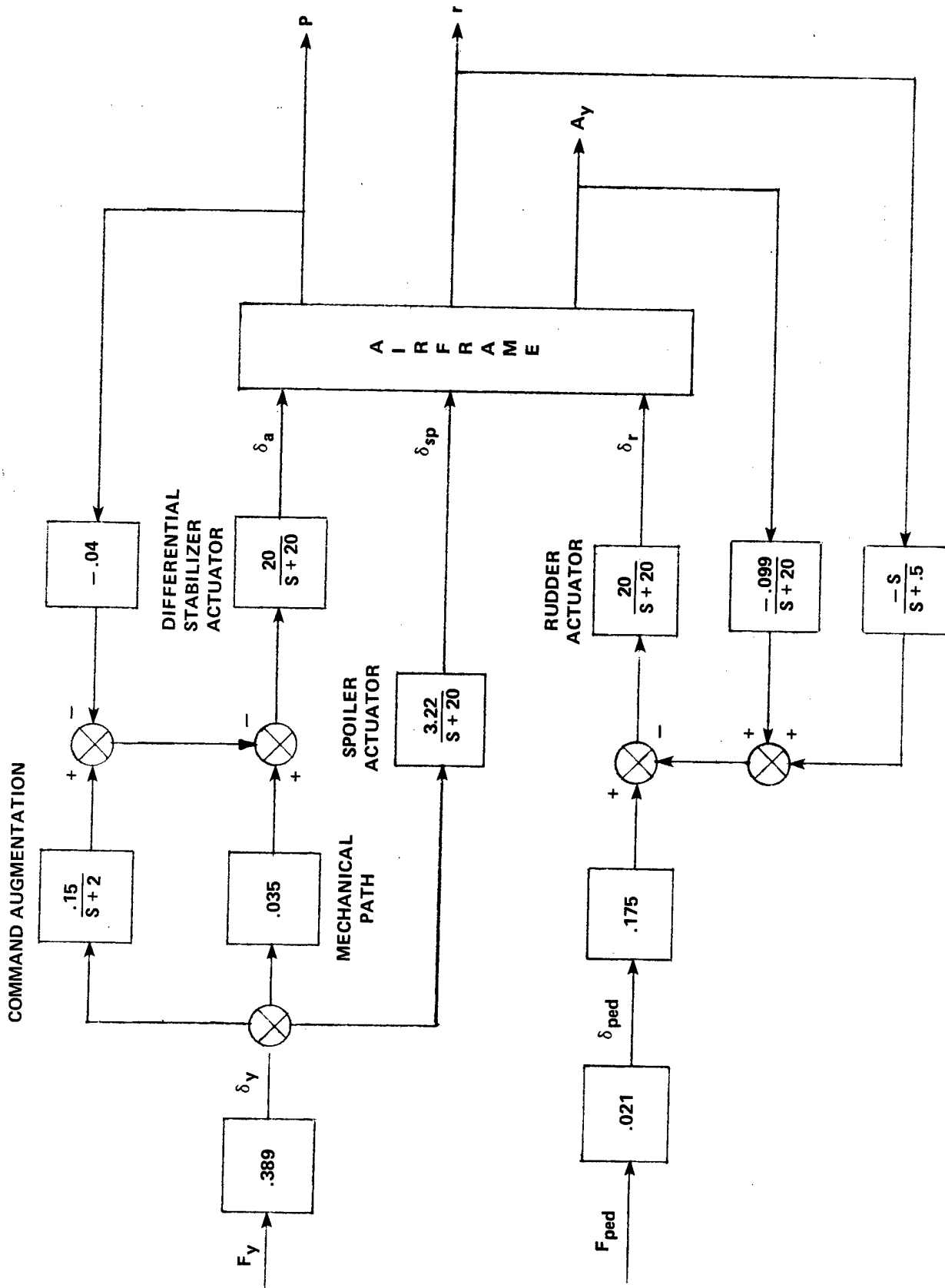


Figure A-4. F-14 Lateral-Directional Control System

TABLE A-IV
F-14 AIRPLANE TRANSFER FUNCTIONS

<u>CONFIGURATION</u>	<u>ALTITUDE (ft)</u>	<u>AIRSPEED (M/KEAS)</u>	<u>TRANSFER FUNCTIONS</u>
CR	15,000	0.40/199	$\frac{\phi}{F_y} = \frac{13.19 (24.66) (13.49) (20.0) (.927) (3.57) [.70, 1.28]}{(24.55) (13.54) (19.65) (20.0) (2.781) (-.016) (2.0) (1.35) [.61, 1.07]}$
			$\frac{\beta}{F_{ped}} = \frac{.111 (49.09) (19.69) (2.577) (-.029) (2.0) (.50) (20.0) (20.0)}{(24.55) (13.54) (19.65) (20.0) (2.781) (-.016) (2.0) (1.35) [.61, 1.07]}$
CR	15,000	0.715/355	$\frac{\phi}{F_y} = \frac{45.41 (.608) (8.13) (3.82) (20.0) (27.2) [.73, 3.56]}{(.697) (2.0) (-.003) (9.1) (18.3) (4.77) (20.0) (26.97) [.72, 3.19]}$
			$\frac{\beta}{F_{ped}} = \frac{.147 (.50) (-.007) (4.99) (2.0) (18.41) (66.06) (20.0) (20.0)}{(.697) (2.0) (-.003) (9.1) (18.3) (4.77) (20.0) (26.97) [.72, 3.19]}$
CR	15,000	0.795/395	$\frac{\phi}{F_y} = \frac{46.80 (4.76) (.581) (7.17) (20.0) (27.39) [.69, 4.32]}{(.65) (2.0) (-.001) (8.54) (17.31) (5.51) (20.0) (27.15) [.68, 3.91]}$
			$\frac{\beta}{F_{ped}} = \frac{.143 (.50) (-.005) (5.96) (2.0) (20.0) (20.0) (17.51) (76.6)}{(.65) (2.0) (-.001) (8.54) (17.31) (5.51) (20.0) (27.15) [.68, 3.91]}$

TABLE A-IV (Continued)
F-14 AIRPLANE TRANSFER FUNCTIONS

<u>CONFIGURATION</u>	<u>ALTITUDE (ft)</u>	<u>AIRSPEED (M/KEAS)</u>	<u>TRANSFER FUNCTIONS</u>
CR	15,000	0.910/452	$\frac{\phi}{F_y} = \frac{42.0 (.554) (7.94) (6.29) (20.0) (27.22) [.58, 4.74]}{(.59) (2.0) (.0003) (9.61) (16.30) (5.05) (20.0) (27.0) [.53, 4.39]}$ $\frac{\beta}{F_{ped}} = \frac{.12 (.50) (-.002) (5.63) (2.0) (16.49) (90.68) (20.0) (20.0)}{(.59) (2.0) (.0003) (9.61) (16.30) (5.05) (20.0) (27.0) [.53, 4.39]}$
PA(1)(1)	SL	.19/126	$\frac{\phi}{F_y} = \frac{5.983 [.46, .921] (.709) (3.493) (23.11) (16.22) (20.0)}{[.361, 1.069] (.855) (1.665) (-.058) (2.0) (20.0) (23.11) (16.22) (19.87)}$ $\frac{\beta}{F_{ped}} = \frac{.094 (.50) (-.161) (2.0) (1.672) (22.93) (19.87) (20.0) (20.0)}{[.361, 1.069] (.855) (1.665) (-.058) (2.0) (20.0) (23.11) (16.22) (19.87)}$

Notes: (1) Direct Lift Control (DLC) ON

F-18 — The F-18 is a single place, turbo powered, land and carrier based, fighter aircraft controlled by a digital flight control system. Separate flight control laws are provided for differing flight regimes. Electrical signals are generated from the pilot's control force inputs, passed to the computer, modified by various gains and shaping networks, and finally passed to the rudder, alleron, and differential tail. Lateral acceleration, roll rate, and yaw rate signals are also input to the computer, where they are shaped and gain scheduled before being summed with the command input signals. The cockpit control feel system dynamics were not included in this analysis. A simplified block diagram of the F-18's lateral directional control system, as modelled in this analysis, is presented in figure A-5. The transfer functions representing the airplane's response to pilot commands are presented in table A-V.

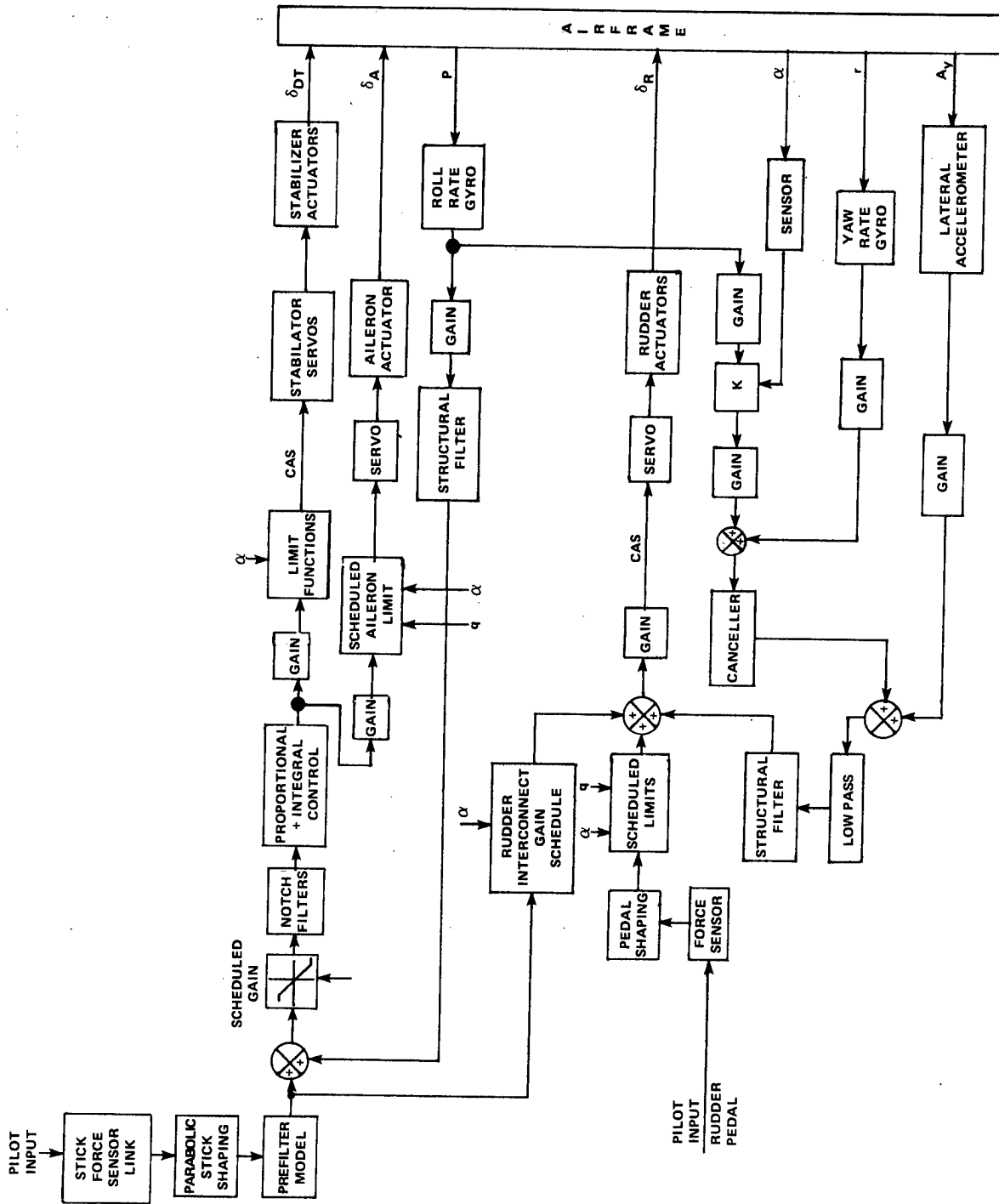


Figure A-5. F-18 Lateral-Directional Control System

TABLE A-V
 F-18 AIRPLANE TRANSFER FUNCTIONS

Configuration CR
 10,000 ft Altitude
 0.5 Mach/274 KEAS

$\frac{\phi}{\delta_{ap}}$	$\frac{.105 \times 10^7 (.64) [.61, 1.46] (2.05) (2.45) [.07, 44.0] (3.11) [.03, 107.0] [.3, 56.6] [.66, 35.1] (46.8) [.69, 71.5] (51.2) [.8, 90.0] (-0032) (.54) [.59, 1.6] (2.03) (2.03) (3.04) (6.67) (6.84) [.33, 52.4] (20.1) [.65, 34.3] [.57, 58.5] [.69, 71.1] [.59, 89.5] [.97, 57.5] (59.3) [.73, 113.4]}$
$\frac{\beta}{\delta_{rp}}$	$\frac{44.8 (-008) (.557) (.938) (1.995) (2.417) (6.622) (6.67) [.33, 52.0] (20.6) [.69, 36.7] [.53, 56.2] (48.6) [.91, 59.0] [.62, 90.0] (56.6) [.69, 116.0] (-0032) (.539) [.59, 1.6] (2.03) (2.03) (3.04) (6.67) (6.84) [.33, 52.0] (20.1) [.65, 34.3] [.57, 58.5] [.69, 71.1] [.59, 89.5] [.97, 57.5] (59.3) [.73, 113.4]}$

APPENDIX B

SUMMARY OF EQUIVALENT SYSTEM MODELS

The equivalent system results for the S-3, A-6, A-7 and F-14 configurations investigated are summarized. (The single F-18 configuration investigated is presented in the body of the report.) The identified modal parameters and quantitative mismatch values are presented in tables B-1 through B-IV, respectively. Graphical comparisons of high- and low-order frequency and time responses, for those configurations not previously shown in the Results and Discussion section, are presented in figures B-1 through B-18.

TABLE B-1
S-3 AIRCRAFT EQUIVALENT PARAMETER RESULTS

CRUISE CONFIGURATION – 15,000 FT ALTITUDE						
0.36 Mach				0.71 Mach		
	APPROX		COMP	APPROX		COMP
	P	β	$\phi + \beta$	P	β	$\phi + \beta$
K_ϕ	58.3	—	54.0	65.7	—	53.9
ζ_ϕ	—	—	.37	—	—	.59
ω_ϕ	—	—	2.00	—	—	3.25
t_ϕ	.069	—	.060	.049	—	.032
K_β	—	24.4	.384	—	70.7	.554
$\tau_{\beta 1}$	—	—	- 60.64*	—	—	-1605.01*
$\tau_{\beta 2}$	—	—	.400	—	—	.327
$\tau_{\beta 3}$	—	—	.015*	—	—	.007*
t_β	—	.013	.034	—	.024	.040
τ_r	.312	—	.355	.183	—	.248
τ_s	—	—	166.69*	—	—	119.6*
ζ_{DR}	—	.28	.29	—	.47	.52
ω_{DR}	—	2.14	2.08	—	3.71	3.43
M_ϕ	18.2	—	1.8	5.4	—	2.4
M_β	—	14.8	2.2	—	4.3	1.8

*Parameter fixed at HOS value

$$\phi/\delta Y_p = \frac{815.4 (.343) (90.52) (26.55) [.53, 3.89]}{(.369) (.008) (6.219) (22.52) (46.0) (26.69) [.51, 3.74]}$$

$$\phi/\delta Y_p = \frac{53.9 [.59, 3.25] e^{-.032}}{(.0084) (4.03) [.52, 3.43]}$$

M=2.4

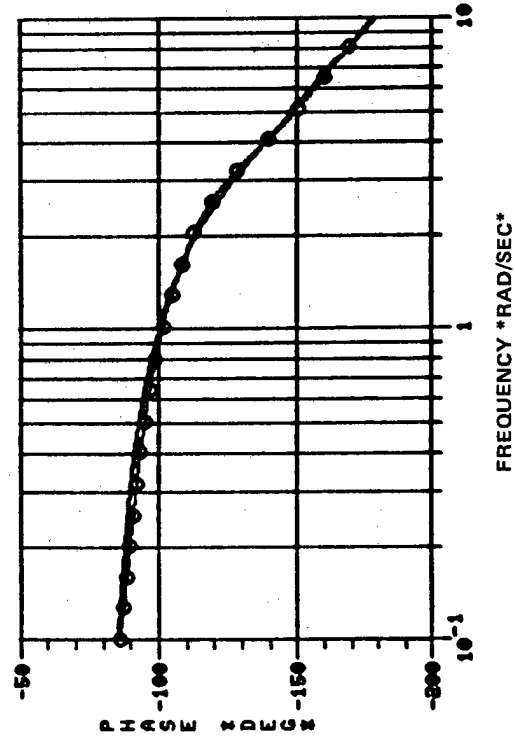
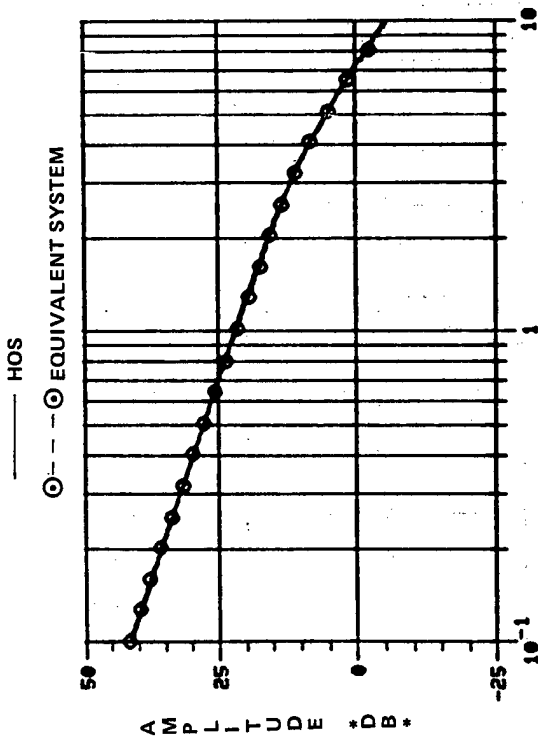
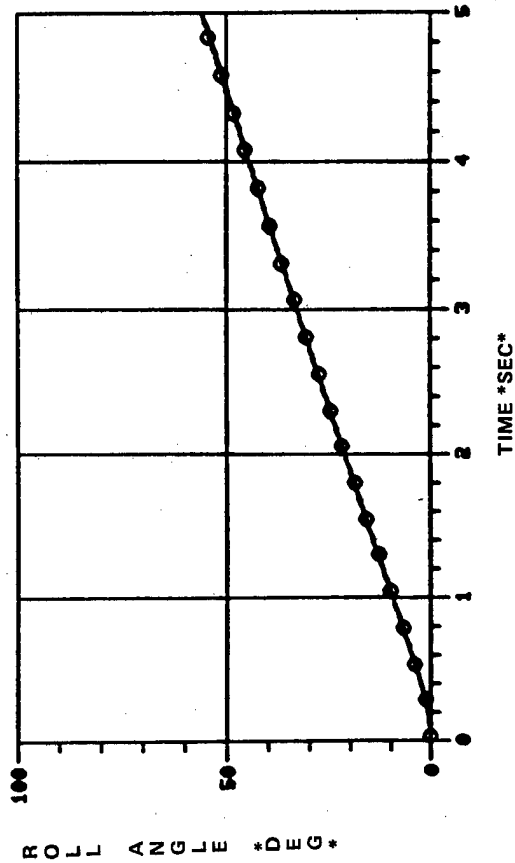
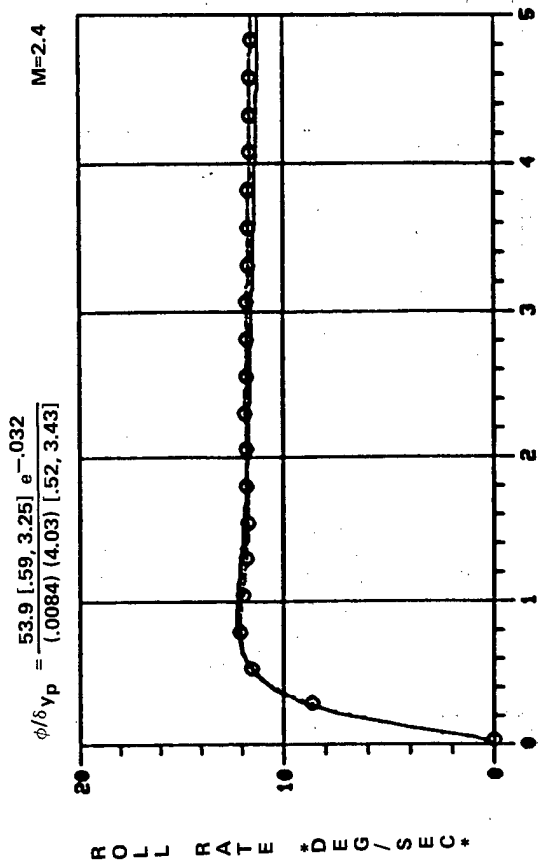


Figure B-1. S-3 Roll Response — Simultaneous Match — .71 Mach

$$\beta/b_{ped} = \frac{13.32 (.333) (-.0006) (151.8) (6.241) (46.0) (22.25)}{(.369) (.008) (6.219) (26.89) (46.0) (22.52) [.51, 3.74]}$$

$$\beta/b_{ped} = \frac{.554 (-.0006) (3.06) (151.8) e^{-.040}}{(.0084) (4.03) [.52, 3.43]}$$

M=1.8

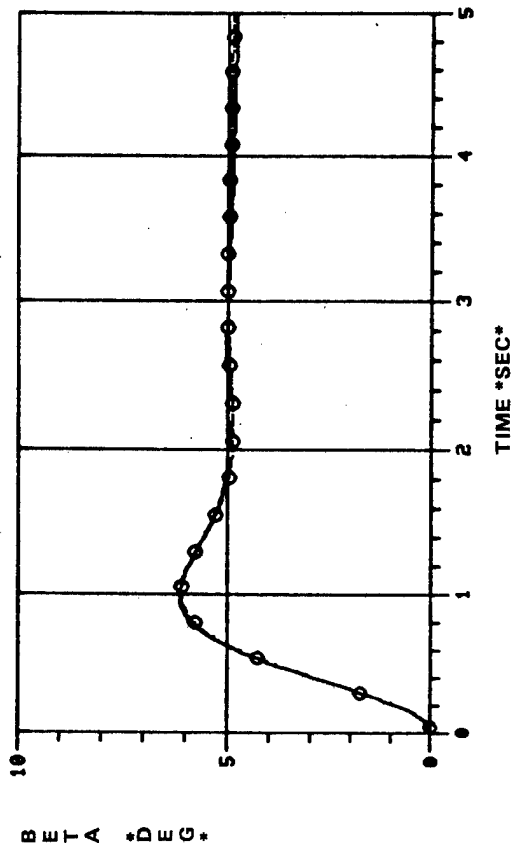
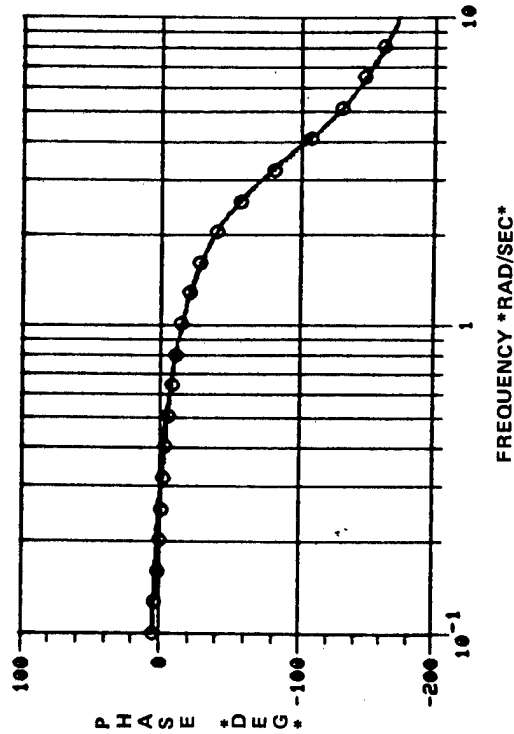
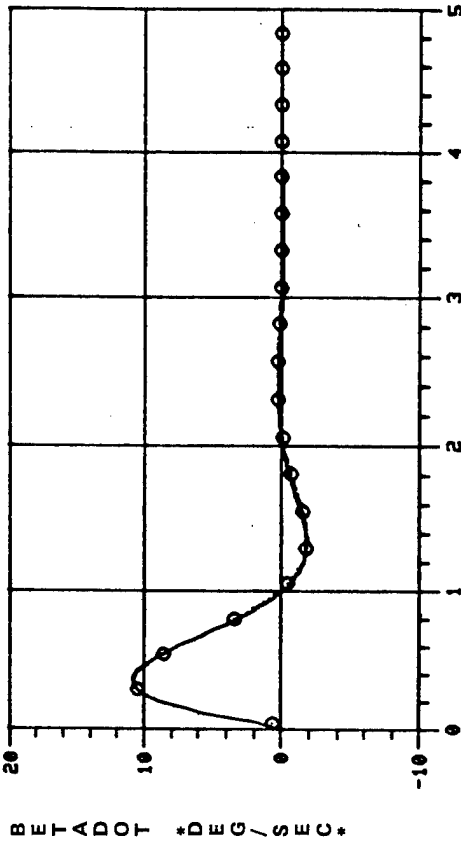
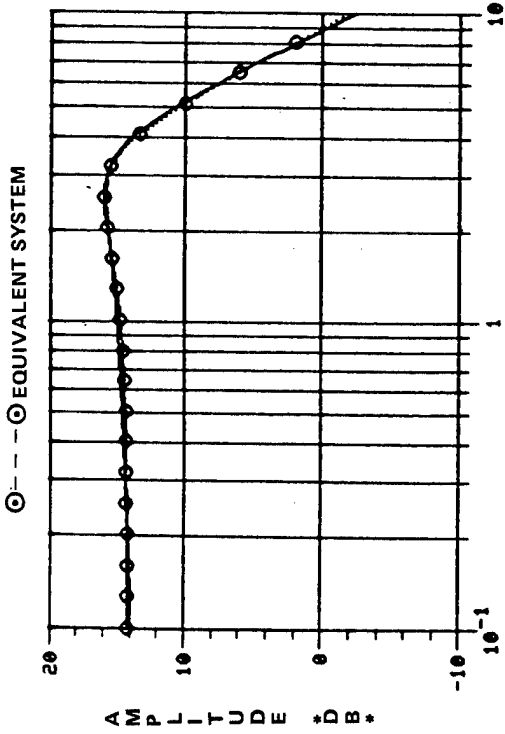


Figure B-2. S-3 Sideslip Response — Simultaneous Match — .71 Mach

TABLE B-II

A-6 AIRCRAFT EQUIVALENT PARAMETER RESULTS

CRUISE CONFIGURATION – 20,000 ft ALTITUDE									
	0.40 Mach			0.72 Mach			0.87 Mach		
	APPROX		COMP	APPROX		COMP	APPROX		COMP
	ϕ	β	$\phi + \beta$	ϕ	β	$\phi + \beta$	ϕ	β	$\phi + \beta$
K_ϕ	.670	—	.646	2.559	—	2.04	4.26	—	3.35
ζ_ϕ	—	—	.194	—	—	.473	—	—	.369
ω_ϕ	—	—	1.56	—	—	2.04	—	—	2.80
t_ϕ	.0076	—	.0077	.0144	—	0	.022	—	.007
K_β	—	.0293	.0003	—	.859	.0068	—	1.004	.0066
τ_{β_1}	—	—	131.58 *	—	—	166.67 *	—	—	175.44 *
τ_{β_2}	—	—	.692	—	—	1.055	—	—	.417
τ_{β_3}	—	—	.010 *	—	—	.007 *	—	—	.006 *
t_β	—	.025	.042	—	.036	.055	—	.033	.048
τ_r	.461	—	.642	.278	—	.873	.166	—	.349
τ_s	—	—	105.26 *	—	—	116.14 *	—	—	144.09 *
ζ_{DR}	—	.251	.299	—	.334	.440	—	.366	.420
ω_{DR}	—	1.736	1.71	—	3.063	2.99	—	3.584	3.46
M_ϕ	145.4	—	121.8	70.5	—	49.9	41.6	—	31.9
M_β	—	4.4	4.2	—	2.3	8.6	—	1.4	2.8

* Fixed Parameter

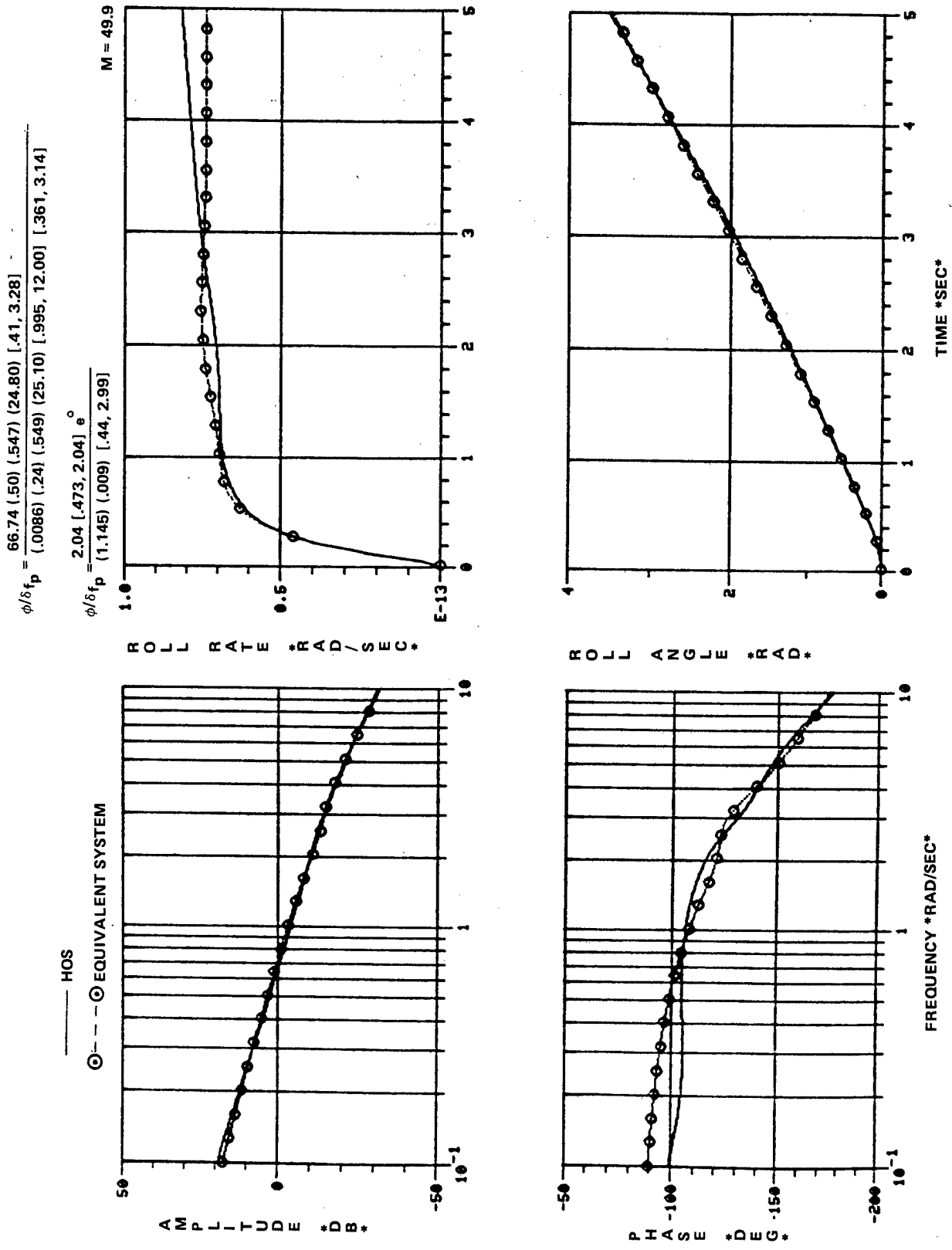


Figure B-3. A-6 Roll Response — Simultaneous Match, .72 Mach

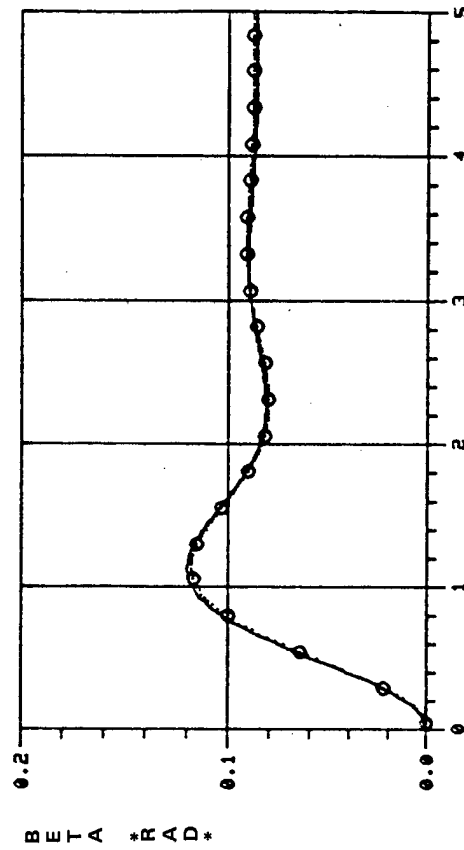
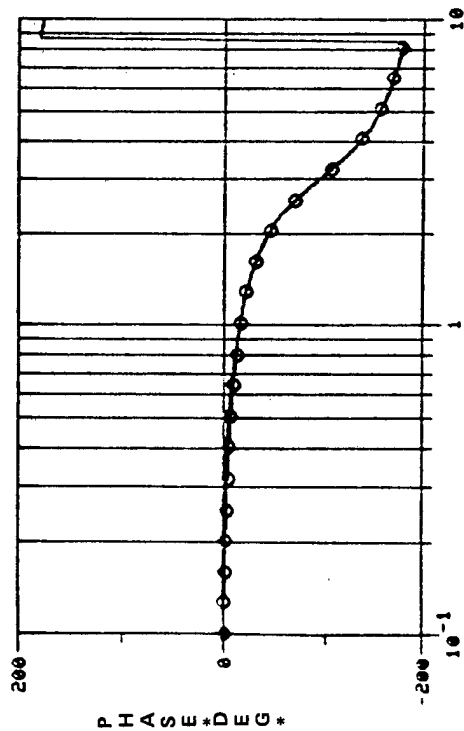
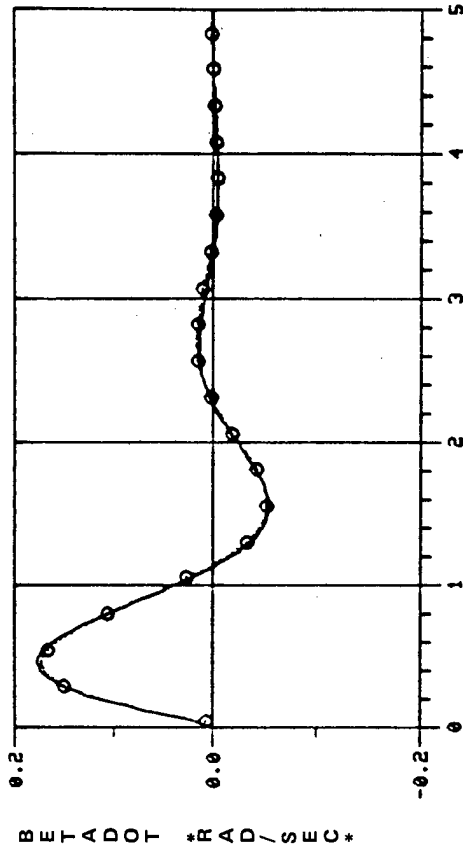
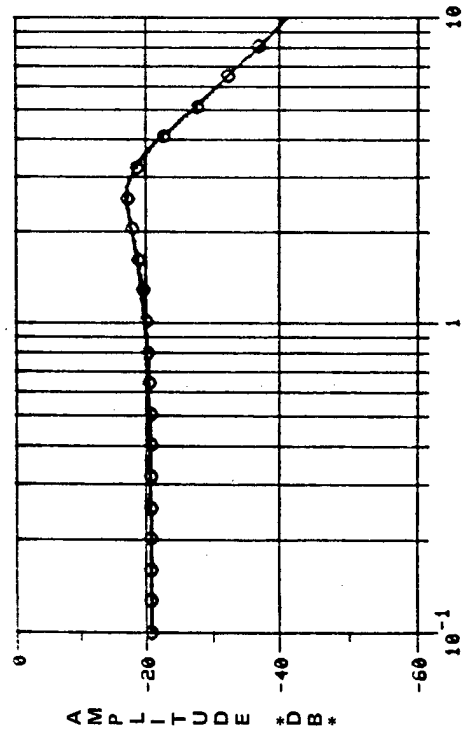
$$\beta/\delta_{ped} = \frac{.148 (.006) (.236) (.507) (141.8) [.928, 12.88]}{(-.0086) (.24) (.549) (25.10) [.995, 12.00] [.361, 3.14]}$$

$$\beta/\delta_{ped} = \frac{.0068 (.006) (.948) (142.86) e^{-.055}}{(1.145) (-.009) [.44, 2.99]}$$

M = 8.6

— HOS

○ --- ○ EQUIVALENT SYSTEM



FREQUENCY *RAD/SEC*

TIME *SEC*

Figure B-4. A-6 Sideslip Response — Simultaneous Match, .72 Mach

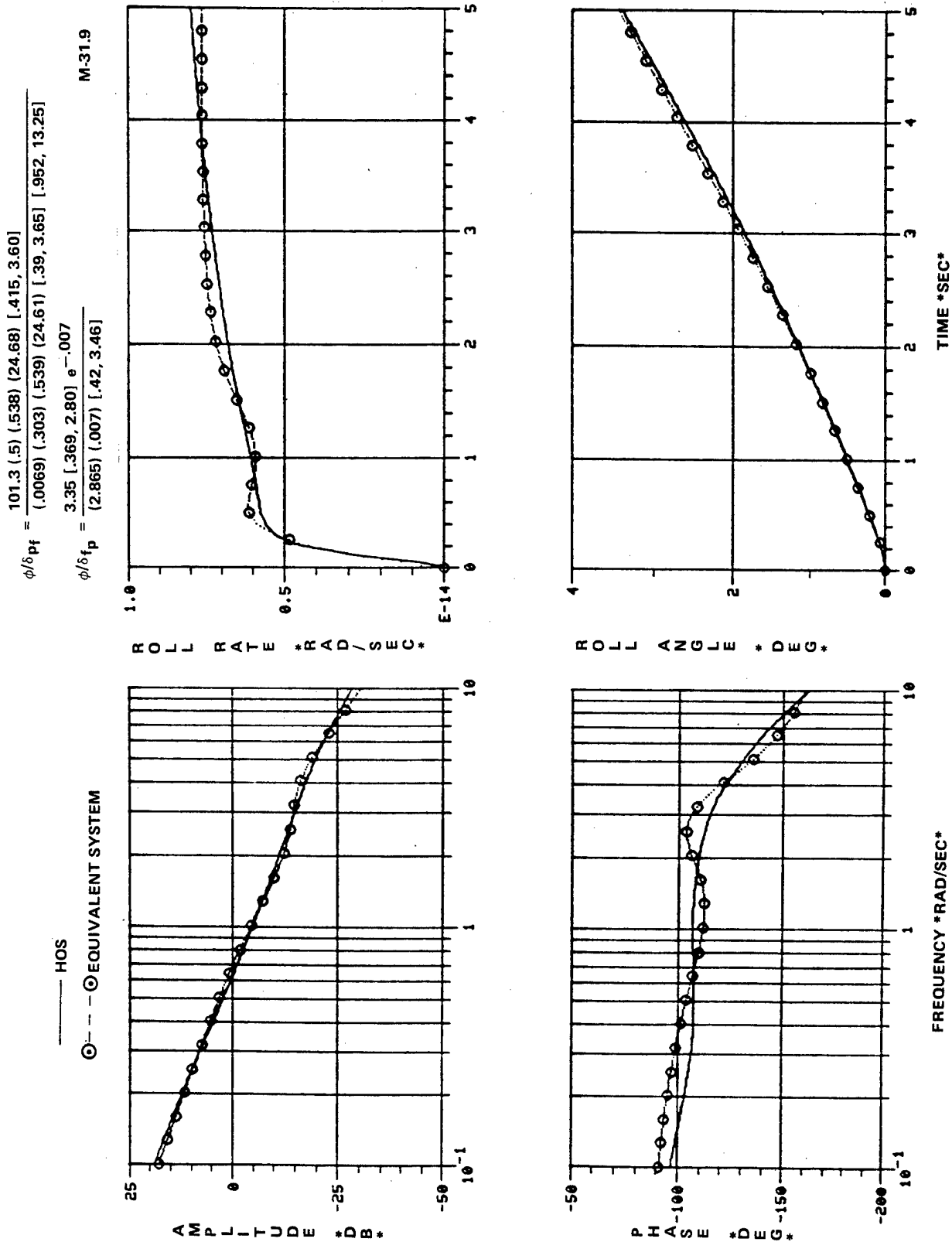


Figure B-5. A-6 Roll Response — Simultaneous Match, .87 Mach

$$\beta/\delta_{ped} = \frac{.156 (.0057) (.30) (.50) (157.8) [.924, 13.89]}{(.0069) (.303) (.539) (24.61) [.39, 3.65] [.952, 13.25]}$$

$$\beta/\delta_{ped} = \frac{.0066 (.006) (2.389) (166.67) e^{-.048}}{(.0069) (.303) (.539) (24.61) [.39, 3.65] [.952, 13.25]} \quad M = 2.8$$

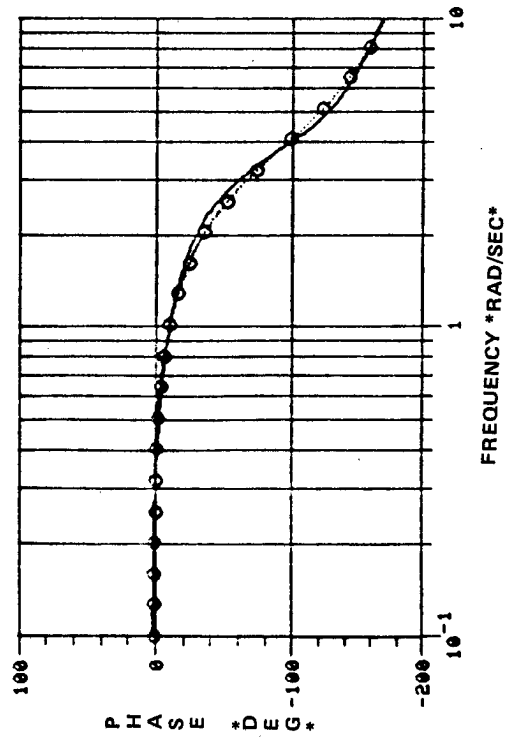
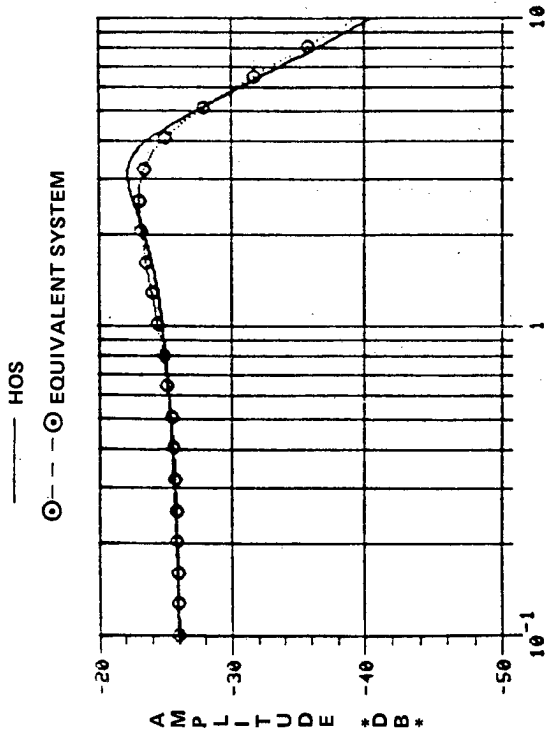
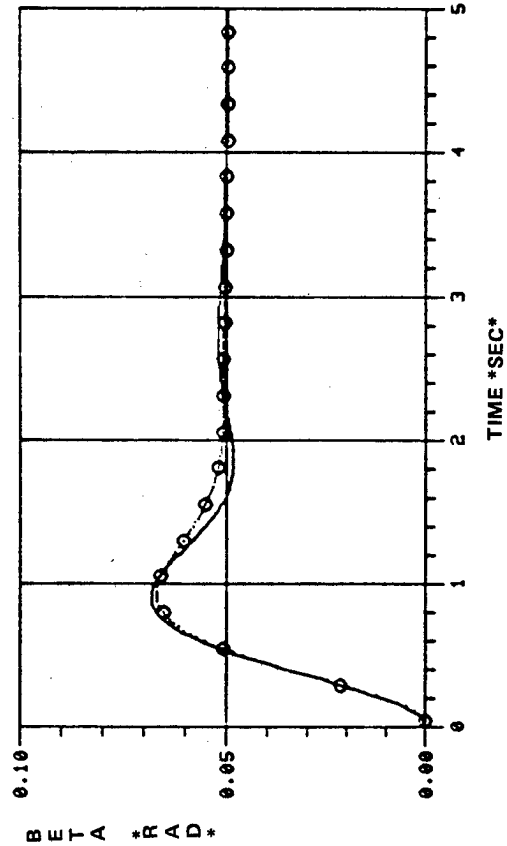
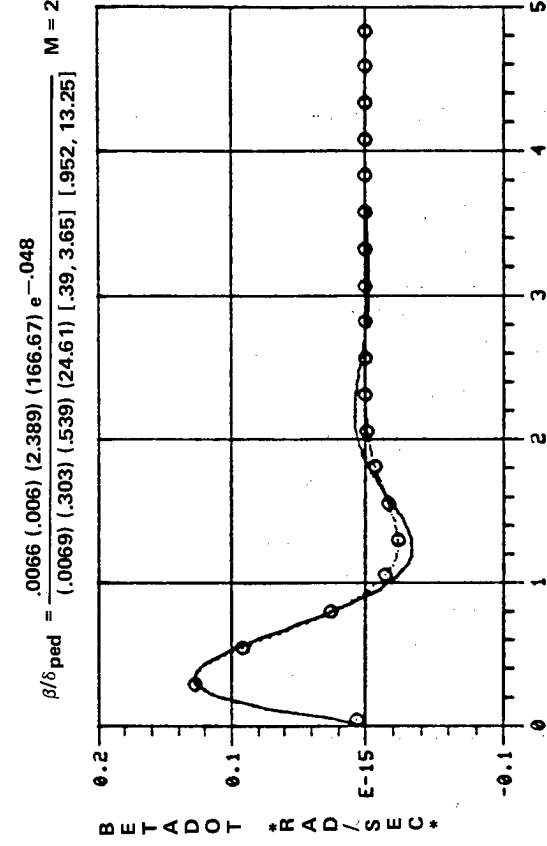


Figure B-6. A-6 Sideslip Response — Simultaneous Match, .87 Mach

TABLE B-III

A-7 AIRCRAFT EQUIVALENT PARAMETER RESULTS

CRUISE CONFIGURATION – 15,000 ft ALTITUDE									
	0.30 Mach			0.60 Mach			0.90 Mach		
	APPROX ϕ	β	COMP $\phi + \beta$	APPROX ϕ	β	COMP $\phi + \beta$	APPROX ϕ	β	COMP $\phi + \beta$
K_ϕ	2.49	—	1.87	7.9	—	5.97	7.2	—	5.19
ζ_ϕ	—	—	.51**	—	—	.69**	—	—	.66**
ω_ϕ	—	—	1.64**	—	—	2.56**	—	—	4.64**
t_ϕ	.267	—	.247	.237	—	.205	.202	—	.166
K_β	—	.002	.00003	—	.0061	.00006	—	.010	.00006
$\tau_{\beta 1}$	—	—	-34.5*	—	—	-1250.0*	—	—	526.3*
$\tau_{\beta 2}$	—	—	.72**	—	—	.64**	—	—	.51**
$\tau_{\beta 3}$	—	—	.015*	—	—	.009*	—	—	.006*
t_β	—	.025	.032	—	.032	.045	—	.038	.052
τ_r	.73	—	1.24	.60	—	.59	.50	—	.44
τ_s	—	—	22.2*	—	—	370.4*	—	—	63.29*
ζ_{DR}	—	.29	.25	—	.40	.42	—	.45	.50
ω_{DR}	—	1.60	1.83	—	2.29	2.27	—	3.80	3.69
M_ϕ	266.1	—	109.5	84.8	—	31.2	45.3	—	6.7
M_β	—	75.8	33.3	—	10.4	7.6	—	9.2	2.2

*Parameter fixed at HOS value

**Parameter iteratively fixed in matching process

$\phi/F_{STK} = 2886 (32.16) (18.8) (1.26) [.996, 11.99] [.30, 1.17]$
 $(32.14) (18.86) (19.57) (12.5) (10.0) (12.12) (3.0) (1.018) (1.525) (.045) [.34, 1.58]$

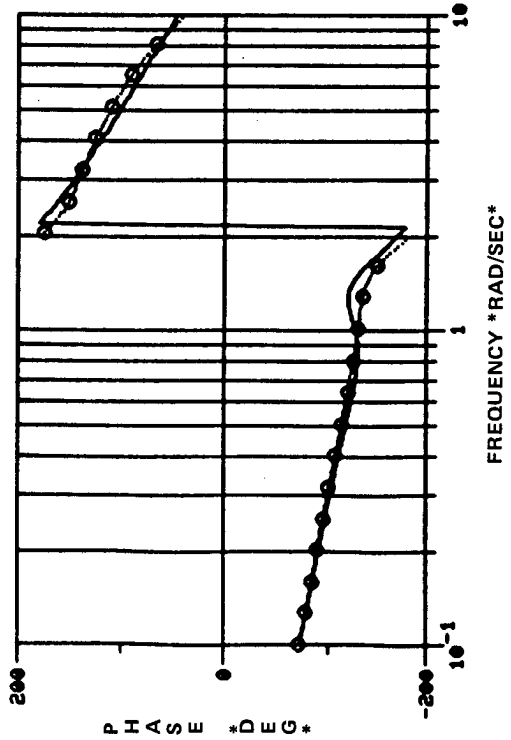
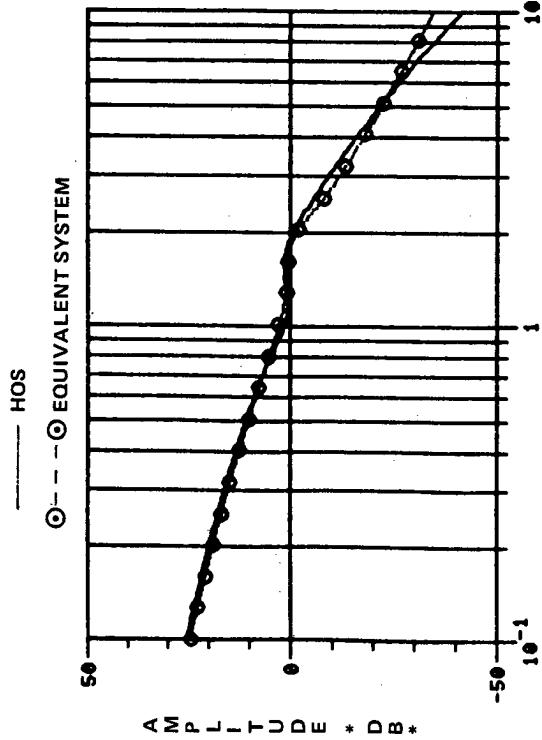
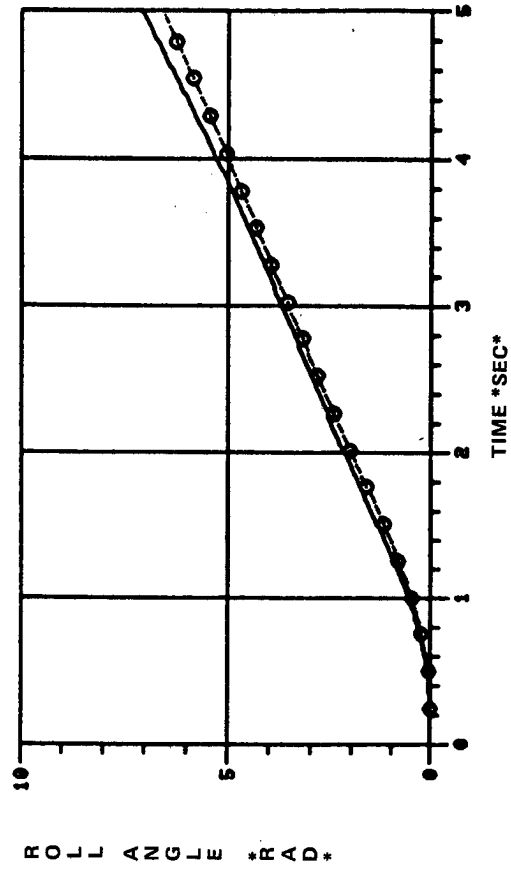
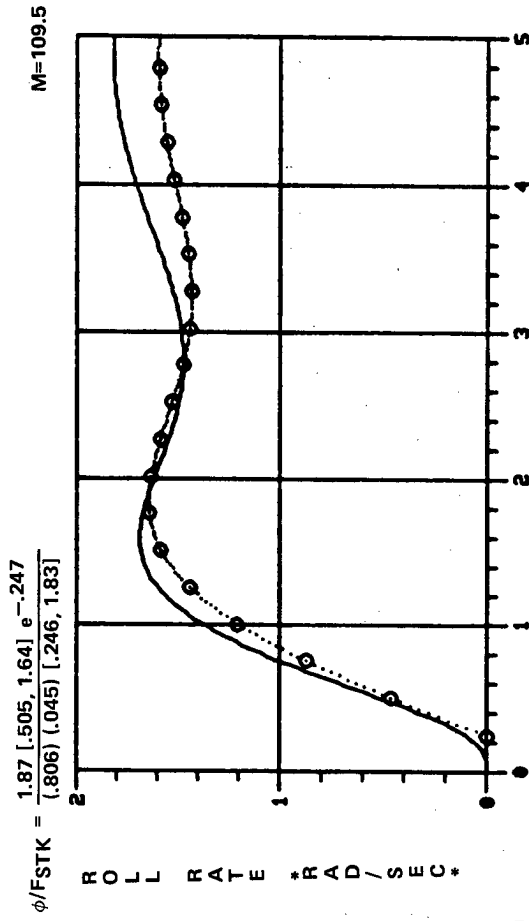


Figure B-7. A-7 Roll Response — Simultaneous Match, .3 Mach

$$\beta/F_{ped} = \frac{.00061 (31.45) (65.08) (19.68) (12.12) (12.5) (10.0) (3.0) (1.485) (1.0) (-.029)}{(32.14) (18.86) (19.57) (12.5) (10.0) (12.12) (3.0) (1.018) (1.525) (.045) [.34, 1.58]}$$

$$\beta/F_{ped} = \frac{.000026 (-.029) (1.395) (66.67) e^{-.032}}{(.806) (.045) [.246, 1.83]}$$

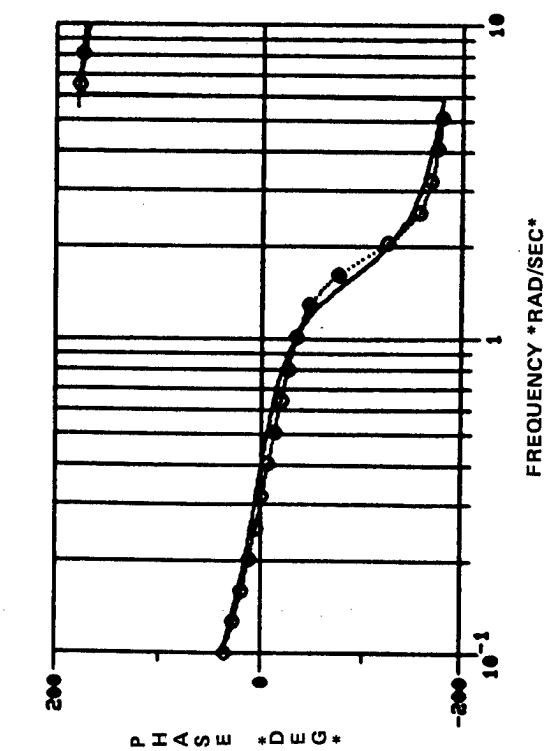
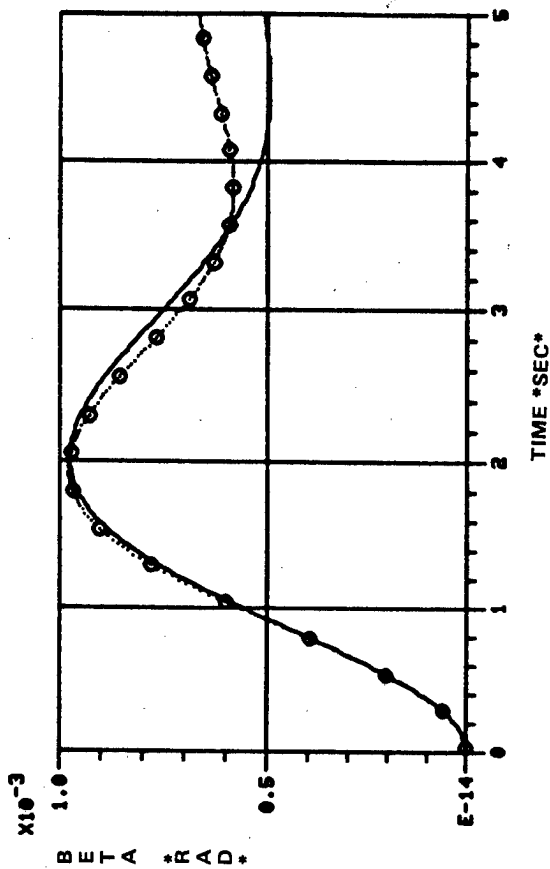
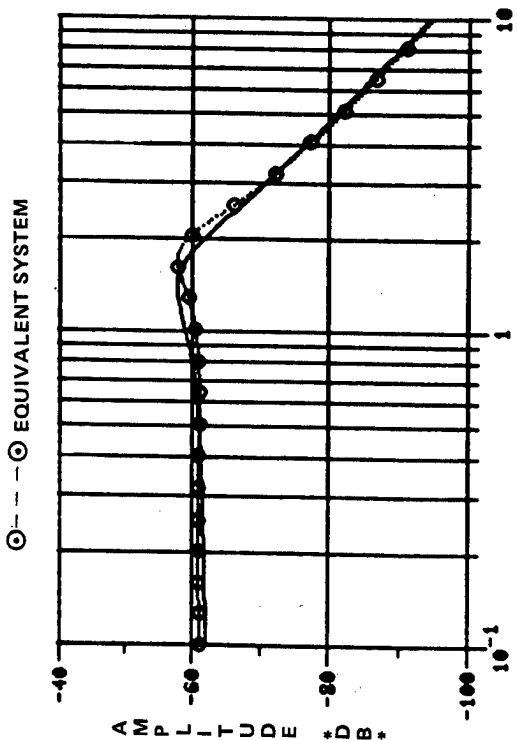
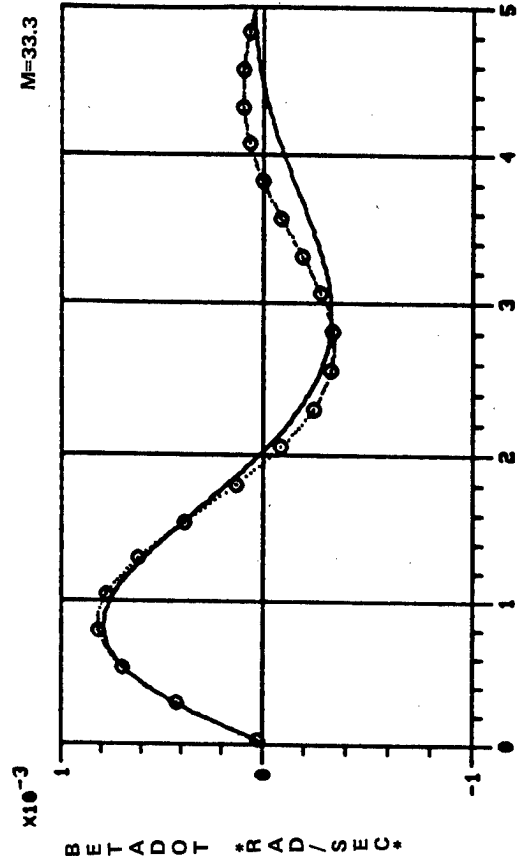


Figure B-8. A-7 Sideslip Response — Simultaneous Match, .3 Mach

$$\phi/FSTK = \frac{18550}{[.57, 3.85]} [4.13, 34.58] [13.27, .996, 11.99] [1.209]$$

$$\phi/FSTK = \frac{5.19}{(2.288)} [659, 4.636] e^{-.166} [503, 3.689]$$

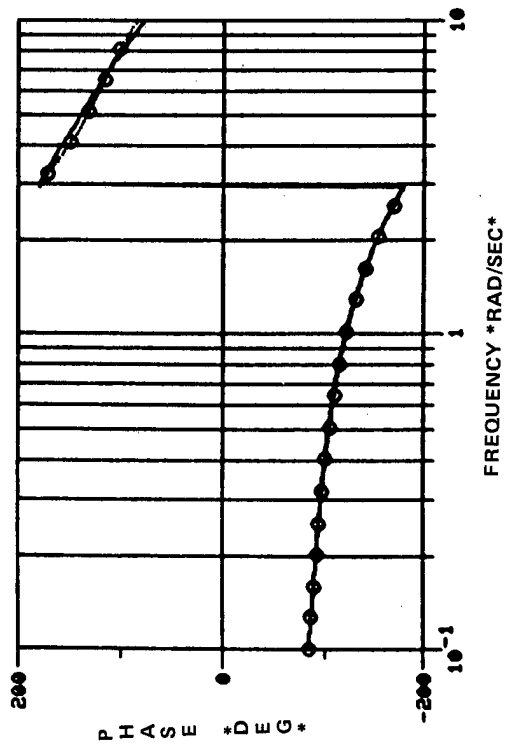
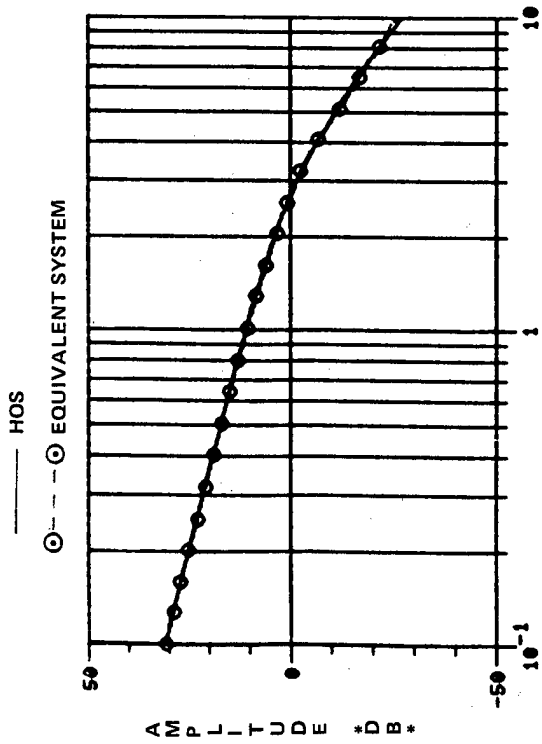
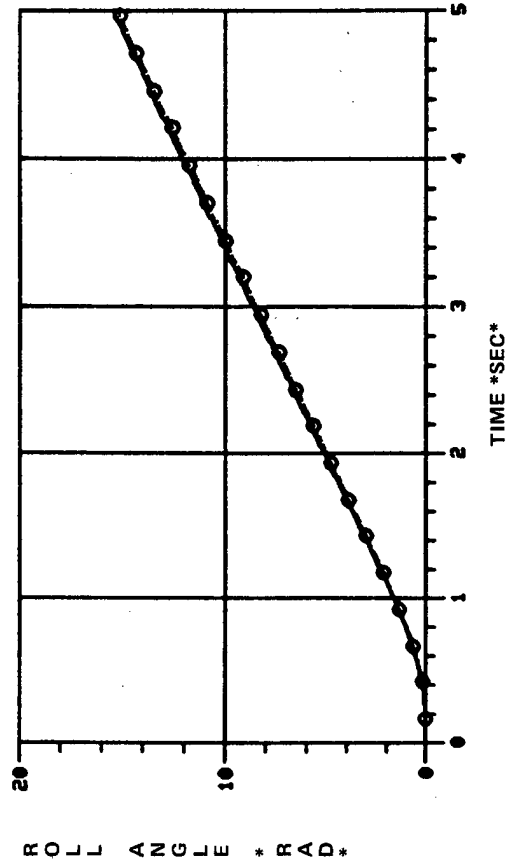
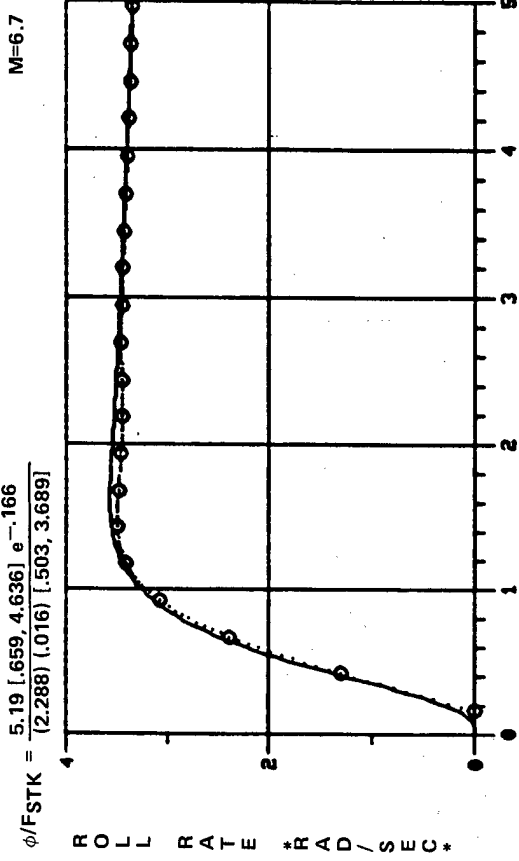


Figure B-9. A-7 Roll Response — Simultaneous Match, .9 Mach

$$\beta/F_{ped} = \frac{.0011 (.0019) (1.0) (3.0) (10.0) (12.12) (12.5) (31.45) (169.9) (.995, 13.15)}{[.57, 3.85] [.992, 14.2] (34.52) (12.12) (12.5) (11.49) (10.0) (3.0) (1.306) (.0158)}$$

$$\beta/F_{ped} = \frac{.000064 (.0019) (1.958) (166.67) e^{-.052}}{[2.288] (.016) [.503, 3.689]} \times 10^{-2}$$

HOS

○ --- ○ EQUIVALENT SYSTEM

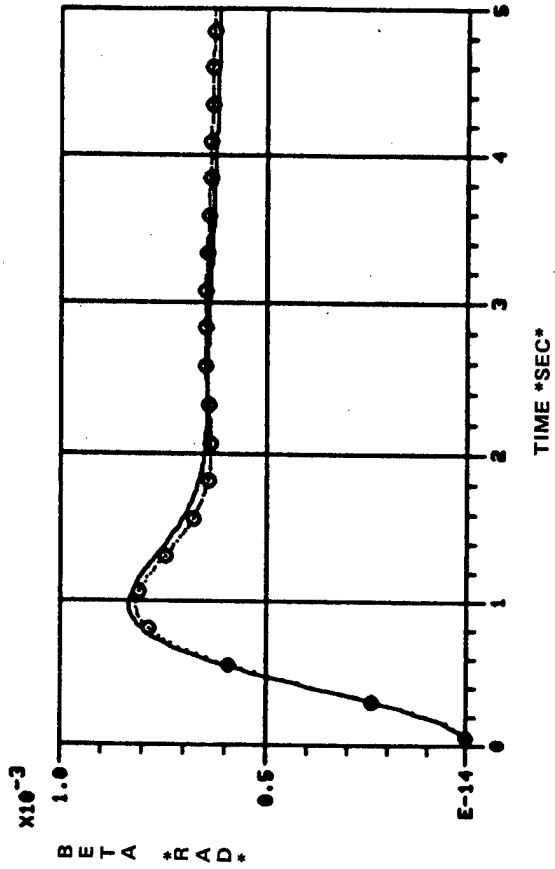
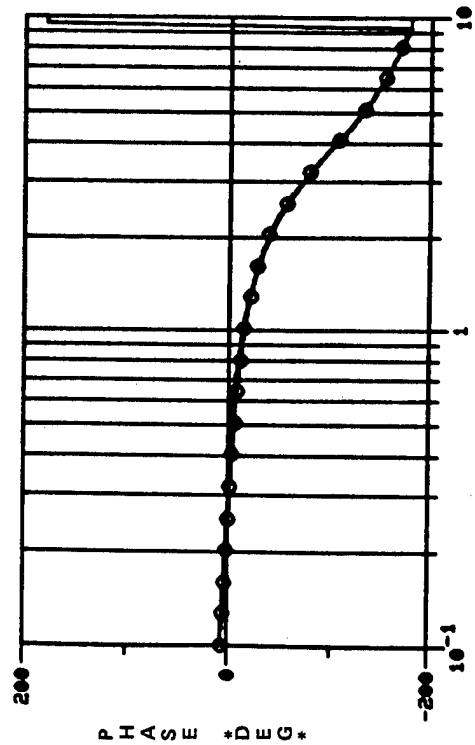
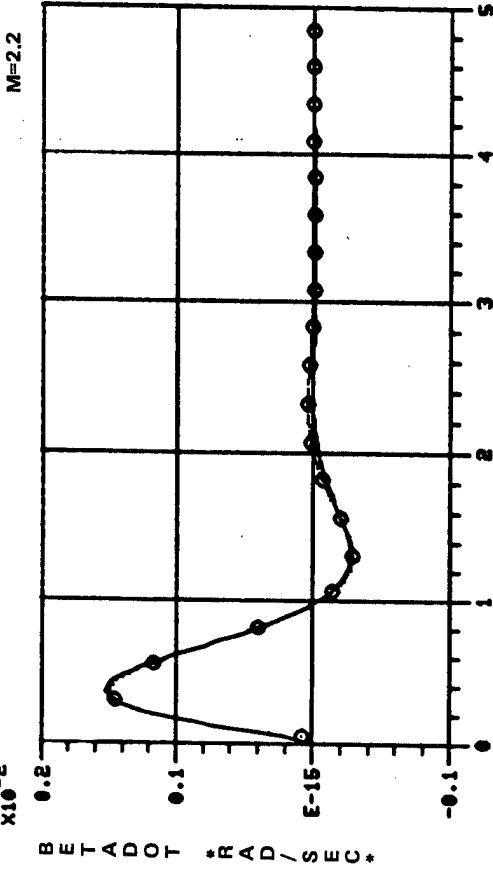
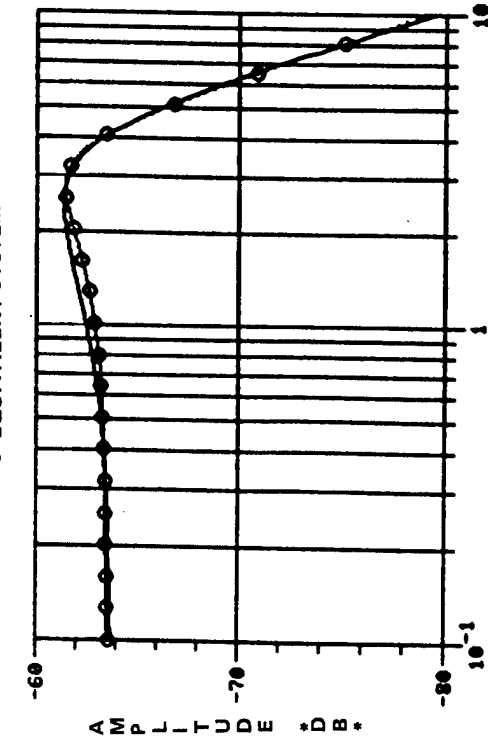


Figure B-10. A-7 Sideslip Response - Simultaneous Match, .9 Mach

TABLE B-IV
F-14 AIRCRAFT EQUIVALENT PARAMETER RESULTS

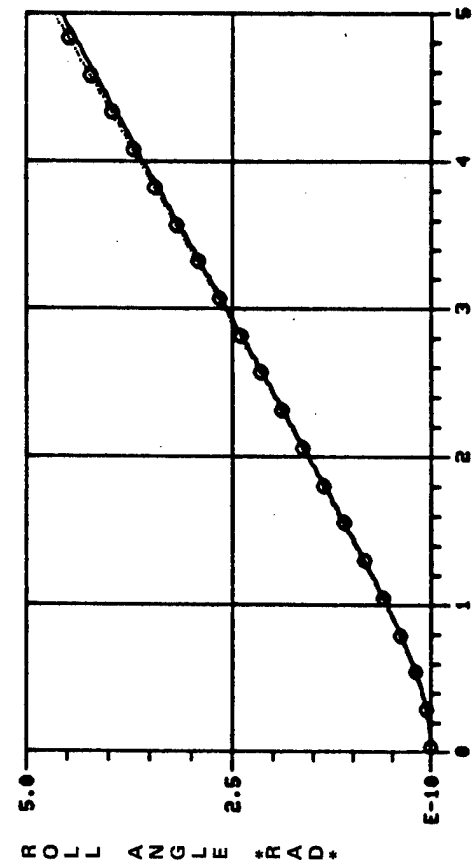
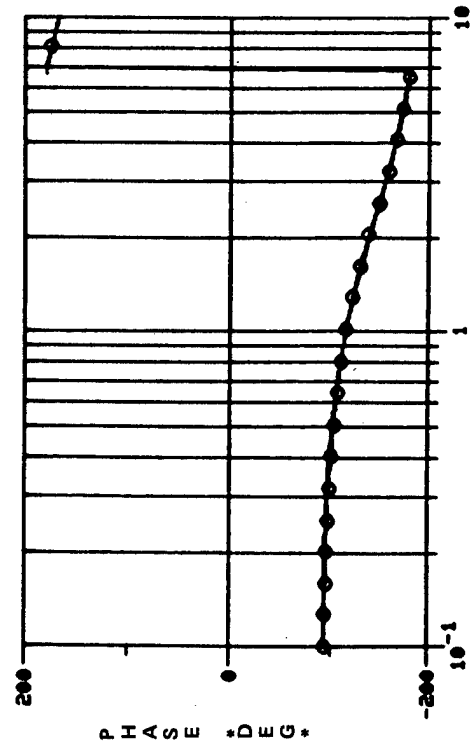
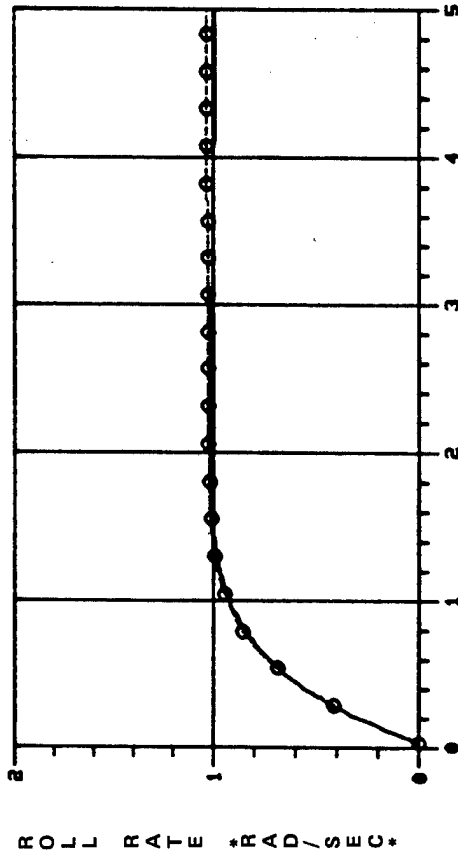
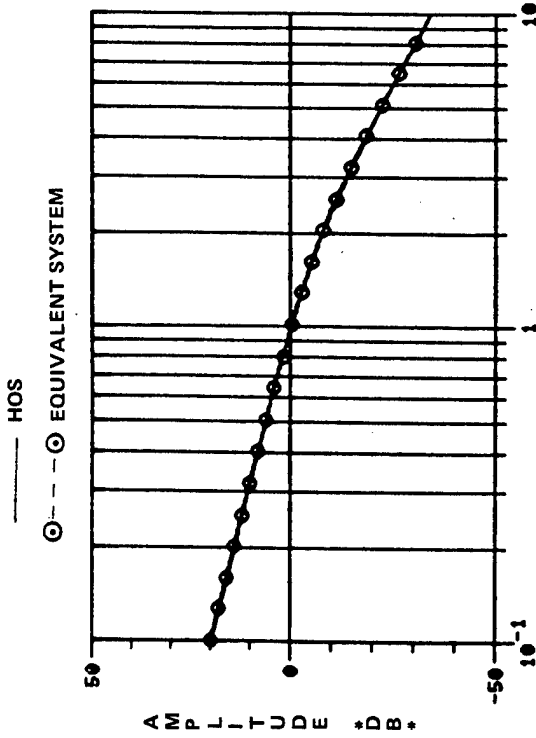
	CRUISE CONFIGURATION - 15,000 ft ALTITUDE															PA CONFIGURATION - SEA LEVEL		
	0.40 Mach			0.715 Mach			0.795 Mach			0.91 Mach			121 KEAS			APPROX P	APPROX β	COMP $\phi + \beta$
	APPROX P	APPROX β	COMP $\phi + \beta$	APPROX P	APPROX β	COMP $\phi + \beta$	APPROX P	APPROX β	COMP $\phi + \beta$	APPROX P	APPROX β	COMP $\phi + \beta$	APPROX P	APPROX β	COMP $\phi + \beta$			
$K\phi$.683	-	.64	2.20	-	2.00	2.35	-	2.14	2.74	-	2.15	.374	-	.33			
$\zeta\phi$	-	-	.73	-	-	.78	-	-	.72	-	-	.64	-	-	.51			
$\omega\phi$	-	-	1.04	-	-	2.53	-	-	3.29	-	-	4.37	-	-	.90			
$t\phi$.054	-	.045	.046	-	.036	.048	-	.038	.072	-	.047	.076	-	.053			
$K\beta$	-	.267	.006	-	.586	.010	-	.682	.010	-	.688	.008	-	.111	.001			
$\tau\beta_1$	-	-	-34.48*	-	-	-142.9*	-	-	-200.0*	-	-	-500.0*	-	-	-6.02			
$\tau\beta_2$	-	-	1.94	-	-	.846	-	-	.671	-	-	.609	-	-	1.58			
$\tau\beta_3$	-	-	.020*	-	-	.015*	-	-	.013*	-	-	.011*	-	-	.008*			
$t\beta$	-	.020	.054	-	.041	.067	-	.045	.067	-	.049	.064	-	0	.018			
τ_r	.671	-	.701	.472	-	.489	.476	-	.466	.551	-	.549	.575	-	.973			
τ_s	-	-	-62.5*	-	-	-333.3*	-	-	-833.3*	-	-	-3333.3*	-	-	-15.6*			
ζDR	-	.491	.59	-	.544	.68	-	.54	.64	-	.47	.51	-	.31	.36			
ωDR	-	1.515	1.06	-	2.98	2.48	-	3.49	3.12	-	3.97	3.89	-	1.26	1.14			
$M\phi$	12.6	-	1.4	3.8	-	1.0	3.6	-	0.8	12.6	-	1.4	98.8	-	0.8			
$M\beta$	-	38.0	1.5	-	10.6	5.8	-	8.2	5.6	-	4.6	4.1	-	109.3	5.4			

*Parameter fixed at HOS value

$$\phi/F_y = \frac{45.41 (.608) (8.13) (3.82) (20.0) (27.2) [.73, 3.56]}{(.697) (2.0) (-.003) (9.1) (18.3) (4.77) (20.0) (26.97) (1.72, 3.19)}$$

$$\phi/F_y = \frac{2.004 [7.77, 2.533] e^{-.036}}{(2.045) (-.003) [.681, 2.484]}$$

M=1.0



FREQUENCY *RAD/SEC*

TIME *SEC*

Figure B-11. F-14 Roll Response -- Simultaneous Match, .715 Mach

$$\beta/F_{ped} = \frac{.147 (.50) (-.007) (4.99) (2.0) (18.41) (66.06) (20.0) (20.0)}{(.697) (2.0) (-.003) (9.1) (18.3) (4.77) (20.0) (26.97) (.72, 3.19)}$$

$$\beta/F_{ped} = \frac{.010 (1.182) (-.007) (66.23) e^{-.067}}{(2.045) (-.003) [.681, 2.484]}$$

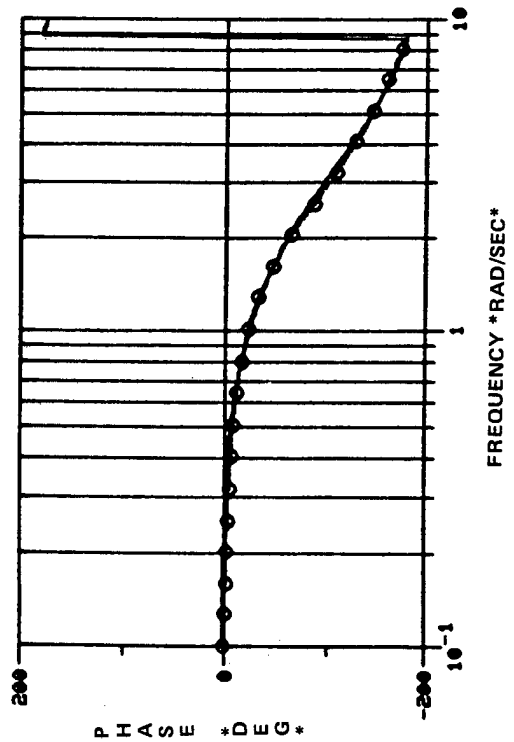
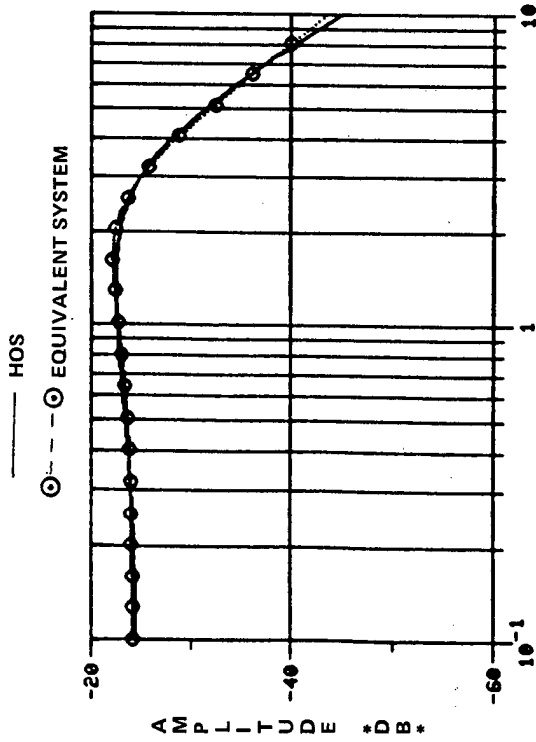
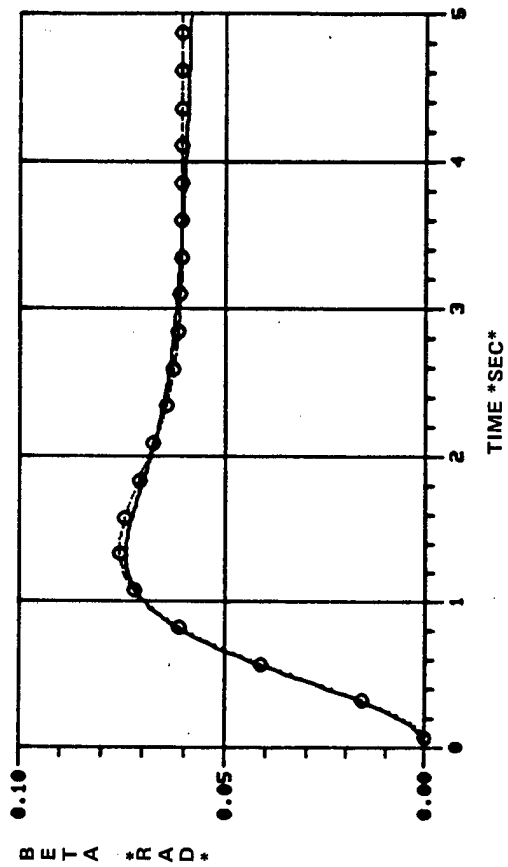
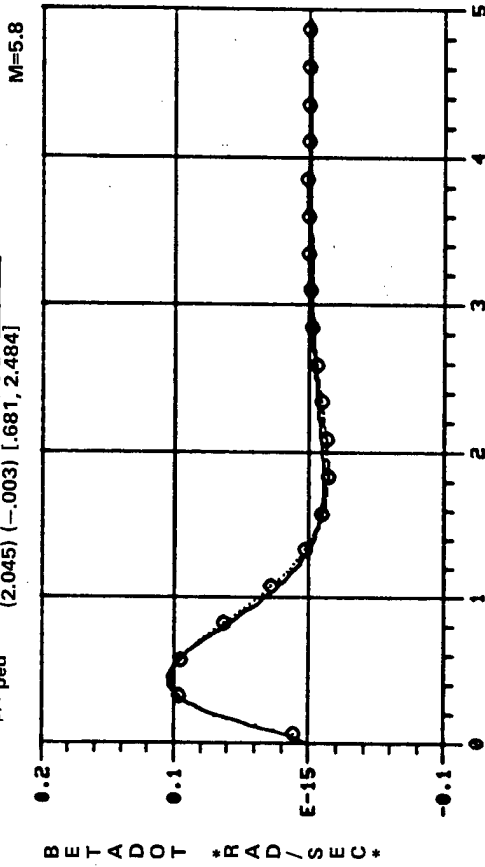


Figure B-12. F-14 Sideslip Response — Simultaneous Match, .715 Mach

$$\phi/F_y = \frac{46.8 (4.76) (.581) (7.17) (20.0) (27.39) [.69, 4.32]}{(.65) (2.0) (-.001) (8.54) (17.31) (5.51) (20.0) (27.15) [.68, 3.91]}$$

$$\phi/F_y = \frac{2.138 [.716, 3.289] e^{-.038}}{(2.146) (-.0012) [.642, 3.122]}$$

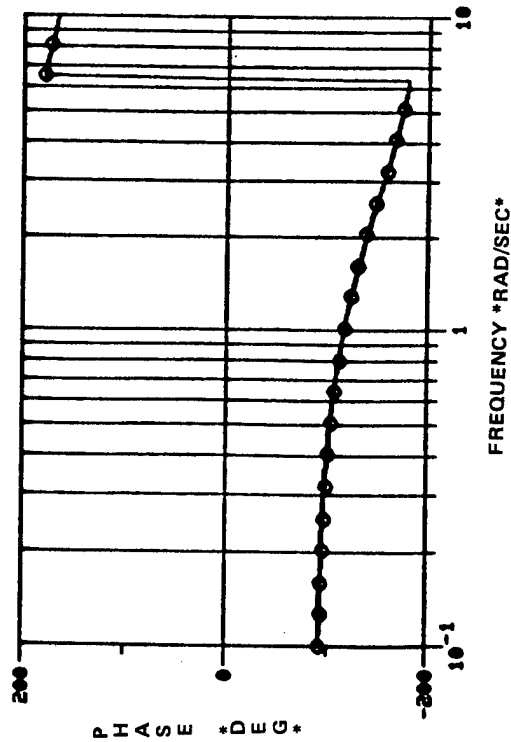
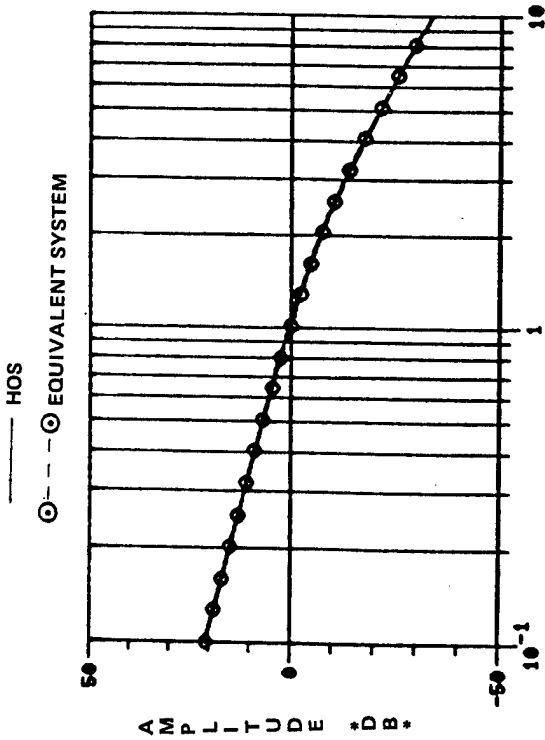
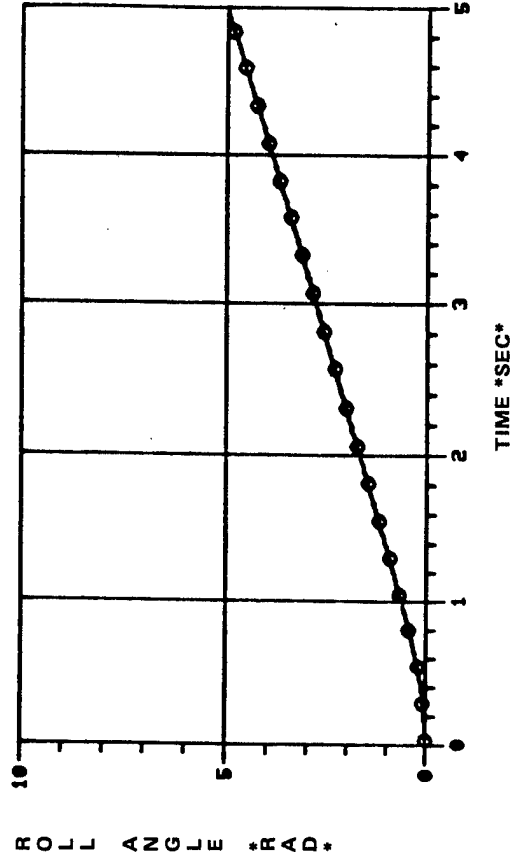
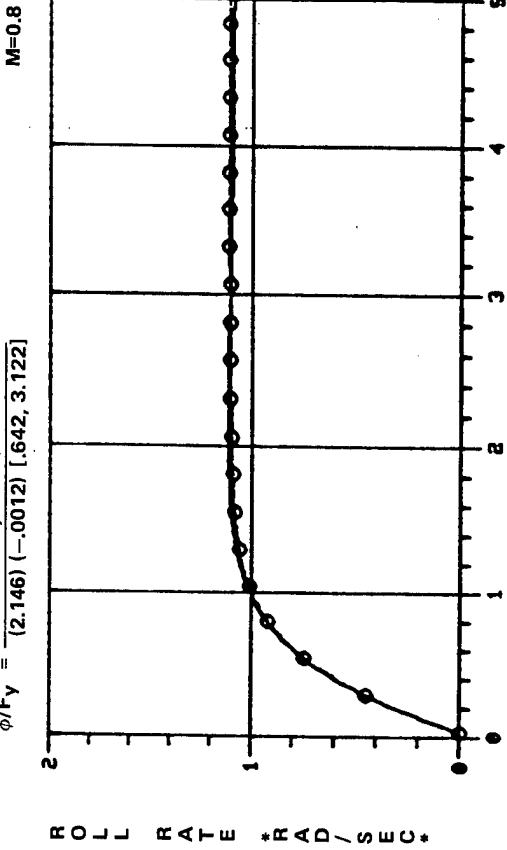


Figure B-13. F-14 Roll Response — Simultaneous Match, .795 Mach

$$\beta/F_{ped} = \frac{.143 (.50) (-.005) (5.96) (2.0) (20.0) (20.0) (17.51) (76.6)}{(.65) (2.0) (-.001) (8.54) (17.31) (5.51) (20.0) (27.15) [.68, 3.91]}$$

$$\beta/F_{ped} = \frac{.0099 (1.49) (-.005) (76.9) e^{-.067}}{(2.146) (-.0012) [.642, 3.122]}$$

M=5.6

HOS

⊙ --- ⊙ EQUIVALENT SYSTEM

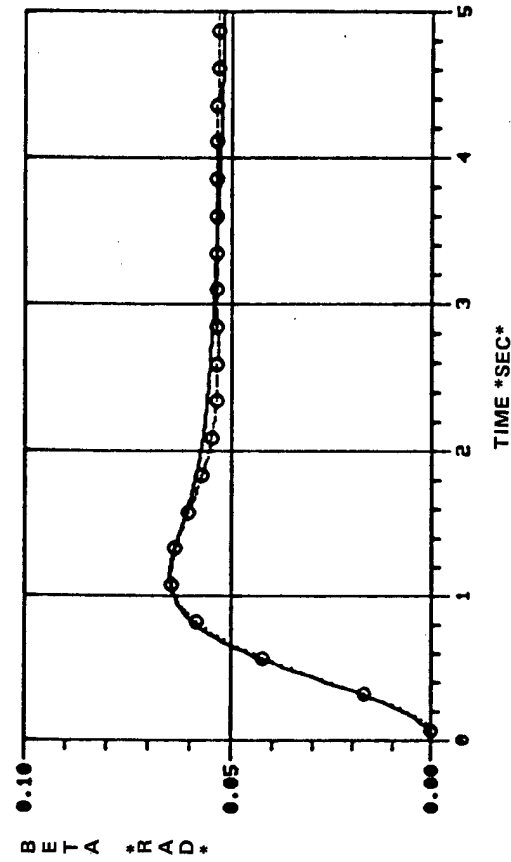
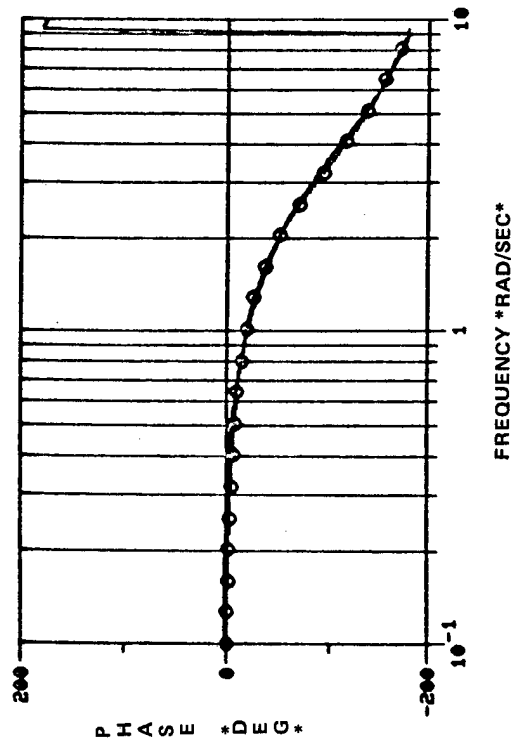
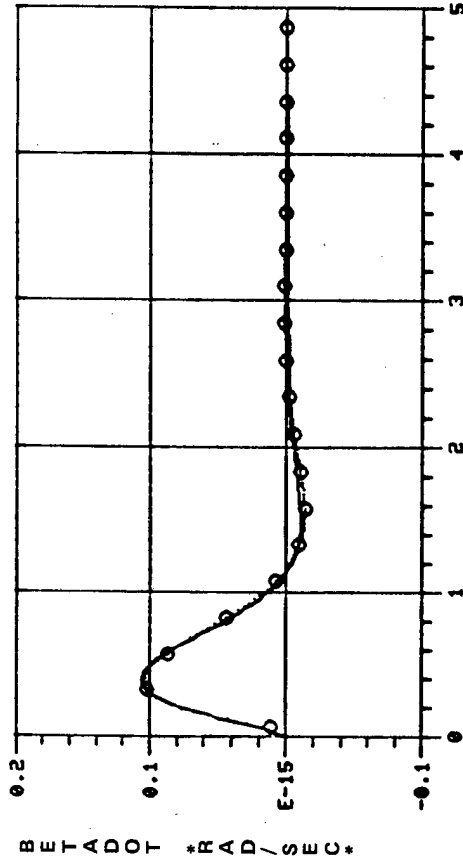
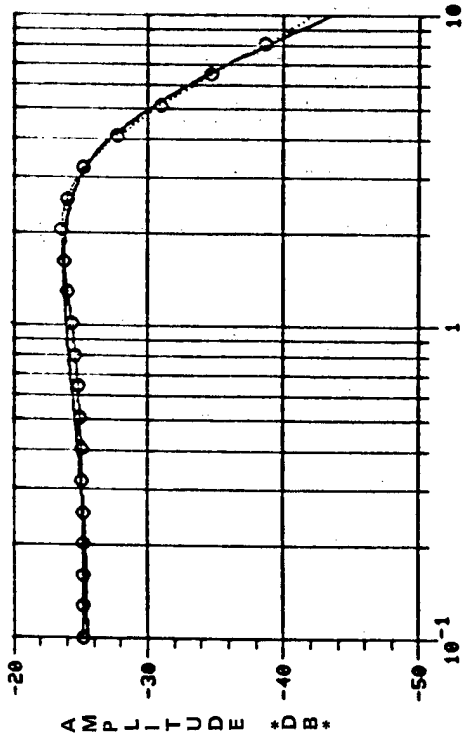
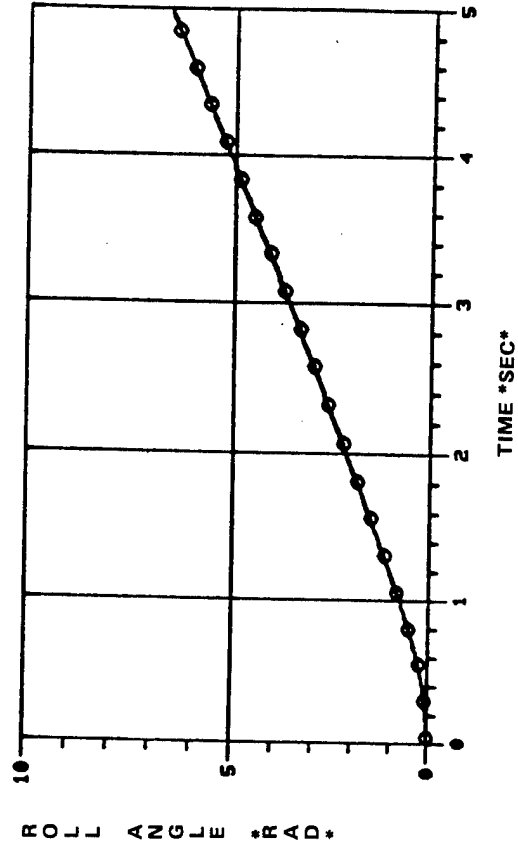
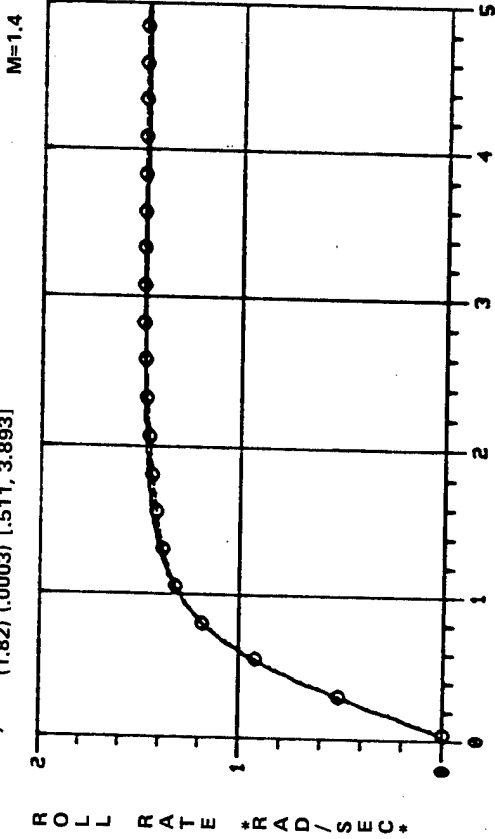


Figure B-14. F-14 Sideslip Response — Simultaneous Match, .795 Mach

$$\phi/F_y = \frac{42.0 (.554) (7.94) (6.29) (20.0) (27.22) [.58, 4.74]}{(.59) (2.0) (.0003) (9.61) (16.3) (5.05) (20.0) (27.0) [.53, 4.39]}$$

$$\phi/F_y = \frac{2.154 [.637, 4.373] e^{-.047}}{(1.82) (.0003) [.511, 3.893]}$$



HOS

⊙ --- ⊙ EQUIVALENT SYSTEM

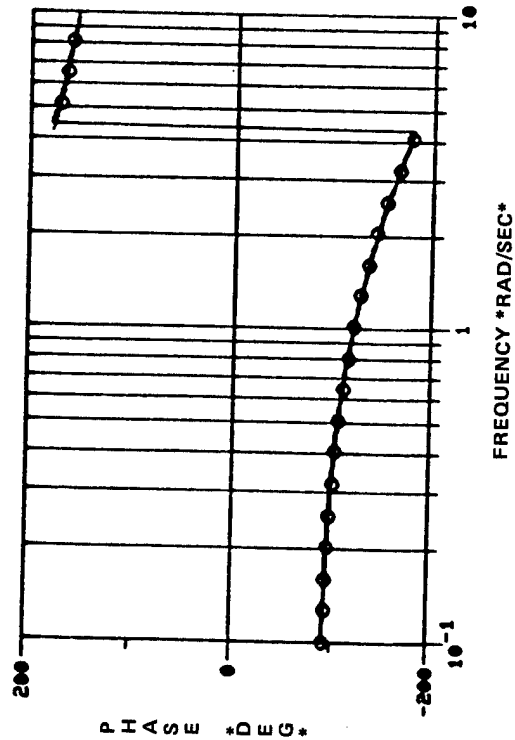
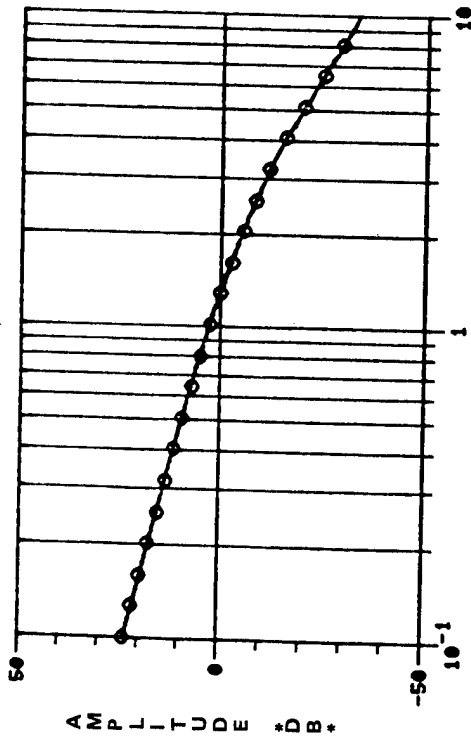


Figure B-15. F-14 Roll Response — Simultaneous Match, .910 Mach

$$\beta/F_{ped} = \frac{.12 (.50) (-.002) (5.63) (2.0) (16.49) (90.68) (20.0) (20.0)}{(.59) (2.0) (.0003) (9.61) (16.3) (5.05) (20.0) (27.0) (.53, 4.39)}$$

$$\beta/F_{ped} = \frac{.00795 (1.642) (-.002) (90.91) e^{-.064}}{(1.82) (.0003) [.511, 3.893]}$$

M=4.1

HOS

⊙ --- ⊙ EQUIVALENT SYSTEM

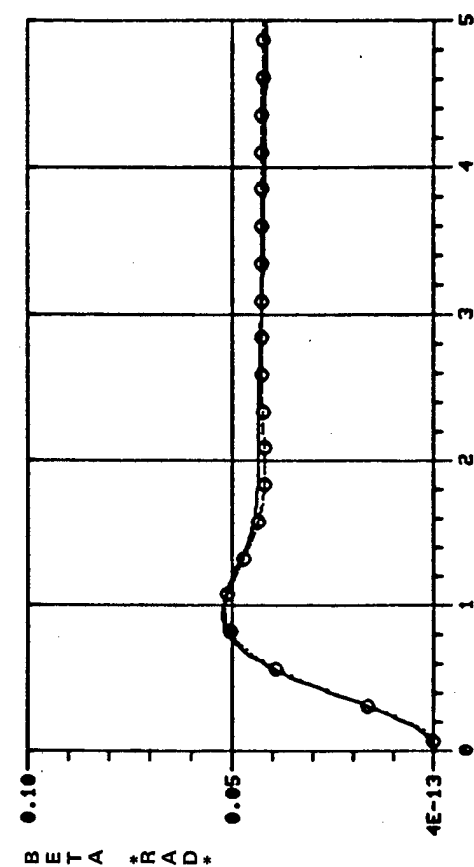
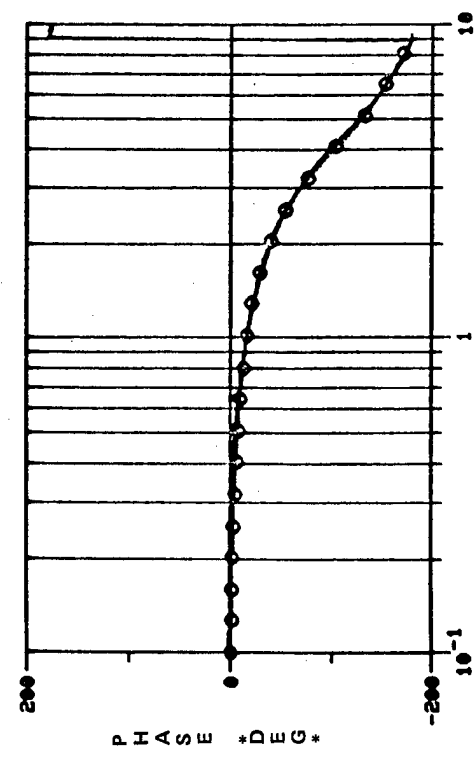
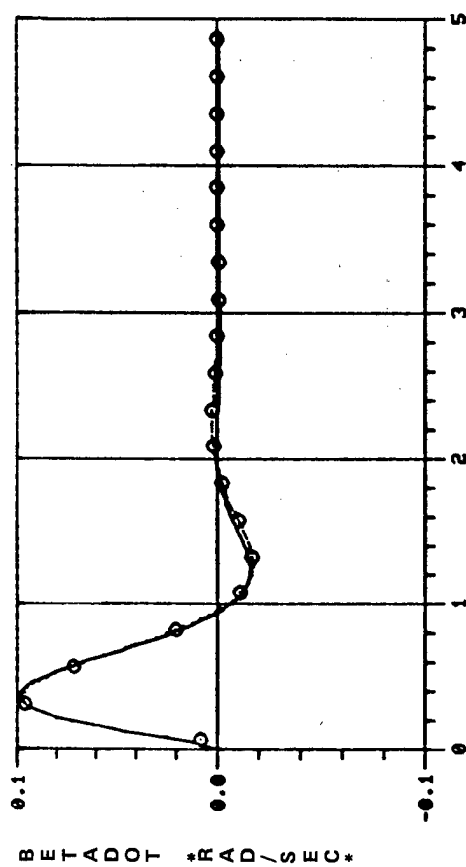
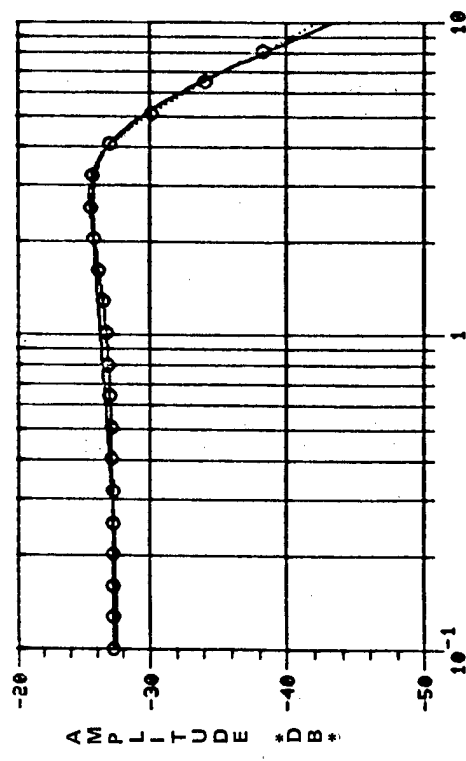


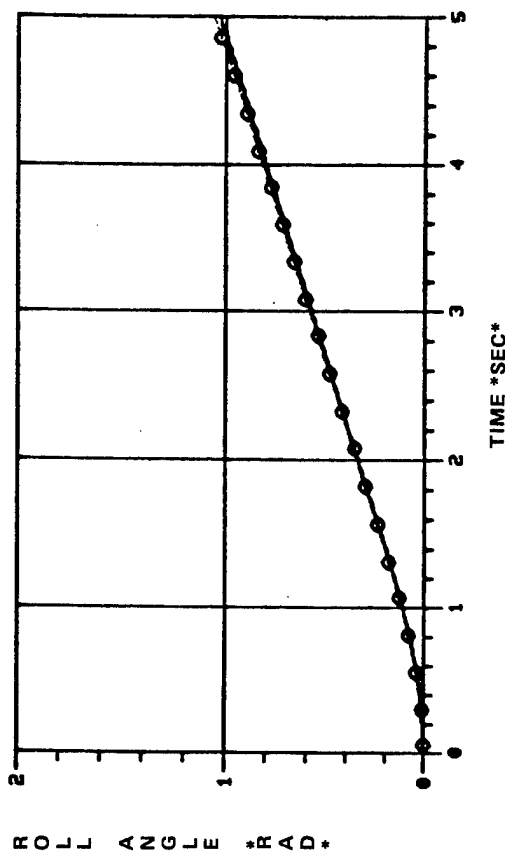
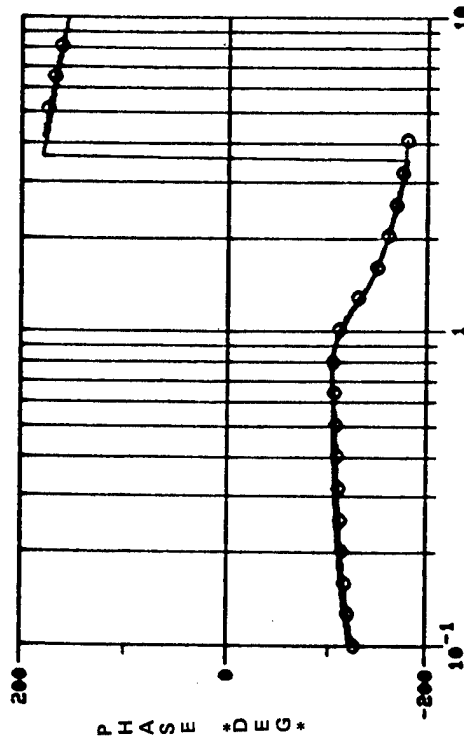
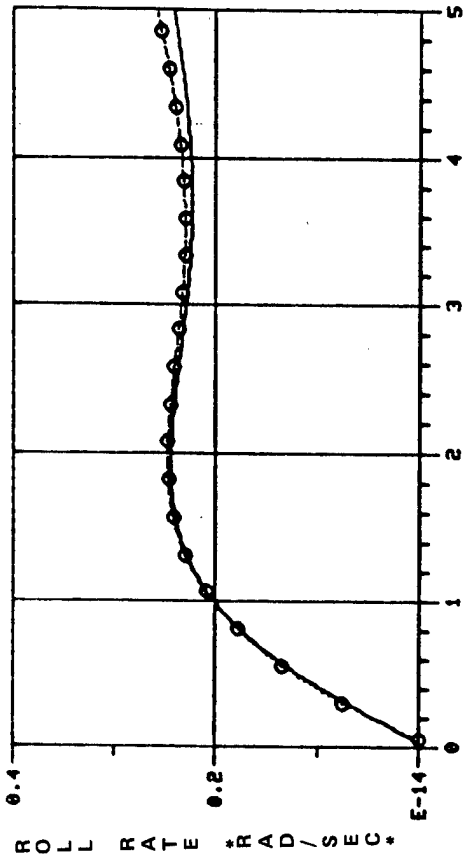
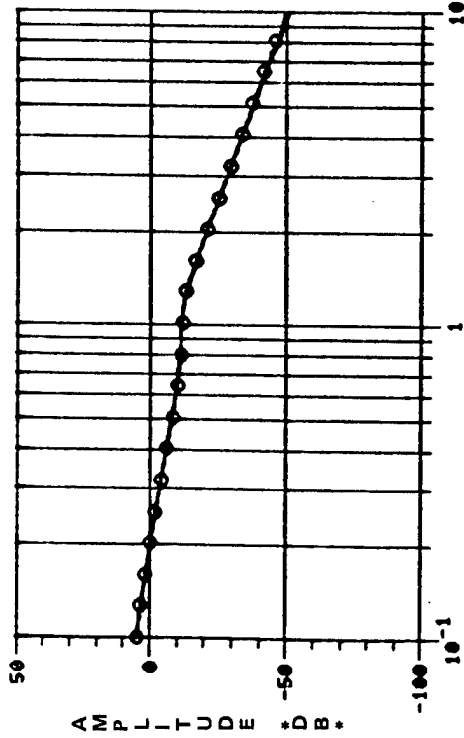
Figure B-16. F-14 Sideslip Response - Simultaneous Match, .910 Mach

$$\phi/F_y = \frac{5.983 \begin{bmatrix} .46 & .921 \end{bmatrix} \begin{bmatrix} .709 & 3.493 \end{bmatrix} \begin{bmatrix} 23.11 & 16.22 \end{bmatrix} \begin{bmatrix} 20.0 \\ 20.0 \end{bmatrix}}{\begin{bmatrix} .361 & 1.069 \end{bmatrix} \begin{bmatrix} .855 & 1.665 \end{bmatrix} \begin{bmatrix} -.058 & 2.0 \end{bmatrix} \begin{bmatrix} 23.11 & 16.22 \end{bmatrix} \begin{bmatrix} 19.87 \\ 20.0 \end{bmatrix}}$$

$$\phi/F_y = \frac{.333 \begin{bmatrix} .505 & .904 \end{bmatrix} e^{-.053}}{\begin{bmatrix} 1.028 & -.064 \end{bmatrix} \begin{bmatrix} .36 & 1.14 \end{bmatrix}} \quad M=0.8$$

HOS

⊙ --- ⊙ EQUIVALENT SYSTEM

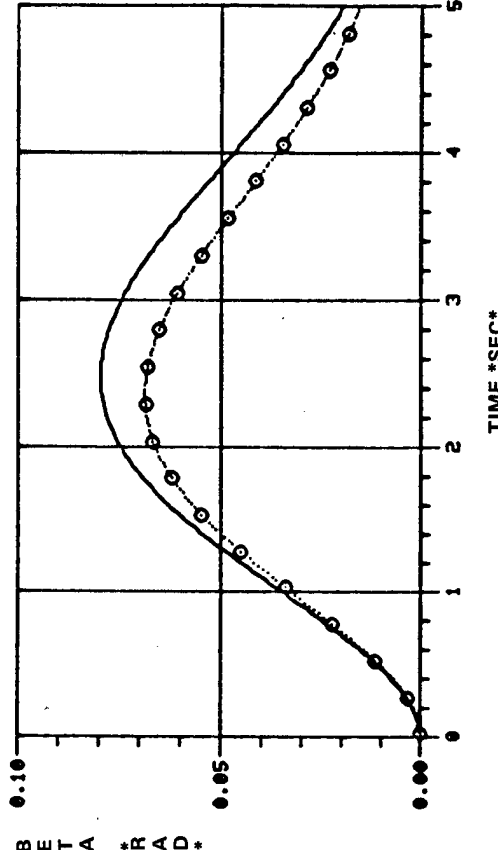
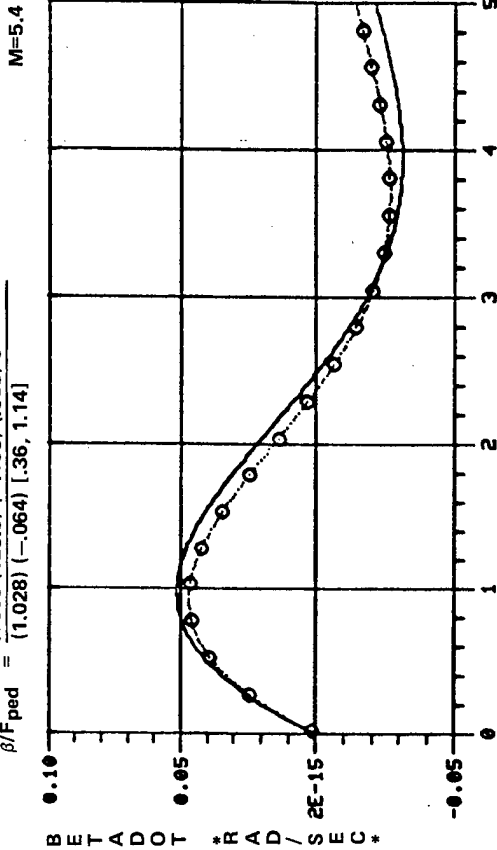


FREQUENCY *RAD/SEC*

Figure B-17. F-14 Roll Response — Simultaneous Match, Power Approach Configuration

$$\beta/F_{ped} = \frac{.094 (.50) (-.161) (2.0) (1.672) (22.93) (19.87) (20.0) (20.0)}{[.361, 1.069] (.855) (1.665) (-.058) (2.0) (20.0) (23.11) (16.22) (19.87)}$$

$$\beta/F_{ped} = \frac{.0009 (123.5) (-.166) (.633) e^{-.018}}{(1.028) (-.064) [.36, 1.14]}$$



HOS

⊙ --- ⊙ EQUIVALENT SYSTEM

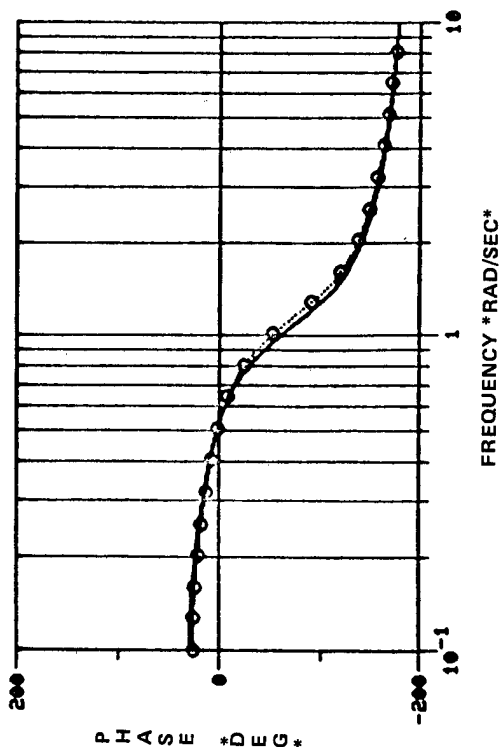
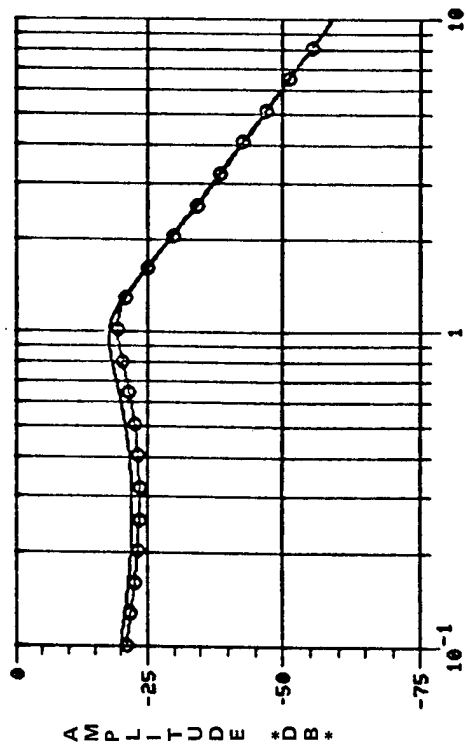


Figure B-18. F-14 Sideslip Response — Simultaneous Match, Power Approach Configuration

DISTRIBUTION LIST

REPORT NO. NADC-83116-60

AIRTASK NO. A034-0000/001B/0F41-400-000

	No. of Copies
NAVAIR (AIR-00D4) (2 for retention) (1 for AIR-530111) (1 for AIR-53014) (1 for AIR-310D)	5
NAVAIRTESTCEN (2 for SA) (2 for AT)	4
Air Force Wright Aeronautical Laboratories (FIGC) Wright Patterson Air Force Base, Ohio 45433 Attention Mr. R. Woodcock	1
McDonnell Douglas Aircraft Co. St. Louis, MO Attention: Mr. W. Moran	1
Systems Technology Incorporated 13766 S. Hawthorne Boulevard Hawthorne, CA 90250 Attention: Mr. R. Hoh	1
NAVAIRDEVCEN (3 for 8131) (15 for 6053)	18
DTIC	12

8400388